AN INVESTIGATION OF THE THERAPEUTIC POTENTIAL OF PHENYLAMINOALKYL SELENIDES THROUGH MECHANISTIC AND BIOLOGICAL STUDIES AND AN EXPLORATION OF CIBER: THE CENTER OF INOVATIVE BIOMATERIAL EDUCATION AND RESEARCH

A Dissertation
Presented To
The Academic Faculty

by

Elizabeth Alice Cowan

In Partial Fulfillment
Of the Requirements for the Degree
Doctor of Philosophy in Chemistry & Biochemistry

Georgia Institute of Technology
December 2011

AN INVESTIGATION OF THE THERAPEUTIC POTENTIAL OF PHENYLAMINOALKYL SELENIDES THROUGH MECHANISTIC AND BIOLOGICAL STUDIES AND AN EXPLORATION OF CIBER: THE CENTER OF INNOVATIVE BIOMATERIAL EDUCATION AND RESEARCH

Approved:

Dr. Sheldon W. May, Advisor
School of Chemistry and Biochemistry
Georgia Institute of Technology

Dr. James Powers
School of Chemistry and Biochemistry
Georgia Institute of Technology

Dr. Donald Doyle
School of Chemistry and Biochemistry
Georgia Institute of Technology

Dr. Nicholas Hud
School of Chemistry and Biochemistry
Georgia Institute of Technology

Dr. Stanley Pollock
Department of Pharmaceutical Sciences
Mercer University

Date Approved: November 14, 2011

Along this journey of highs and lows, I have lost and gained family and friends. Therefore, I dedicated this work to Roselle, James, and Howell. I miss you deeply and hope that I have made you proud. I also dedicated this work to my amazing nephews, Luke and Mark and my precious niece, Maggie. It is my wish that I am always there to provide inspiration and support for you as you have done for me.

ACKNOWLEDGEMENTS

My time at Georgia Tech has been filled with frustrations and constant mixed emotions of achievements and failures. Although there were times when I doubted my capabilities, I now know that with God's help, I am strong and capable. I have learned a lot about myself and built relationships that I have no doubt will remain strong for many years.

I would first like to thank my family for all their support. I would like to thank my parents for teaching me the importance of education and never showing any doubt in me. To the most wonderful, supportive sisters anyone could ask for, I say thank you for listening, for wiping tears and for providing much needed distractions. I love you all deeply and will never be able to fully describe how much you have helped me.

I would like to thank Dr. Sheldon May for helping me to develop into the scientist I am today. You have provided me with skills and opportunities that I will carry with me as I start my journey as a professional scientist. I would also like to thank Dr. May for allowing me to be a teaching assistant in the Georgia Tech Mass spectrometry Facilities. Although it took time away from research in your laboratory, this opportunity was a valuable and priceless experience that I will always be grateful for. I would also like to thank current and former members of the May lab for their experiences, expertise, and critical review of experiments. Dr. Charlie Oldham has been an amazing help throughout this entire process. Showing me around the lab when I first joined the May group, listening to rants about broken instruments and failed experiments, proofing dozens of reports, articles, etc., and being a wealth of knowledge are just some of the ways you

have supported me and for all those reasons and more I give you my thanks. I am truly honored to have been able to work with each of you.

There are several other people who have also been involved in helping me through this process. I would like to thank Dr. Rusty Arnold and Jeong Kang at the University of Georgia for their help with the xenograft prostate model studies. I would like to thank Dr. Donald Doyle and Dr. Jennifer Taylor for their help with the human embryonic kidney cell studies. I would also like to thank Dr. Niren Murthy and Dr. Madhuri Dasari for help with the synthesis of the peroxalate polymer. I would like to thank Dr. Cameron Sullards, Mr. David Bostwick, and the Georgia Tech Mass Spectrometry Facilities for the opportunity to learn valuable skills that have helped me start my career. I would also like to thank Dr. Tiffany Seyler at the Centers for Disease Control for giving me an opportunity that I have dreamed about for years, and for being patient with me throughout the last two years of this process. I look forward to working alongside you and making a real difference through Tobacco Exposure Biomarkers.

There are many people that are not mentioned here that contributed to this success. Many family members and friends have provided encouragement, support and stress relief throughout my graduate career and deserve gratitude. You are all important to me and I thank you all.

TABLE OF CONTENTS

LIST OF TABLES

LIST OF FIGURES

LIST OF SYMBOLS AND ABBREVIATIONS

ANOVA	Analysis of Variance
Ca^{+2}	Intracellular Calcium
CE	Capillary Energy
ClPAESe	Chlorophenylaminoethyl Selenide
ClPAESeO	Chlorophenylaminoethyl Selenoxide
CM-H_2DCFDA	(5-(and-6)-chloromethyldihydrofluorescein Diacetate Acetyl Ester
CO_2	Carbon Dioxide
CV	Cone Voltage
DLS	Dynamic Light Scattering
DMSO	Dimethylsulfoxide
DNA	Deoxyribose Nucleic Acid
DOX	Doxorubicin
DβM	Dopamine β-monoxygenase
EDTA	Ethylenediaminetetraacetic Acid
FBA	Fetal Bovine Serum
FDA	U.S. Food and Drug Administration
FPAESe	Fluorophenylaminoethyl Selenide
FPAESeO	Fluorophenylaminoethyl Selenoxide
GSH	Reduced Glutathione
GSSG	Glutathione Disulfide

H&E	Hematoylin and Eosin
H_2O_2	Hydrogen Peroxide
HIV	Human Immunodeficiency Virus
HOCl	Hypochlorous Acid
HPLC	High Pressure Liquid Chromatography
LPS	Lipopolysaccharide
MTT	3-(4,5-Dimethylthiazol-2-yl)-2,5-diphenyltetrazolium Bromide
Nac-FPAESe	*N*-acetyl Fluorophenylaminoethyl Selenide
NADPH	Nicotinamide Adenine Dinucleotide Phosphate
NCr	Spontaneous Mutant T-cell Deficient Mice
NMR	Nuclear Magnetic Resonance
NOX	Nicotinamide Adenine Dinucleotide Phosphate Oxidase
O_2^-	Superoxide
$OH^\cdot$	Hydroxyl Radical
$ONOO^-$	Peroxynitrite
PAESe	Phenylaminoethyl Selenide
PAESeO	Phenylaminoethyl Selenoxide
PC-3	Human Prostate Epithelial Cells
PCL	Poly(ε-caprolactone)
PDI	Polydispersity Index
PLA	Poly(lactic) Acid
PLGA	Poly(lactic-co-glycolic) Acid
ROS	Reactive Oxygen Species

Se	Selenium
SOD	Superoxide Dismutase
SRB	Sulforhodamine B
SVD	Singular Value Decomposition
TBHP	Tert-butylhydroperoxide
TCA	Trichloroacetic Acid
TMS	Trimethylsilane
TRIS	Tris(hydroxymethyl)aminomethane

SUMMARY

The overproduction of reactive oxygen species (ROS) has been linked to diseases and other pathologies. As therapeutic agents, antioxidants have been tested and some shown to attenuate these diseases by relieving oxidative stress. The May laboratory has previously developed a family of phenylaminoalkyl selenides and has demonstrated the antihypertensive and antioxidant properties of these compounds.

To further understand the antioxidant property of these selenide compounds, the two step mechanism of the reaction between the selenoxide form and glutathione was investigated by stopped-flow and mass spectrometry, leading to the detection and characterization of a novel thioselenurane intermediate. Mass spectrometry studies supported the redox cycle of the selenide compounds as a straightforward cycle with no byproducts or side reactions and was the first evidence reported of a thioselenurane intermediate present in a reduction reaction of a selenoxide.

The therapeutic potential of these compounds is further supported by cell and histological studies demonstrating their ability to alleviate the cardiotoxic effect of anthracyclines without affecting the anti-cancer property of the drugs. Codosage of a phenylaminoethyl selenide with Doxorubicin decreased the infiltration of inflammation cells in the myocardium of mice. Phenylaminoethyl selenides were also able to maintain the body weight of mice treated with Doxorubicin, compared to mice treated with Doxorubicin alone.

To make the possibility of using Phenylaminoalkyl selenides as therapeutic agents or supplements with other agents, delivery of the compounds was investigated. *N* acetyl

phenylaminoethyl selenides were successfully encapsulated into poly(lactic-*co*-glycolic) (PLGA) nanoparticles using the nanoprecipitation technique. An attempt was made to demonstrate the ability of these selenide- nanoparticles to reduce cellular oxidative stress caused by incubation with LPS. Future studies are needed to optimize the loading of the selenide compounds into nanocarriers and to demonstrate the ability of the encapsulated drug to work as the free drug. The long term goal of this research is to fully understand the potential of phenylaminoalkyl selenides as an efficient therapeutic agent for ailments derived from increased levels of ROS and a state of oxidative stress.

As a supplemental project funded by the National Science Foundation, the Center for Innovative Biomaterial Education and Research (CIBER) was created. Enzymatically catalyzed reaction and polymerizations were investigated using *Candida antarctica* Lipase B (CALB). Several CALB catalyzed Michael addition reactions were successful and yielded compounds that could be used as future reactants and monomers. As an education requirement of the project a website was created to educate the public of the importance, sources and uses of biomaterials. The website provides information for all levels of students and educators. This center has allowed The Georgia Institute of Technology to form relationships and exchange programs with leading universities around the world allowing the exchange of knowledge and research in biomaterials.

CHAPTER 1

INTRODUCTION

1.1 Reactive Oxygen Species: Cellular Functions and Toxicity

Life essentially developed in the absence of oxygen. The advent of O_2-evolving photosynthesis, including novel metabolic transformations, the generation of heat and light, and the ability to solubilize and detoxify compounds, lead to an increased rate of mutations and evolution. Organisms were forced to either develop defenses against the toxic gas or to find anaerobic niches. The thought that oxygen is toxic to life forms for which it has become an essential component, is the "Oxygen Paradox".

The toxicity of oxygen gas is a result from its paramagnetic electronic structure, containing two unpaired electrons with the same spin state. This feature makes the reaction of two oxygen molecules energetically unfavorable, as explained by the Pauli Exclusion Principle. This is overcome by the fact that electronic spins can be inverted by the interaction with nuclear spins. Therefore, the reduction of oxygen takes place through the accepting of free electrons one at a time, in separate univalent electron transfers. Superoxide ($O_2^{\cdot-}$), hydrogen peroxide (H_2O_2), hypochlorous acid (HOCl), peroxynitrite ($ONOO^-$), and hydroxyl radical ($HO^{\cdot}$) are intermediates produced either directly or secondarily through the reduction of oxygen. These compounds belong to a class of radical and non-radical compounds known as reactive oxygen species (ROS) and are responsible for the toxic effects of oxygen, listed in Table 1.1.[1, 2]

Table 1.1. Radical and Non-Radical Reactive Oxygen Species

Radical Species	Non-Radical Species
$O_2^{\cdot-}$ superoxide radical	H_2O_2 hydrogen peroxide
$HO^{\cdot}$ hydroxyl radical	HOCl hypochlorous acid
$ROO^{\cdot}$ peroxyl radical	O_3 ozone
$RO^{\cdot}$ alkoxy radical	$^1O_2$ singlet oxygen
$HOO^{\cdot}$ hydroperoxyl radical	

Reactive oxidants are products of cellular metabolism, being produced by the mitochondrial electron-transport chain and oxygen-metabolizing enzymatic reactions such as xanthine oxidases, the cytochrome P450 system, NADPH oxidases, myeloperoxidases, and nitric oxide peroxidases.[3, 4] Although high concentrations of ROS can be cytotoxic; the generation of these small molecules, within certain concentrations, is necessary to maintain homeostasis. At physiological concentrations, ROS, specifically H_2O_2, are known to play a role in cell signaling. Intracellular redox environment has been linked to cell proliferation and differentiation, activation and inhibition of apoptosis, and the induction of necrosis.[5-7] H_2O_2 plays a role in gene regulation, growth factor signaling, host defense, and wound detection and healing.[3, 7-12]

Under normal physiological conditions, the production and elimination of reactive oxidants is maintained in balance by enzymes (catalase, glutathione peroxidase, thioredoxin, superoxide dismutase (SOD), etc.) and cellular small molecule antioxidants, including ascorbate and glutathione. The natural production of ROS can be shifted by environmental stimuli, such as ionizing and UV radiation, and by the metabolism of drugs and xenobiotics, or by biochemical stimuli such as the over stimulation of deactivation of endogenous enzymes. When this balance between cellular production and elimination of ROS is disrupted, a state of excess cellular oxidants occurs and is referred to as “oxidative stress”.

1.2. Oxidative Stress

The state of oxidative stress causes various responses within a cell. Gene expression modulation, growth stimulation, temporary growth-arrest and apoptosis are all observed in stressed cells. Necrosis, direct cell destruction, is the most extreme outcome of oxidative stress.[13] ROS activate a number of nuclear transcription factors, cytokines, kinases and other immune system cells. These activations lead to increased inflammatory cytokine activation, and T cell apoptosis, resulting in a reduction in immune tolerance.[14-17] Due to these changes through redox signaling, oxidative stress has been found to be a cause of some diseases, and a secondary, contributing factor of others. It is known to play a role in various pathological phenomena including but not limited to cancer, hypertension, asthma, renal failure, atherosclerosis, Parkinson's disease and HIV.[3, 6, 13, 18-23]

Oxidative stress has been shown to contribute to immune alterations and inflammatory conditions such as increased virulence.[2,3,4] Studies by Beck *et al.* demonstrated that states of oxidative stress causes increased pathology, viral virulence and viral mutation.[24] Vitamin E deficient and selenium deficient mice both showed increased susceptibility to the cardiotoxic effects of a myocarditic coxsackievirus. In the same report, a benign strain of the virus, showing no cardiotoxic effects, caused heart damage when inoculated into vitamin E deficient mice.[6] These studies lead to the conclusions that oxidative stress not only plays an important role in host resistance of viral infections, but also a role in the progression and pathology of the infection.

Evidence suggests that patients infected with the human immunodeficiency virus (HIV) are under chronic oxidative stress. Elevated serum levels of lipid peroxidation byproducts, increased oxygen consumption, and increased free radical production by neutrophils implies increased oxidative stress in asymptomatic HIV-infected and AIDS patients. HIV replication is increased under oxidative stress conditions *in vitro*. These effects of oxidants on viral replication have been demonstrated in studies in which antioxidants inhibited viral replication.[13, 25-27]

1.3 Anti-oxidant Properties of Selenium

Selenium (Se), discovered in 1817 by Jöns Jakob Berzelius, is an essential element and micronutrient. The micronutrient enters the food chain via plants and vegetables through which it is taken up from the soil. Human consumption of Se comes primarily from shellfish, fish, and meat. Differences in soil selenium concentrations provide an explanation for greater Se deficiencies in some geographic areas than others. Although the average US resident meets the daily requirement of Se (55µg) with an average intake of 70-100µg/day, in many populations in Asia, Europe and parts of Africa the average daily intake is much lower than the normal nutritional requirement at less than 25µg/day.[28, 29] Deficiency in dietary Se has been associated with diseases and aliments such as white muscle disease, heart disease, arthritis, cancer, and impaired immune response. [30-33]

In 1957, the biological importance of selenium was demonstrated by the work with Schwarz and Foliz and Patterson *et al.*[34, 35] The discovery of selenoproteins and selenocysteine further established the necessity of the element and initiated the ever-

expanding field of biological and medicinal selenium research. The importance of selenium became clearer in 1973 when Rotruck et al. discovered its role in the formation of glutathione peroxidase, an enzyme that protects against oxidative injury. [36] Through the amino acid selenocysteine, Se is a component of at least 25 human selenoenzymes, playing a critical role in the redox center of several of these. It has been proposed that this role in selenoproteins is the origin of the anti-oxidant and anticancer properties observed in selenium and organoselenium compounds. In 1969, Shamberger and Frost reported the first suggestion of selenium's protective effect against cancer.[37] With the discovery of this property, small molecule selenium compounds increased in popularity for therapeutics for oxidative stress and its related diseases.

1.4 Phenylaminoalkyl Selenides and Selenoxides

Phenylaminoalkyl selenides (Figure1.1) were originally synthesized in the May laboratory as substrate analogs for Dopamine β-monooxygenase (DβM, 1.14.17.1), the key enzyme involved in catecholamine metabolism. DβM catalyzes the ascorbate-

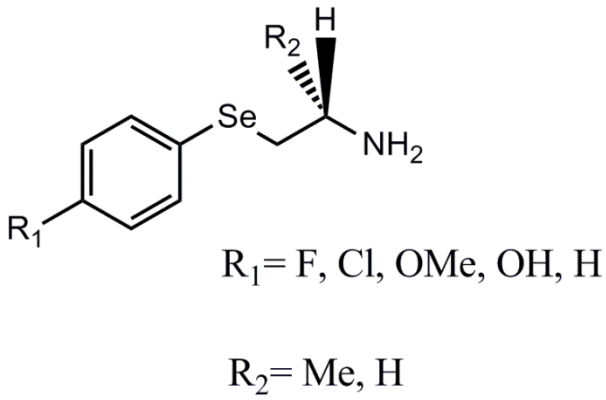

Figure1.1. Phenylaminoalkyl Selenides

dependent hydroxylation of dopamine to R-norepinephrine and is a target for modulating the peripheral adrenergic activity. Experimental evidence demonstrated that phenylaminoalkyl selenides are oxidized by DβM to the corresponding selenoxides. The inactivation of ascorbate-dependent DβM activity was achieved by the recycling of the selenoxide product back to the selenide form with the concomitant oxidation of reduced ascorbate.[38-40]

The May laboratory later reported these compounds to exhibit dose-dependent antihypertensive properties in spontaneously hypertensive rats.[39, 41] The compounds gain access to the peripheral adrenergic nerve terminal via a cocaine sensitive neuronal uptake mechanism, where they enter the adrenergic storage vesicles and inhibit the synthesis of norepinephrine. This has further been demonstrated by the reduction of norepinephrine levels in cardiac tissue at levels that lower blood pressure.[42, 43] More recently the antioxidant property of phenylaminoalkyl selenides was established in our laboratory, through the work of Woznichak *et al.* and De Silva *et al.*[11, 44] Our lab showed that phenylaminoalkyl selenides react with cellular oxidants, peroxynitrite and hydrogen peroxide, in a stochiometric 1:1 molar ratio yielding the respective selenoxides.[44] We also reported that the selenoxides are reduced back to the original selenide form via a redox reaction with cellular reductants.[11] Antihypertensive and antioxidant properties make phenylaminoethyl selenides very attractive organoselenium compounds for therapeutic agents and worthy of the further investigative research discussed herein.

1.5 REFERENCES

1. Auten, R. L.; Davis, J. M., The role of oxygen in health and disease - A series of reviews. *Pediatric Research* **2009,** 66, (2), 121-127.

2. Fridovich, I., Oxygen toxicity: a radical explanation *The Journal of Experimental Biology* **1998,** 201, 1203-1209.

3. Sarsour, E. H.; Kumar, M., G.; Chaudhuri, L.; Kalen, A. L.; Goweami, P. C., Redox control of the cell cycle in health and disease. *Antioxidants and redox signaling* **2009,** 11, (12), 2985-3011

4. Winterbourn, C. C., Reconciling the chemistry and biology of reactive oxygen species. *Nature Chemical Biology* **2008,** 4, (5), 278-286.

5. Davies, K. J. A., Oxidative stress, antioxidant defenses, and damage removal, repair, and replacement systems. *Life* **2000,** 50, 279-289.

6. Sies, H.; Cadenas, E., Oxidative stress: damage to intact cells and organs. *Philosophical translations of the Royal Society of London B* **1985,** 311, 617-631.

7. Hancock, J. T.; Desikan, R.; Neill, S. J., Role of reactive oxygen species in cell signaling pathways. *Biochemical Societey Transactions* **2001,** 29, 345-350.

8. Finkel, T., Oxidant signals and oxidative stress. *Current Opinion in Cell Biology* **2003,** 15, 247-254.

9. Rhee, S. G., H_2O_2, a necessary evil for cell signaling. *Science* **2006,** 312, 1882-1883.

10. Niethammer, P.; Grabher, C.; Look, A. T.; Mitchinson, T., A tissue-scale gradient of hydrogen peroxide mediates rapid wound detection in zeba fish. *Nature* **2009,** 459, 996-1000.

11. De Silva, V.; Woznichak, M. M.; Burns, K. L.; Grant, K. B.; May, S. W., Selenium redox cycling in the protective effects of organoselenides against oxidant-induced DNA damage. *Journal of the American Chemical Society* **2004,** 126, 2409-2413.

12. Woo, H. A.; Yim, S. H.; Shin, D. H.; Kang, D.; Yu, D.-Y.; Rhee, S. G., Inactivation of Peroxiredoxin I by phosphorylation allows localized H_2O_2 accumulation for cell signaling. *Cell* **2010,** 140, 517-528.

13. Pace, G. W.; Leaf, C. D., The role of oxidative stress in HIV disease. *Free Radical Biology and Medicine* **1995,** 19, 523-528.

14. Griffiths, H., ROS signaling molecules in T cells- evidence for abnormal redox signaling in the autoimmune disease, rheumatoid arthritis. *Redox Report* **2005,** 10, (6), 273-280.

15. Maziere, C.; Maziere, J.-C., Activation of transcription factors and gene expression by oxidized low-density lipoprotein. *Free Radical Biol. Med.* **2009,** 46, 127-137.

16. Mukhopadhyay, S.; Sen, S.; Majhi, B.; Das, K. P.; Kar, M., Methyl glyoxyl elevation is associated with oxidative stress in rheumatoid arthritis. *Free Radical Research* **2007,** 41, (5), 507-514.

17. Tsukahara, H., Biomarkers for oxidative stress: Clinical application in pediatric medicine. *Current Medicinal Chemistry* **2007,** 14, (339-351), 339.

18. Wu, D.; Cederbaum, A. I., Alcohol, oxidative stress, and free radical damage. *Alcohol Research and Health* **2003,** 27, (4), 277-284.

19. Wang, Y. W.; Qiao, B.; Wang, Y.; Han, X.; Chu, Y.; Xiong, S., Autoantibodies closely related to the elevation level of *in vivo* hydrogen peroxide and tissue damage in systemic lupus erythematosus. *DNA and Cell Biology* **2006,** 25, 563-570.

20. Spector, A., Review: oxidative stress and disease. *Journal of Ocular Phamracology* **2000,** 16, (2), 193-199.

21. Lander, H. M., An essential role for free radicals and derived species insignal transduction. *FASEB J.* **1997,** 11, 118-124.

22. Kovacic, P.; Jacintho, J. D., Systemic lupus erythematosus and other autoimmune diseases from endogenous and exogenous agents: unifying theme of oxidative stress. *Mini Reviews in Medicinal Chemistry* **2003,** 3, 568-575.

23. Kehrer, J. P., Free Radicals as mediators of tissue injury and disease. *Critical Reviews in Toxicology* **1993,** 23, 21-48.

24. Beck, M. A.; Shi, Q.; Morris, V. C.; Levander, O. A., Rapid genomic evolution of a non-virulent Coxsackievirus B3 in selenium-deficient mice results in selection of identical virulent isolates. *Nature Medicine* **1995,** 1, 433-436.

25. Harakeh, S.; Jariwalla, R. J., Comparative study of the anti-HIV activities of ascorbate and thiol-containing reducing agents in chronically HIV-infected cells. *Americal Journal of Clinical Nutrition* **1991,** 54, 1231-1235.

26. Mihm, S.; Ennen, J.; Pessara, U.; Kurth, R.; Droge, W., Inhibition of HIV-1 replication and NF-8β activity by cysteine and cysteine derivatives. *AIDS* **1991,** 5, (5), 497-504.

27. Kalebic, T.; Kinter, A.; Poli, G.; Anderson, M. E.; Meister, A.; Fauci, A. S., Supression of human immunodeficiency virus expression in chronically infected monocytic cells by glutathione, glutathione ester and *N*-acetylcysteine. *Proc. Natl. Acad. Sci. USA* **1991,** 88, 986-990.

28. El-Bayoumy, K., The protective role of selenium on genetic damage and on cancer. *Mutation Research* **2001,** 475, 123-139.

29. Zeng, H., Selenium as an essential micronutrient: Roles in cell cycle and apoptosis. *molecules* **2009,** 14, 1263-1278.

30. Baum, M. K.; Shor-Posner, G.; Lai, S. H.; Zhang, G. Y.; Fletcher, M. A.; Sauberlich, H.; Page, J. B., High risk of HIV-related mortality is associated with selenium deficiency. *Journal of Acquired Immune Deficiency Syndromes and Human Retrovirology* **1997,** 15, 370-374.

31. Manteroatienza, E.; Sotomayor, M. G.; Shor-Posner, G.; Fletcher, M. A.; Sauberlich, H. E.; Beach, R. S.; Baum, M. K., Selenium status and immune function in asymptomatic HIV-1 seropositive men. *Nutrition Research* **1991,** 11, 1237-1250.

32. Parham, M. E.; Loudon, G. M., Carboxyl-terminal sequential degradation of peptides. *Biochem. Biophys. Res. Commun.* **1978,** 80, 1-6.

33. Parham, M. E.; Loudon, G. M., A new method of determination of the carboxyl-terminal residue of peptides. *Biochem. Biophys. Res. Commun.* **1978,** 80, 7-13.

34. Patterson, E. L.; Milstrey, R.; Stokstad, E. L. R., Effect of selenium in preventing exudative diathesis in chicks. *Proceedings of the Society for Experimental Biology and Medicine* **1957,** 95, 617-620.

35. Schwarz, K.; Foltz, C. M., Selenium as in integral part of factor 3 against dietary liver degeneration. *Journal of the American Chemical Society* **1957,** 70, 3292-3293.

36. Rotruck, J. T.; Pope, A. L.; Ganther, H. E.; Swanson, A. B.; Hafeman, D. G.; Hoekstra, W. G., Selenium: Biochemical role as a component of glutathione peroxidase. *Science* **1973,** 179, 588-590.

37. Shamberger, R. J.; Douglas, F. V., Possible protective effect of selenium against human cancer. *Canadian Medical Association Journal* **1969,** 100, 682.

38. May, S. W.; Herman, H. H.; Roberts, S. F.; Ciccarello, M. C., Ascorbate depletion as a consequence of product recycling during dopamine β-monooxygenase catalyzed selenoxidation. *Biochemistry* **1987,** 26, 1626-1633.

39. May, S. W.; Pollock, S. H., Selenium-based antihypertensives. Rationale and potential. *Drugs* **1998,** 56, 959-964.

40. John Wiley: New York, 1981.

41. May, S. W.; Wang, L.; Gill-Woznichak, M. M.; Browner, R. F.; Ogonowski, A. A.; Smith, J. B.; Pollock, S. H., An orally active selenium-based antihypertensive agent with restricted CNS permeability. *J. Pharmacol. Exp. Ther.* **1997,** 283, 470-477.

42. Pollock, S. H.; Herman, H. H.; Fowler, L. C.; Edwards, A. S.; Evans, C. O.; May, S. W., Demonstration of the antihypertensive activity of phenyl-2-aminoethyl selenide. *Journal of Pharmacology and Experimental Therapeutics* **1988,** 246, 227-234.

43. Powers, J. L.; Plaskon, R. R.; Olsen, G. A.; May, S. W., Structural requirements for cocaine-sensitive and -insensitive uptake of phenethylamines into the adrenal chromaffin cell. *J. Neurochem.* **1995,** 65, 2031-2042.

44. Woznichak, M. M.; Overcast, J. D.; Robertson, K.; Neumann, H. M.; May, S. W., Reaction of phenylaminoethyl selenides with peroxynitrite and hydrogen peroxide. *Archives of Biochemistry and Biophysics* **2000,** 379, 314-320.

CHAPTER 2

IDENTIFICATION OF A THIOSELENURANE INTERMEDIATE IN THE REACTION BETWEEN PHENYLAMINOALKYL SELENOXIDES AND GLUTATHIONE

2.1 Introduction

In epidemiological studies, a low concentration of selenium in plasma has been identified as a risk factor for many of the same diseases associated with oxidative stress.[1-6] A number of investigators have suggested that organoselenium compounds capable of propagating a selenium redox cycle might supplement natural cellular defenses against oxidants, and indeed, several organoselenium compounds with antioxidant, anti-hypertensive or anti-cancer activity have been reported.[7-25]

As discussed in chapter 1, a family of novel phenylaminoalkyl selenides has been developed in our laboratory. We have shown that these compounds are potent antioxidants, reacting rapidly with a variety of metabolic oxidants ($ONOO^-$, H_2O_2, etc.), and that they are readily taken up into cells and have low toxicity *in vivo* (mice and rats).[7, 20, 21] Moreover, the selenoxide products generated from the antioxidant activity of these selenides are readily recycled back to the selenide form by cellular reductants such as glutathione (GSH).[9, 20, 22-24, 26, 27] We have also shown that as a consequence of this selenium redox cycling, our compounds protect DNA against damage caused by the reactive cellular oxidant, peroxynitrite (Figure 2.1).[16]

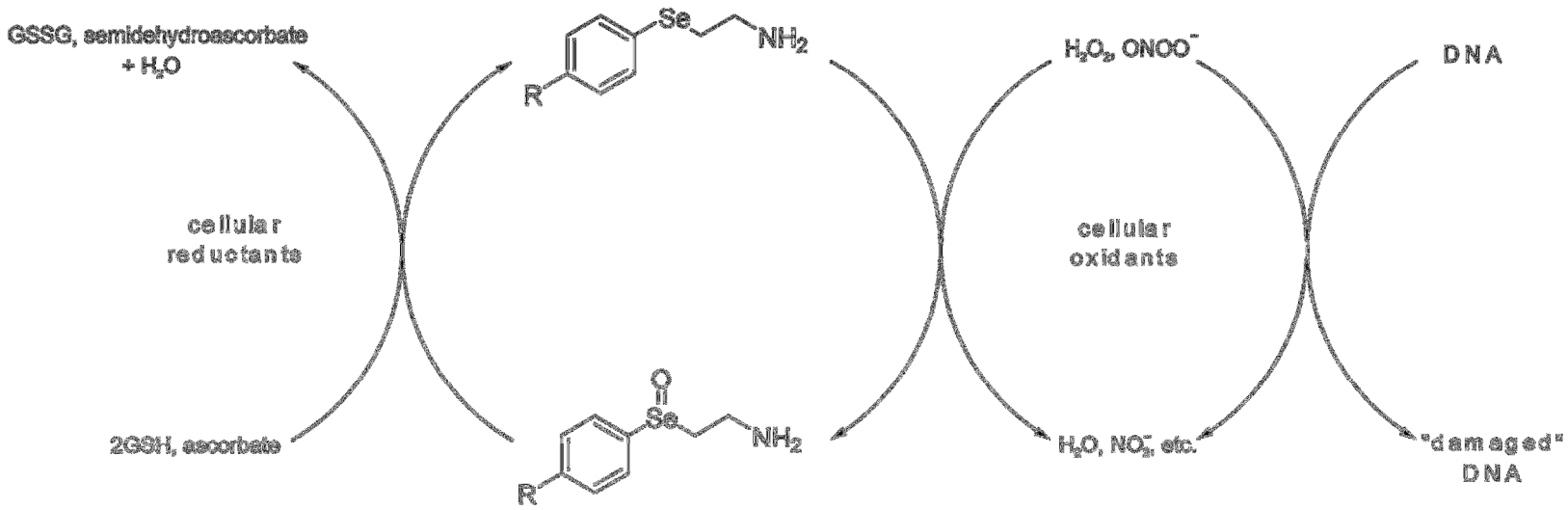

Figure 2.1. Phenylaminoalkyl Selenide Redox Cycle

Among the proposed selenium intermediates in the oxidation-reduction reactions of organoselenium compounds are species such as selenenic and seleninic acids, selenones, spirodioxaselenanonanes and thiolseleninates, Table 1.1.[12, 18, 25, 28-31] Thus, for example, evidence has been reported for formation of a thiolseleninate intermediate in the reactions between Ebselen oxide and certain thiols[30, 32], a spirodioxaselenanonane intermediate in the reaction between di(3-hydroxypropyl) selenide and *tert*-butyl hydroperoxide[12], and a thioselenurane intermediate for the reaction between benzenethiol and a substituted phenyl benzyl selenoxide.[30] The reactivity and instability of some tetra-coordinate selenium compounds, coupled with fast reaction rates for the reactions of organoselenium compounds with oxidants or with reducing agents such as thiols, have made it difficult to clearly characterize thioselenurane-like intermediates.[28, 32-34] We now report evidence from stopped-flow kinetic and mass spectrometry experiments that the oxidation-reduction reaction between phenylaminoalkyl selenoxides and glutathione indeed occurs via a two-step process that entails the intermediacy of a thioselenurane species.

Table 2.1. Common intermediates in redox reactions of organoselenium compounds

Selenium Compounds			Sulfur-Selenium Compounds	
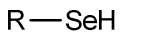 Selenol	 Diselenide	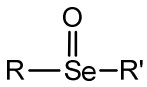 Selenoxide	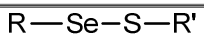 Selenyl sulfide	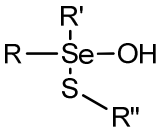 Hydroxythioselenurane
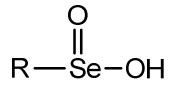 Seleninic acid	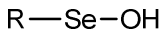 Selenenic acid	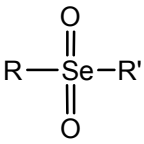 Selenone	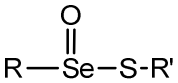 Thioseleninate	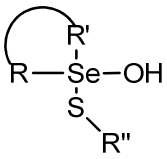 Cyclic Hydroxythioselenurane
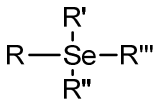 Hydroxyselenurane	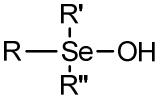 Selenurane		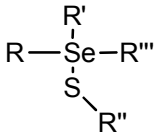 Thioselenurane	

2.2 METHODS AND MATERIALS

2.2.1 Materials All chemicals and solvents were used without further purification as received unless otherwise noted. Reduced and oxidized glutathione (GSH and GSSG), 30% hydrogen peroxide solution (H_2O_2) and manganese dioxide were obtained from Sigma Chemical Co. (St. Louis, MO). Deuterated solvents were purchased from Cambridge Isotope Laboratories, Inc. (Andover, MA). All other chemicals were purchased from standard commercial sources and were of the highest grade available. Allsphere C8 HPLC column was obtained from Alltech (Deerfield, IL).

2.2.2 Synthesis of Phenylaminoethyl Selenides PAESe and PAES were synthesized and characterized by Dr. James E. Colbert as previously reported.[21] Fluorophenylaminoethyl selenide (FPAESe) and chlorophenylaminoethyl selenide (ClPAESe) were prepared and characterized by Dr. Michelle M. Woznichak as reported in the literature.[20]

2.2.3 Synthesis of Phenylaminoalkyl Selenoxides Phenylaminoalkyl selenoxides were synthesized as previously described.[24, 27] Selenides were dissolved in H_2O and reacted with 30% H_2O_2 in a 1:2 molar ratio. The reaction was monitored by HPLC (UV detection at 266nm, Alltech Allsphere Octyl (C8) 5u, 250mmx 4.6 mm; mobile phase: 20% acetonitrile, 0.1% TFA, flow rate 1mL/min). The completed reaction was quenched with the addition of MnO_2, filtered and lyophilized overnight.

2.2.4 Spectrophotometric Experiments The reduction of selenoxides, FPAESeO and ClPAESeO with GSH was investigated on a Hewlett Packard 8453 diode-array spectrophotometer equipped with an HP 89090 temperature-control accessory.

Extinction coefficients were determined by taking the slope of the absorbance of multiple concentrations of selenide or selenoxide.

2.2.5 Stopped-flow Kinetic Experiments Stopped-flow experiments were carried out on an OLIS UV/VIS RSM 1000 rapid-scanning spectrophotometer (Bogart, GA, USA) with 3.16 entrance and exit slits, 600 lines/mm gratings and a Xenon 75 Watt lamp. Syringes and flow cell were thermostated by a Fisher Scientific Isotemp 3016 circulating water bath. A 0.75mL stop volume was used for all experiments. Reactant solutions and buffers were made fresh before each experiment and kept on ice during the course of the experiment. Stock solutions and dilutions of GSH and selenoxides were prepared in buffer. Stopped-flow syringes and flow cell were rinsed thoroughly with distilled water and buffer before collection of data. Syringes were filled with GSH (100-1600μM) and selenoxides (50-1600μM) in 100mM buffers ranging in pH from 1.7 to 9.0. Loaded syringes were allowed to set for 10 minutes in order equilibrate with the temperature of the water in the syringe chamber. Absorbance data were collected from 240-300nm for 3 to 500 seconds. Wavelengths and collection times were adjusted according to concentration, pH and temperature.

2.2.5.1 Olis Global Works Software Olis GlobalWorks software was used to fit the stopped-flow data with a three species A→B→C fast/slow kinetic model. The software uses Singular Value Decomposition (SVD) and Matrix Exponentiation to analyze the three-dimensional data (absorbance data collected with respect to wavelength and time).[35-37] SVD determines the number of species present in the reaction, while Matrix Exponentiation global fitting is used to fit the data with a chosen kinetic model. SVD uses matrices to manage complex 3-dimensional data and to distinguish unique spectral

patterns. The varying patterns are referred to as eigenvectors, because they represent an accumulation of data rather than one specific piece of information. The number of eigenvectors and how they change as a function of time is used to determine the number of components in the reaction and the kinetic trace for these components.

2.2.6 Mass Spectroscopy Positive mode ion electrospray ionization mass spectroscopy (ESI-MS) and tandem ESI mass spectrometry (ESI-MS/MS) experiments were performed on a triple quadrupole tandem mass spectrometer (Micromass Quattro LC) coupled with an Agilent 1100 binary HPLC system. Source and desolvation temperatures were maintained at 100ºC and150ºC respectively for all experiments.

2.2.6.1 Flow Injection Experiments ESI-MS spectra were acquired by 10µL injections of selenoxide solution via an Agilent 1100 autosampler (pump flow rate of 200µL methanol/min) into a continuous stream of a GSH generated by a KD Scientific syringe pump (flow rate of 50µL/min). The two solutions were mixed in a tee located as close to the mass spectrometer source as possible and the LC and syringe pump flow rates, concentration of GSH and selenoxide, and injection volume of selenoxide were all optimized. Optimal voltages for ESI-MS were cone voltage (CV) 20V and capillary energy (CE) 3.5V.

2.2.6.2 Tandem Mass Spectrometry For tandem mass spectrometry (ESI-MS/MS) experiments the reactants were diluted in 50/50 water/acetonitrile with 0.1% formic acid. The same setup used in the ESI-MS experiments was used except 100µL injections of FPAESeO were made at a flow rate of 200 µL/min into a stream of GSH (flow rate 300 µL/min). The mass spectrometer conditions were optimized to achieve the

fragmentation of the precursor ion *m/z* 543. Voltages were optimized to be CV 55V and CE 25V.

2.2.7 77Se NMR Experiments ^{77}Se nuclear magnetic resonance (NMR) spectroscopy experiments were performed on a Bruker DMX 400 NMR spectrometer. Tetramethylsilane (TMS) and dimethyl selenide were used as standards for ^{1}H, ^{13}C and ^{77}Se experiments and methanol was used for temperature calibration. Reactions were carried out at temperatures ranging from -45 to 3°C. Samples were prepared in 80/20 deuterated methanol/ deuterated water and were kept on ice until analysis. Deuterated acetic acid was used in samples where the pH was lowered. A reaction setup that allowed for the constant formation of the intermediate was used. Selenoxide solution was placed in an NMR tube and tubing (O.D. 1/8", I.D. 1/16") cut at a slant was inserted into the NMR tube until it almost touched the bottom of the tube. The tubing allowed for the continuous addition of GSH into the FPAESeO sample via a syringe pump (flow rate 3.5mL/0.5hr) and sample spinning was omitted during experiment.

2.3 RESULTS AND DISCUSSION

2.3.1 Stopped-flow Experiments

Stopped-flow experiments were conducted to determine whether or not a reaction intermediate is kinetically detectable for the reaction between fluorophenylaminoethyl and chlorophenylaminoethyl selenoxides and glutathione. We have previously shown that this is a facile process and the stoichiometry for the overall reaction is one molecule of selenoxide reacting with two molecules of GSH to produce one selenide molecule plus one molecule of GSSG [24]. Supplemental data for stopped-flow experiments was gathered on a Hewlett Packard HP 8453 diode-array spectrophotometer, including expected changes in absorbance for the conversion from selenoxide to selenide (Figure 2.3) and extinction coefficients for selenides and selenoxides.

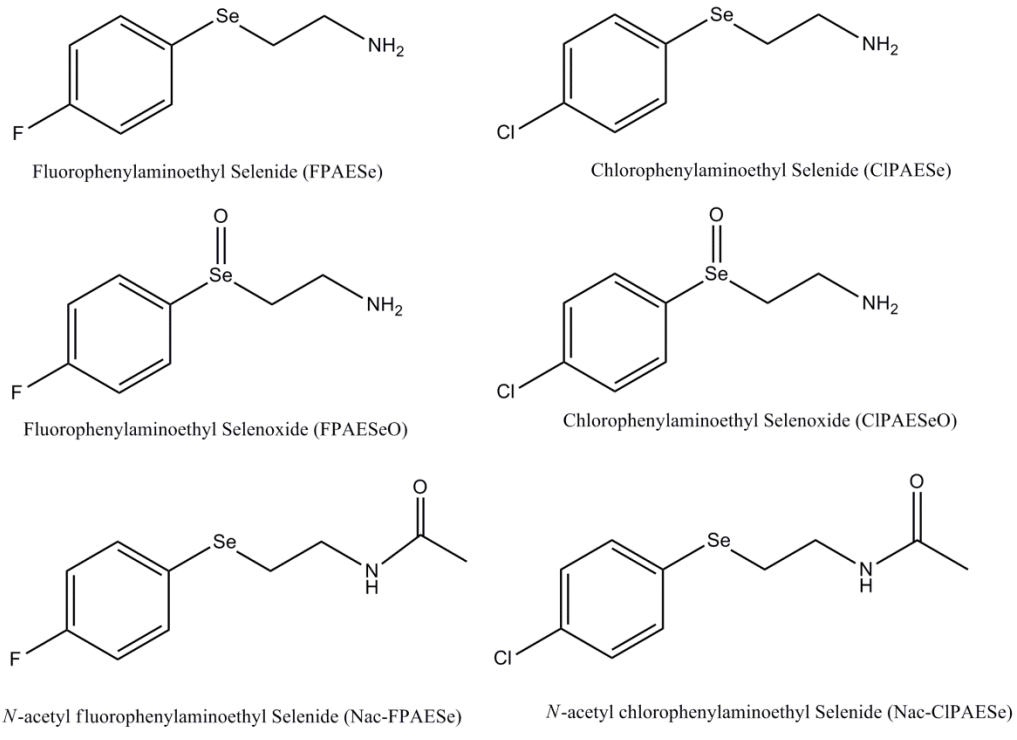

Figure 2.2. Fluorophenylaminoethyl and Chlorophenylaminoethyl Selenides and Selenoxides

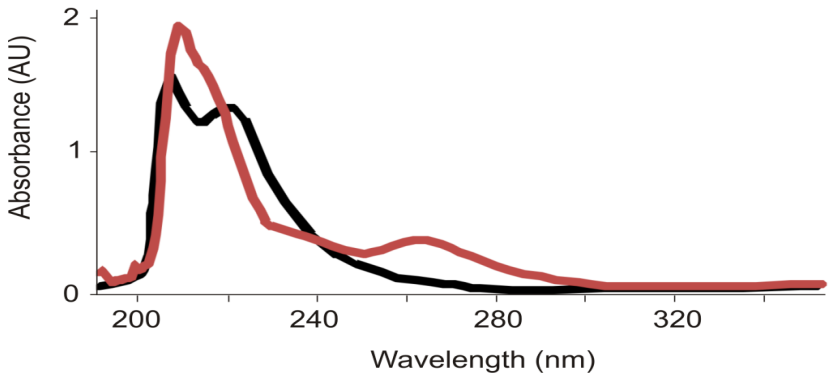

Figure 2.3. ClPAESeO (Black) and ClPAESe (Red) UV Absorbance

Figure 2.4A illustrates typical absorbance changes recorded by the photomultiplier tube detector of the stopped-flow instrument over a 2.6 sec reaction period for the reaction of ClPAESeO with GSH. The overall increase in absorbance in the 262nm region reflects formation of the selenide product, which has a greater extinction coefficient than the selenoxide at this wavelength (5288 $M^{-1}cm^{-1}$ vs. 4134 $M^{-1}cm^{-1}$). Control experiments confirmed that, as expected, no reaction is detectable when either GSSG and ClPAESeO or GSH and ClPAESe are mixed in the stopped-flow instrument.

Figure 2.4B illustrates the results obtained when Olis GlobalWorks software was used to fit the raw data to a three species A → B → C fast/slow kinetic model. This software uses Singular Value Decomposition (SVD) and Matrix Exponentiation to analyze the three-dimensional stopped-flow data (absorbance data collected with respect to wavelength and time). [35-37] Traces A and C are kinetic traces of the eigenvectors for the selenoxide substrate and the selenide product, respectively. Formation, buildup and decomposition of a reaction intermediate are clearly evident as seen in the kinetic trace of eigenvector B.

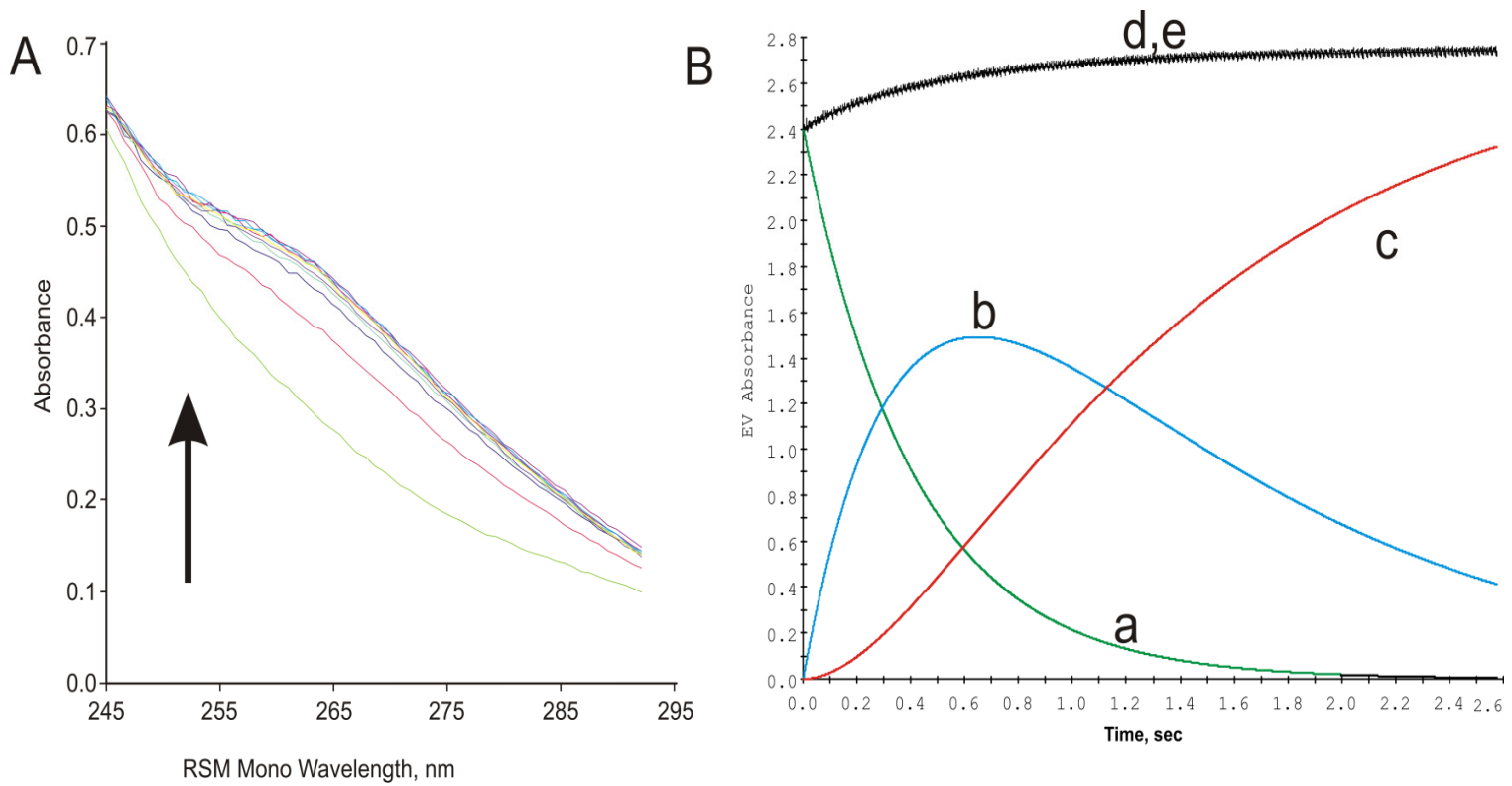

Figure 2.4. Stopped-flow spectra of the oxidation of glutathione by ClPAESeO. A) Raw absorbance data collected. B) GlobalWorks calculated (a) decrease of reactant selenoxide, (b) build-up and decomposition of the intermediate, and (c) increase of selenide product. (d and e) The GlobalWorks results of the calculated data (d) and the sum of the eigenvectors (e).

Traces A and C are kinetic traces of the eigenvectors for the selenoxide substrate and the selenide product, respectively. Formation, buildup and decomposition of a reaction intermediate are clearly evident as seen in the kinetic trace of eigenvector B. Traces D and E are the sum of the eigenvector absorbances and the predicted results from the chosen model, respectively. The excellent overlay of these traces and the equal randomness of the residuals (Figure 2.5) indicate that the kinetic model chosen is appropriate for the data. Several two and three species models within Olis GlobalWorks software were tried, but based on the criteria discussed by Matheson, Parkhurst, and DeSa [35-37], none of the other models gave a good fit to the kinetic data set. The second order rate constants calculated by Olis GlobalWorks for intermediate formation and decomposition at 10˚C were 4010 and 1120 $M^{-1}s^{-1}$ for FPAESeO (pH 7.0), and 5844 and 1412 $M^{-1}s^{-1}$ for ClPAESeO (pH 7.5), respectively.

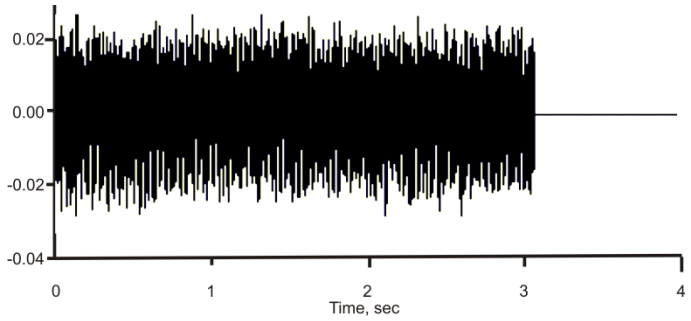

Figure 2.5. GlobalWorks residuals from oxidation of GSH with ClPAESeO.

A reaction scheme consistent with these kinetic results is shown in Figure 2.6. As shown, initial attack of a thiolate on a selenoxide moiety should generate a thioselenurane adduct. Subsequent reaction with a molecule of GSH would then produce the final

products, GSSG and selenide. This reaction scheme is consistent with our stoichiometry results and the stopped-flow kinetic data indicate that the rate of formation of the intermediate is approximately 4-fold faster than its decomposition under our reaction conditions. We therefore reasoned that it might be possible to obtain direct structural confirmation that the intermediate suggested by our kinetic results is indeed the thioselenurane.

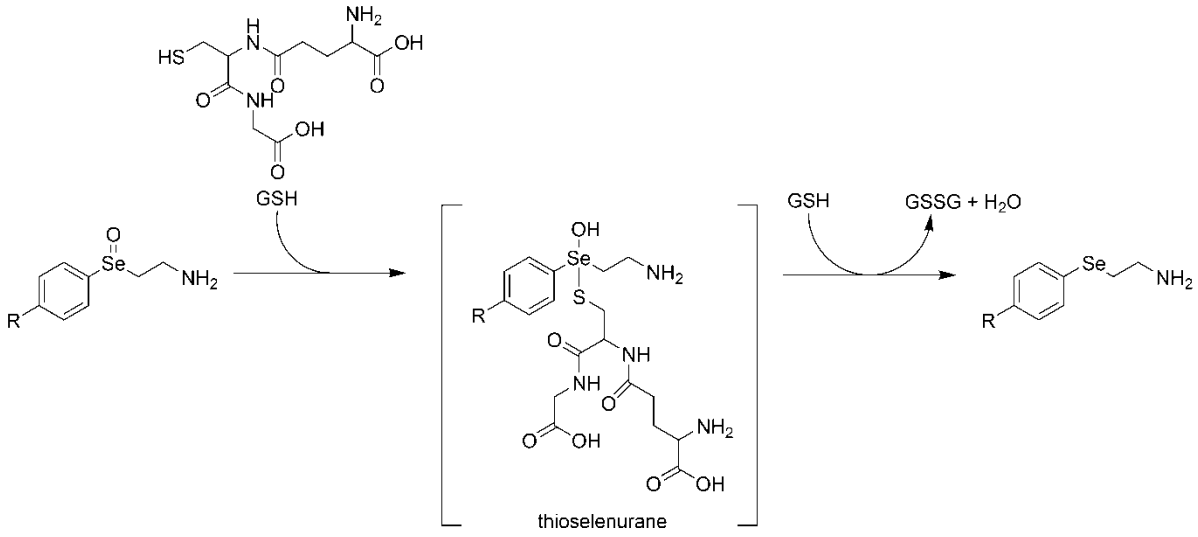

Figure 2.6. Reduction of selenoxide with glutathione showing the thioselenurane intermediate.

2.3.2 ^{77}Se NMR

Kumakura *et al* .[34] and Haenen *et al.* [38] were unsuccessful in attempts to use NMR to visualize and characterize thioselenurane-like intermediates in the reaction between selenoxides and thiols. Nevertheless, we attempted to detect the putative thioselenurane intermediate through the use of ^{77}Se, ^{1}H, and ^{13}C NMR. These experiments were carried out at various temperatures between -25°C and room temperature using an experimental

setup designed to allow for constant formation of the intermediate, thereby increasing the likelihood of its detection by NMR. As demonstrated in Figure 2.7, we observed a kinetic decrease in selenoxide (871.16 ppm) and increase in selenide (254.66 ppm), but were unable to detect any other selenium-containing species. Our results are therefore consistent with the previous reports by Kumakura *et al.*[34], Glass *et al.*[39], and Haenen *et al.*[38]who were also unable to detect intermediates in reactions between selenoxides and thiols via NMR.

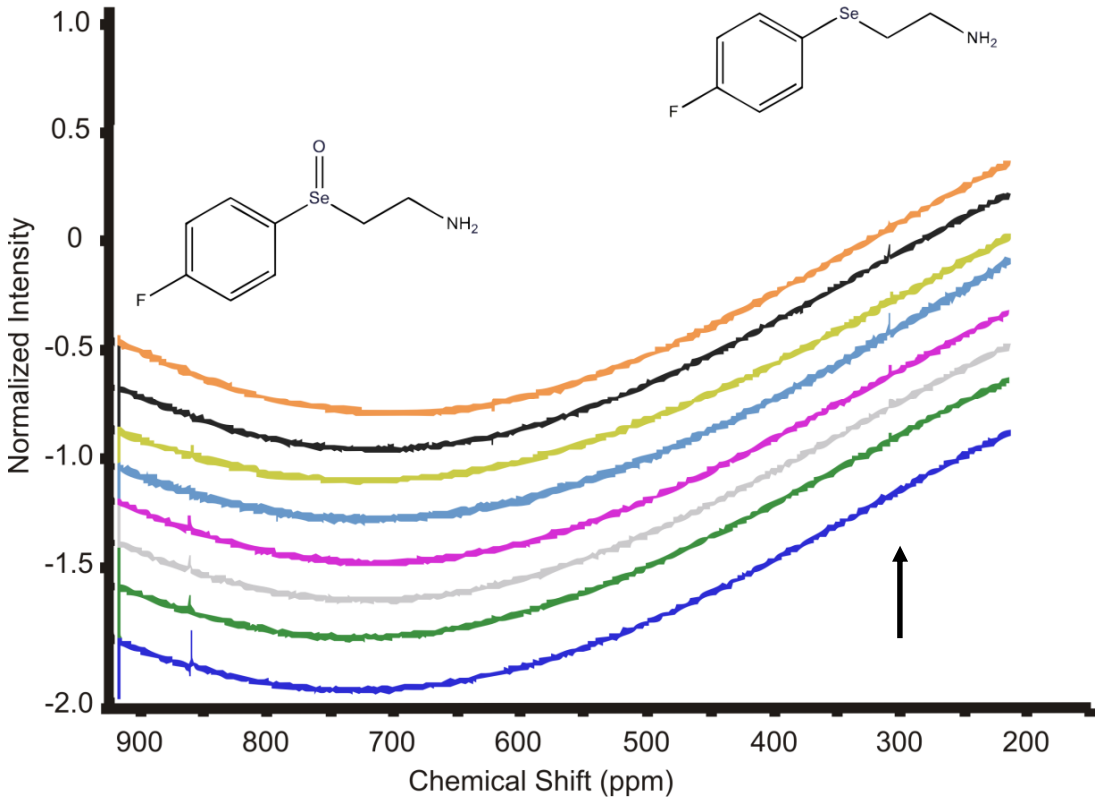

Figure 2.7. Stacked ^{77}Se NMR showing decrease of selenoxide and increase of selenide, arrow indicates an increase in time.

2.3.3 Tandem Mass Spectrometry

An alternative approach is exemplified by the work of Santos [40], Greip-Raming *et al*. [41], and many others who have successfully used ESI-MS and ESI-MS/MS for the detection of short-lived reaction intermediates in solution. Among the advantages of this approach are the mild formation of ions in ESI and the high sensitivity of mass spectrometry [40, 42-44]. Generally, intermediates have been studied using ESI-MS through one of two major techniques; the first of these is "ion-fishing", in which intermediates are transferred to the gas phase and then trapped with a charge-labeled compound [41, 45, 46]. The second technique entails the mixing of two or more reactants via a microreactor before the ions enter the ionization source; this latter technique was utilized here to monitor the reaction between selenoxides and GSH [46, 47]. Injections of selenoxide were made, via a liquid chromatography pump, into a continuous stream of GSH, created by a syringe pump, immediately before entering the ESI source.

An additional aspect of ESI-MS is that certain elements can be identified based on their isotope patterns. Selenium has six naturally occurring isotopes, ^{74}Se 0.89%, ^{76}Se 9.37%, ^{77}Se 7.63%, ^{78}Se 23.77%, ^{80}Se 49.61% and ^{82}Se 8.73%; the most abundant of these is ^{80}Se. This creates a very distinct isotopic pattern and makes any selenium-containing species easily distinguishable in the mass spectrum of a complex mixture. Figure 2.8 shows a series of ESI-MS spectra obtained for the reaction between ClPAESeO and GSH (Panels A, B and C) and between FPAESeO and GSH (Panels D, E and F). The spectrum from 300 to 620 *m/z* for the ClPAESeO reaction is shown in panel A. Peaks for GSH ($[M+H]^+$ *m/z* 307.9), GSSG ($[M+H]^+$ *m/z* 614.9), and proton-bound dimers of selenium-containing compounds ($[2M+H]^+$ *m/z* 449.7 and 502.7) are present. Additionally, a peak

arising from a selenium species is observed at *m/z* 559. This peak was not observed when either GSH or the selenoxide was omitted from the reactions, demonstrating that the formation of the ion at *m/z* 559 only occurs when both selenoxide and GSH are present. Similar results were obtained for the reaction between FPAESeO and GSH (Panels D, E and F), with a new selenium-containing peak appearing at *m/z* 43.

It is evident by the isotopic pattern of the intermediate *m/z* 559 and *m/z* 543 ions (Panels B and E) that selenium is indeed present in the intermediate. The comparison of the intermediate peaks with the theoretical isotope modeling (MassLynx NT) of the proposed intermediates is shown in panels B and C (ClPAESeO reaction intermediate) and panels E and F (FPAESeO reaction intermediate). As seen in these panels, the masses and isotope pattern of the experimental and theoretical spectra are in excellent agreement. These results provide initial evidence that the intermediate formed in the reaction of the phenylaminoalkyl selenoxides and GSH is indeed a selenium-containing species, which corresponds to the molecular mass of the thioselenurane intermediate previously shown in Figure 2.6.

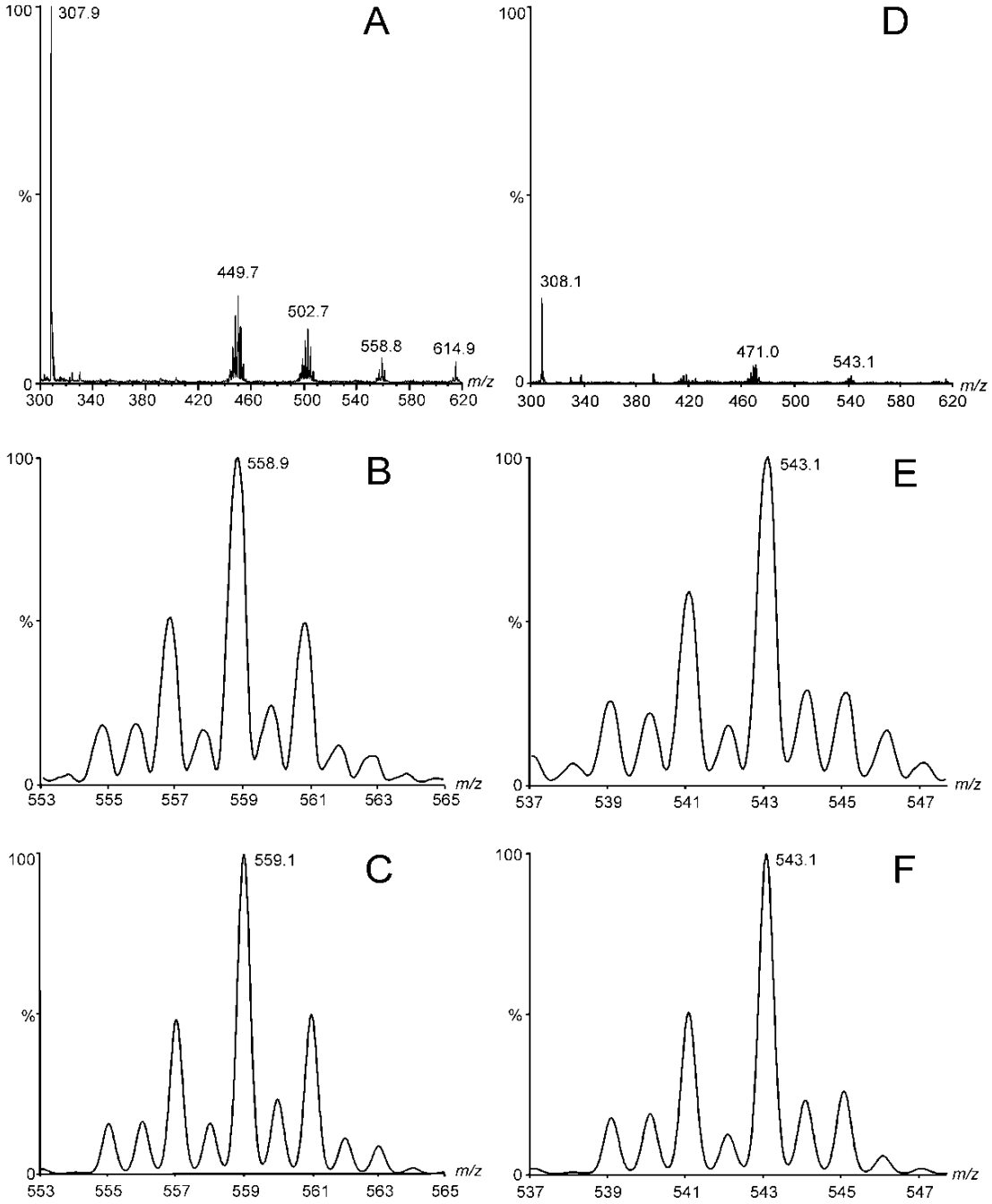

Figure 2.8. Mass spectroscopy of the reaction between phenylaminoethyl selenides and GSH. (A) ESI (+) mass spectrum of the reaction between ClPAESeO and GSH. (B) ESI (+) experimental mass spectrum for 559 *m/z*. (C) Theoretical isotope model of thioselenurane intermediate ($[M+H]^+$ $C_{18}H_{28}ClN_4O_7SSe$). (D) ESI (+) mass spectrum of the reaction between FPAESeO and GSH. (E) ESI (+) experimental mass spectrum for 534 *m/z*. (C) Theoretical isotope model of thioselenurane intermediate ($[M+H]^+$ $C_{18}H_{28}FN_4O_7SSe$).

Flow injection ESI-MS/MS experiments were carried out in order to obtain further characterization of the intermediate. As seen in Figure 2.9, product ion scans of the thioselenurane intermediate present in the reaction between FPAESe and GSH (*m/z* 543 cation) resulted in daughter ions of glutathione ($[M+H]^+$, *m/z* 308) and selenoxide ($[M+H]^+$, FPAESeO *m/z* 236). The observed daughter ions agree with the expected fragmentation pathways for the thioselenurane intermediate (Figure 2.10). The two observed peaks of equal intensity observed in Figure 2.8 can be explained by the ability of both fragments to stabilize the charge and Stevenson's rule, which states that the charge will remain on the fragment with the lower ionization energy [48]

The results reported here provide, to our knowledge, the first evidence for the intermediacy of a thioselenurane species in the reaction of a thiol with a selenoxide. As evidenced by stopped-flow kinetic data, a rapid and stoichiometric initial reaction of either fluoro- or chlorophenylaminoethyl selenoxide with GSH generates a kinetically-detectable intermediate, and a subsequent slower reaction of this intermediate with a second molecule of GSH produces the final selenide and GSSG products. Flow injection ESI-MS experiments confirmed that the reaction intermediate is indeed a selenium-containing species with a molecular mass and selenium isotopic pattern corresponding to that of the thioselenurane that would be produced by attack of GSH on a phenylaminoalkyl selenoxide. Final structural characterization of the thioselenurane intermediate was obtained from analysis of the daughter ions produced in flow injection ESI-MS/MS experiments.

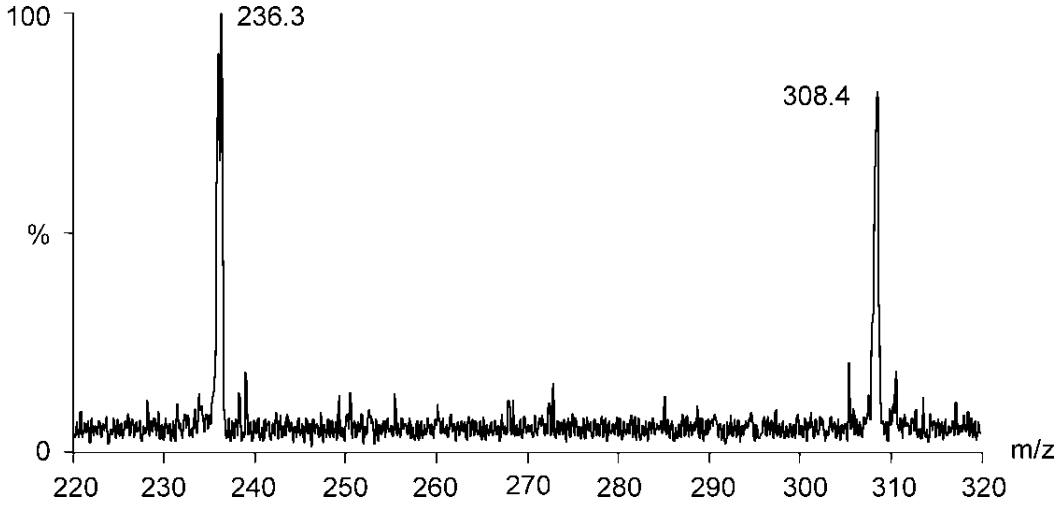

Figure 2.9. ESI-MS/MS results showing the daughter peaks for the 543 *m/z* ion

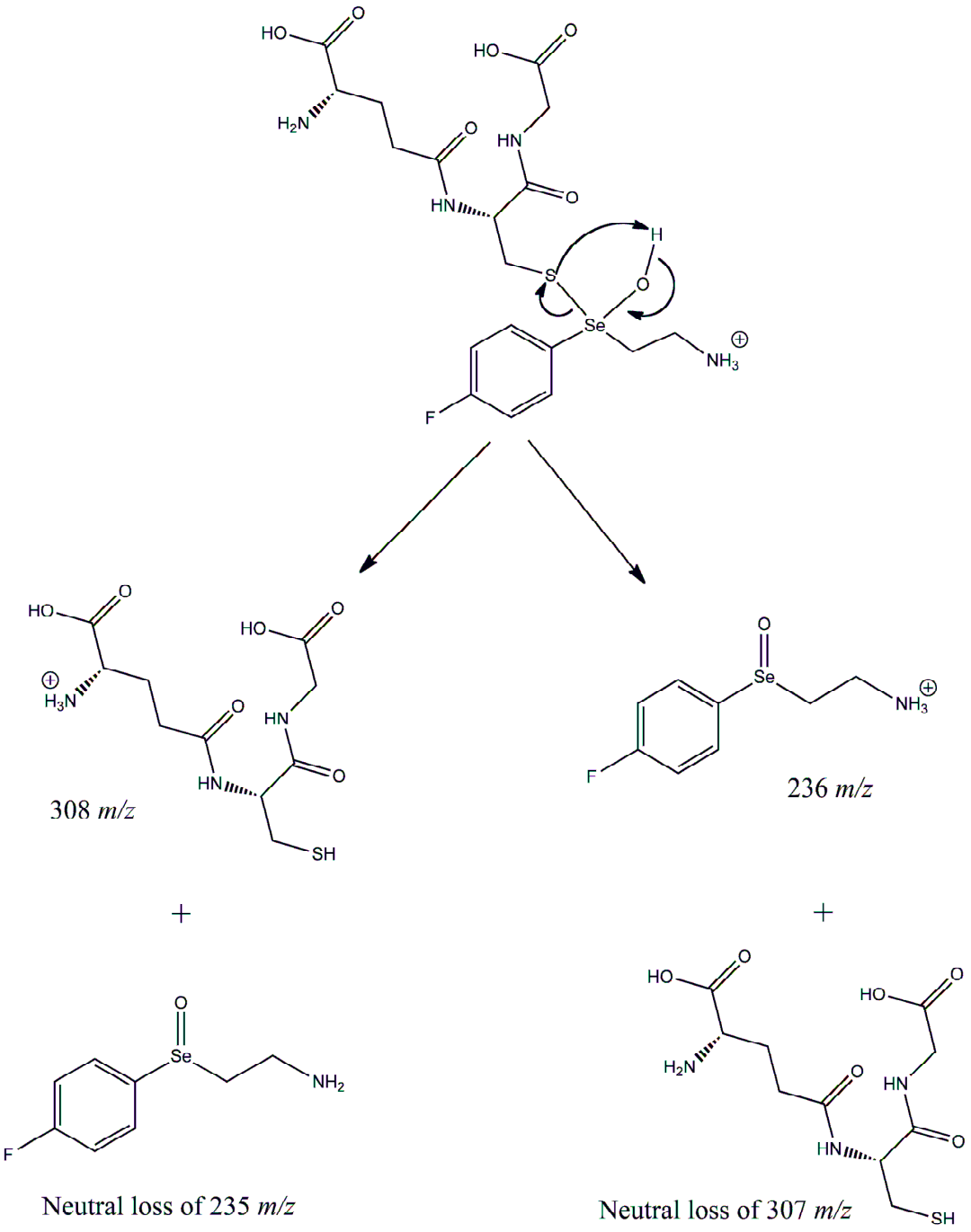

Figure 2.10. Fragmentation pathways of the thioselenurane intermediate showing ionized and neutral loss products.

2.4 Conclusions

Over the years, a number of investigators have proposed the formation of intermediates in the reaction of selenoxides with reducing agents. In 1978, Kice and Lee [28] detected the presence of an intermediate via UV absorption in the reaction between benzeneseleninic acid and 1-butanethiol or 2-methyl-2-propanethiol. Because of instability of this intermediate, the authors were unable to obtain structural information confirming its structure. However, they suggested it might be either a thioseleninate or a thioselenurane, with the more likely possibility being the former. Kumar *et al.* [30] proposed the formation of a thioselenurane in the reaction between benzenethiol and a substituted phenyl benzyl selenoxide. They were unable to obtain any structural evidence for this species, but did observe, via ESI-MS, a cyclization product that could arise from this proposed intermediate. The authors also acknowledged the possibility of an alternative pathway of direct formation of the cyclic product that does not proceed via the thioselenurane intermediate. Very recently, Kumakura *et al*. proposed the possible intermediacy of a thioselenurane in the reaction of *trans*-3,4-dihydroxyselenoxolane with thiols, but were unable to obtain any evidence for formation of this species [34]. Turning to Ebselen oxide, Fischer and Dereu [33] first proposed that the reaction between Ebselen oxide and benzylmercaptan might proceed via the initial formation of a transient cyclic thioselenurane intermediate, whereas a thioseleninate intermediate was observed by Kumar *et al*. in the reaction of Ebselen oxide and benzenethiol using ESI-MS [30]. However, to our knowledge, actual evidence for the intermediacy of a thioselenurane species in any of these systems has never been reported.

We have previously shown that phenylaminoalkyl selenides react stoichiometrically with hydrogen peroxide and peroxynitrite, and that the resulting selenoxide products are readily recycled back to the corresponding selenides by cellular reductants such as GSH [7-9, 21, 24]. We have further demonstrated that these phenylaminoalkyl selenides protect DNA against peroxynitrite-induced damage, and that GSH-mediated redox cycling results in enhanced protection of DNA against peroxynitrite-induced damage [16]. The results reported here elucidate the chemical nature of this redox cycling process, and demonstrate that redox cycling of phenylaminoalkyl selenides is an efficient cycle consisting of a rapid two-step process with initial formation of a thioselenurane intermediate followed by complete regeneration of the original selenide. This contrasts sharply to the complicated redox cycle of the well-studied organoselenium compound, Ebselen, which consists of multiple reaction pathways with several intermediates and byproducts [12, 13, 18, 25]. Recent investigations have shown that Ebselen is an inefficient catalyst due to deactivating pathways, where unreactive intermediates hinder the regeneration of the original compound [18, 40, 49, 50]. Thus, the results reported here enhance the attractiveness of phenylaminoalkyl selenides as potential agents for supplementing cellular defenses against reactive oxygen species.

2.5 REFERENCES

1. Brenneisen, P.; Steinbrenner, H.; Sies, H., Selenium, oxidative stress, and health aspects. *Molecular Aspects of Medicine* **2005,** 26, (4-5), 256-267.

2. Beck, M. A.; Shi, Q.; Morris, V. C.; Levander, O. A., Rapid genomic evolution of a non-virulent Coxsackievirus B3 in selenium-deficient mice results in selection of identical virulent isolates. *Nature Medicine* **1995,** 1, 433-436.

3. Baum, M. K.; Shor-Posner, G.; Lai, S. H.; Zhang, G. Y.; Fletcher, M. A.; Sauberlich, H.; Page, J. B., High risk of HIV-related mortality is associated with selenium deficiency. *Journal of Acquired Immune Deficiency Syndromes and Human Retrovirology* **1997,** 15, 370-374.

4. Clark, L. C.; Combs, G. F.; Turnbull, B. W.; Slate, E. H.; Chalker, D. K.; Chow, J.; Davis, L. S.; Glover, R. A.; Graham, G. F.; Gross, E. G.; Krongrad, A.; Lesher, J. L.; Park, K.; Sanders, B. B.; Smith, C. L.; J., T. R., Effects of selenium supplementation for cancer prevention in patients with carcinoma of the skin. *Journal of the American Medical Association* **1996,** 276, 1957-1963.

5. Duntas, L. H., Selenium and inflammation: underlying anti-inflammatory mechanisms. *Hormone and Metabolic Research* **2009,** 41, 443-447.

6. Micke, O.; Schomburg, L.; Buentzel, J.; Kisters, K.; Meuecke, R., Selenium in oncology: from chemistry to clinics. *Molecules* **2009,** 14, 3975-3988.

7. May, S. W., Selenium-based drug design: rationale and therapeutic potential. *Expert Opinion on Investigational Drugs* **1999,** 8, 1017-1030.

8. May, S. W., Selenium-based pharmacological agents: an update. *Expert Opinion on Investigational Drugs* **2002,** 11, 1261-1269.

9. May, S. W.; Pollock, S. H., Selenium-based antihypertensives. Rationale and potential. *Drugs* **1998,** 56, 959-964.

10. Klotz, L. O.; Sies, H., Defenses against peroxynitrite: selenocompounds and flavonoids. *Toxicology Letters* **2003,** 140-141, (125-132), 125.

11. Alberto, E. E.; Soares, L. C.; Sudati, J. H.; Borges, A. C. A.; Rocha, J. B. T.; Braga, A. L., Efficient synthesis of modular amino acid derivatives containing selenium with pronounced GPx-like activity. *European Journal of Organic Chemistry* **2009**, 4211-4214.

12. Back, T. G.; Moussa, Z.; Parvez, M., The exceptional glutathione peroxidase-like activity of di(3-hydroxypropyl) selenide and the unexpected role of a novel spirodioxaselenanonane intermediate in the catalytic cycle. *Angewandte Chemie International Edition* **2004,** 43, 1268-1270.

13. Kunwar, A.; Mishra, B.; Barik, A.; Kumbhare, L. B.; Pandey, R.; Jain, V. K.; Priyadarsini, K. I., 3,3'-Diselenodipropionic acid, an efficient peroxyl radical scavenger and a GPx mimic, protects erythrocytes (RBCs) from AAPH-induced hemolysis. *Chemical Research in Toxicology* **2007,** 20, 1482-1487.

14. Mugesh, G.; Panda, A.; Singh, H. B.; Punekar, N. S.; Butcher, R. J., Glutathione peroxidase-like antioxidant activity of diaryl diselenides: a mechanistic study. *Journal of the American Chemical Society* **2001,** 123, 839-850.

15. Wilson, S. R.; Zucker, P. A.; Huang, R.-R. C.; Spector, A., Development of synthetic compounds with glutathione peroxidase activity. *Journal of the American Chemical Society* **1989,** 111, 5936-5939.

16. De Silva, V.; Woznichak, M. M.; Burns, K. L.; Grant, K. B.; May, S. W., Selenium redox cycling in the protective effects of organoselenides against oxidant-induced DNA damage. *Journal of the American Chemical Society* **2004,** 126, 2409-2413.

17. Pearson, J. K.; Boyd, R. J., Density functional theory study of the reaction mechanism and energetics of the reduction of hydrogen peroxide by Ebselen, Ebselen diselenide, and Ebselen selenol. *Journal of Physical Chemistry* **2007,** 111, 3152-3160.

18. Sarma, B. K.; Mugesh, G., Antioxidant activity of the anti-inflammatory compound Ebselen: a reversible cyclization pathway via selenenic and seleninic acid intermediates. *Chemical European Journal* **2008,** 14, 10603-10614.

19. Zhao, R.; Holmgren, A., A novel antioxidant mechanism of Ebselen involving Ebselen diselenide, a substrate of mammalian thioredoxin and thioredoxin reductase. *Journal of Biological Chemistry* **2002,** 277, 39456-39462.

20. May, S. W.; Wang, L. Q.; Gill-Woznichak, M. M.; Browner, R. F.; Ogonowski, A. A.; Smith, J. B.; Pollock, S. H., An orally active selenium-based antihypertensive agent with restricted CNS permeability. *Journal of Pharmacology and Experimental Therapeutics* **1997,** 283, 470-477.

21. May, S. W.; Herman, H. H.; Roberts, S. F.; Ciccarello, M. C., Ascorbate depletion as a consequence of product recycling during dopamine beta-monooxygenase catalyzed selenoxidation. *Biochemistry* **1987,** 26, 1626-1633.

22. Overcast, J. D.; Ensley, A. E.; Buccafusco, C. J.; Cundy, C.; Broadnax, R. A.; He, S. Q.; Yoganathan, A. P.; Pollock, S. H.; Hartley, C. J.; May, S. W., Evaluation of cardiovascular parameters of a selenium-based antihypertensive using pulsed Doppler ultrasound. *Journal of Cardiovascular Pharmacology* **2001,** 38, 337-346.

23. Pollock, S. H.; Herman, H. H.; Fowler, L. C.; Edwards, A. S.; Evans, C. O.; May, S. W., Demonstration of the antihypertensive activity of phenyl-2-aminoethyl selenide. *Journal of Pharmacology and Experimental Therapeutics* **1988,** 246, 227-234.

24. Woznichak, M. M.; Overcast, J. D.; Robertson, K.; Neumann, H. M.; May, S. W., Reaction of phenylaminoethyl selenides with peroxynitrite and hydrogen peroxide. *Archives of Biochemistry and Biophysics* **2000,** 379, 314-320.

25. Back, T. G.; Moussa, Z., Diselenides and allyl selenides as glutathione peroxidase mimetics. Remarkable activity of cyclic seleninates produced *in situ* by the oxidation of allyl ω-hydroxyalkyl selenides. *Journal of the American Chemical Society* **2003,** 125, 13455-13460.

26. Woznichak, M. M.; Ogonowski, A. A.; Wang, L.; Overcast, J. D.; Smith, J. B.; Browner, R. F.; Pollock, S. H.; May, S. W., Biochemistry and pharmacology of novel selenium compounds. *FASEB Journal* **1997,** 11, A1153-A1153.

27. May, S. W.; Herman, H. H.; Pollock, S., H.; Fowler, L. C.; Wimalasena, K.; Ciccarello, M. C., Antihypertensive activity and ascorbate depletion via product recycling by DBM-targeted selenides. *Federation Proceedings* **1987,** 46, 1940-1940.

28. Kice, J. L.; Lee, T. W., Oxidation-reduction reactions of organoselenium compounds. 1. Mechanism of the reaction between seleninic acids and thiols. *Journal of the American Chemical Society* **1978,** 100, 5094-5102.

29. Ritchey, J. A.; Davis, B. M.; Pleban, P. A.; Bayse, C. A., Experimental and theoretical evidence for cyclic selenurane formation during selenomethionine oxidation. *Organic and Biomolecular Chemistry* **2005,** 3, 4337-4342.

30. Kumar, S.; Singh, H. B.; Wolmershauser, G., Protection against peroxynitrite-mediated nitration reaction by intramolecularly coordinated diorganoselenides. *Organometallics* **2006,** 25, 382-393.

31. Chen, G.-P.; Ziegler, D. M., Liver microsome and flavin-containing monooxygenase catalyzed oxidation of organic selenium compounds. *Archives of Biochemistry and Biophysics* **1994,** 312, 566-572.

32. Reich, H. J.; Jasperse, C. P., Organoselenium chemistry. Redox cheimstry of selenocysteine model systems. *Journal of the American Chemical Society* **1987,** 109, 5549-5551.

33. Fischer, H.; Dereu, N., Mechanism of the catalytic reduction of hydroperoxides by ebselen: a selenium-77 NMR study. *Bulletin des Societes Chimiques Belges* **1987,** 96, 757-769.

34. Kumakura, F.; Mishra, B.; Priyadarsini, K. I.; Iwaoka, M., A water-soluble cyclic selenide with enhanced glutathione peroxidase-like catalytic activities. *European Journal of Organic Chemistry* **2010**, 440-445.

35. DeSa, R. J.; Matheson, I. B. C., A practical approach to interpretation of singular value decomposition results. *Methods in Enzymology* **2004,** 384, 1-8.

36. Matheson, I. B. C.; Parkhurst, L. J.; DeSa, R. J., Efficient integration of kinetic differential equation sets using matrix exponentiation. *Methods in Enzymology* **2004,** 384, 18-39.

37. Matheson, I. B. C., Large reduction in singular value decomposition calculation time using Savitzsky-Golay data precompression. *Methods in Enzymology* **2004,** 384, 9-17.

38. Haenen, G. R. M. M.; De Rooij, B. M.; Vermeulen, N. P. E.; Bast, A., Mechanism of the reaction of Ebselen and endogenous thiols: Dihydrolipoate is a better cofactor than glutathione in the peroxidase activity of Ebselen. *Molecular Pharmacology* **1990,** 37, 412-422.

39. Glass, R. S.; Farooqui, F.; Sabahi, M.; Ehler, K., Formation of thiocarbonyl compounds in the reaction of Ebselen oxide with thiols. *Journal of Organic Chemistry* **1989,** 54, 1092-1097.

40. Santos, L. S.; Knaack, L.; Metzger, J. O., Investigation of chemical reactions in solution using API-MS. *International Journal of Mass Spectrometry* **2005,** 246, 84-104.

41. Griep-Raming, J.; Meyer, S.; Bruhn, T.; Metzger, J. O., Investigation of reactive intermediates of chemical reactions in solutions by electrospray ionization mass spectrometry: radical chain reactions. *Angewandte Chemie International Edition* **2002,** 41, 2738-2741.

42. Eberlin, M. N., Electrospray ionization mass spectrometry: a major tool to investigate reaction mechanisms in both solution and the gas phase. *European Journal of Mass Spectrometry* **2007,** 13, 19-28.

43. Cui, S.-Y.; Jin, H.; Kim, S.-J.; Kumar, A. P.; Lee, Y.-I., Interaction of glutathione and sodium selenite *in vitro* investigated by electrospray ionization tandem mass spectrometry. *Journal of Biochemistry* **2008,** 143, 685-693.

44. Regazzoni, L.; Panusa, A.; Yeum, K.-J.; Carini, M.; Aldini, G., Hemoglobin glutathionylation can occur through cysteine sulfenic acid intermediate: electrospray ionization LQT-Orbitrap hybrid mass spectrometry studies. *Journal of Chromatography B* **2009,** 877, 34565-3461.

45. Adlhart, C.; Chen, P., Fishing for catalysts: mechanism-based probes for active species in solution. *Helvetica Chimica Acta* **2000,** 83, 2192-2196.

46. Meyer, S.; Metzger, J. O., Use of electrospray ionization mass spectrometry for the investigation of radical cation chain reactions in solution: detection of transient radical cations. *Analytical and Bioanalytical Chemistry* **2003,** 377, 1108-1114.

47. Sam, J. W.; Tang, X.-J.; Magliozzo, R. S.; Peisach, J., Electrospray mass spectrometry of iron Bleomycin II: investigation of the reaction of Fe(III)-Bleomycin with iodosylbenzene. *Journal of the American Chemical Society* **1995,** 117, 1012-1018.

48. Gross, J. H., *Mass Spectrometry. A textbook*. Springer-Verlag: Berlin, 2004.

49. Sarma, B. K.; Mugesh, G., Glutathione peroxidase (GPx)-like antioxidant activity of the organoselenium drug Ebselen: Unexpected complications with thiol exchange reactions. *Journal of the American Chemical Society* **2005,** 127, 11477-11485.

50. Davies, R.; Bartholomeusz, D. A.; Andrade, J., Personal sensors for the diagnosis and management of metabolic disorders. *IEEE Eng. Med. Biol. Mag.* **2003**, 32-42.

CHAPTER 3

INVESTIGATIONS INTO THE THERAPEUTIC ANTIOXIDANT PROPERTIES OF PHENYLAMINOETHYL SELENIDES AND THEIR ENCAPSULATION IN NANOCARRIERS

3.1 Introduction

Hydrogen peroxide (H_2O_2) is the product of superoxide ($O_2^{\cdot-}$) degradation via superoxide dismutases (SOD) or spontaneous breakdown. H_2O_2 originates endogenously from a variety of enzymes (*i.e.*oxidases). Being a small, stable, molecule capable of diffusing through cellular membranes, gives H_2O_2 the characteristics needed to be a highly effective signaling molecule.[1-4] At low concentrations, H_2O_2, is capable of inhibiting many proteins through the oxidation of unprotonated cysteine residues and Fe^{+2} cofactors (*i.e.,* phosphatases, caspases, and transcription factors). Reversible oxidation of target molecules via H_2O_2 has been linked to phosphatase activity, gene transcription, epidermal growth factor, and insulin signaling, inflammation, etc.[5-9]

Although at low concentrations, H_2O_2 acts as a signaling molecule, at high concentrations this small molecule becomes cytotoxic and is well known to induce DNA and cellular membrane damage, eventually leading to apoptosis.[10, 11] Furthermore, in the presence of metals such as iron and copper, H_2O_2, is converted to more reactive ROS through Fenton chemistry. The simplest form of the Fenton reaction, in which hydroxyl radicals are formed from ferrous iron and H_2O_2, can be written as a two-step process (Equations 1 and 2). In the literature, there is a continuous debate on whether the product of the Fenton reaction is the free hydroxyl radical (shown in Equation 2), a bound

"crypto" radical or a ferryl species.[4, 12-16] Because of this controversy, there are two additional alternatives to step 1 of the Fenton reaction (Equations 1a and b).[4, 17] The damage created by the overproduction of H_2O_2 and other ROS, either generated secondarily from H_2O_2 or created by other cellular processes, is referred to as oxidative stress and has been linked to pathologies such as cancers, cardiovascular disorders, hypertension, Alzheimer's and other related neurodegenerative diseases.[9, 18-22]

$$Fe^{+2} + H_2O_2 \rightarrow Fe^{+3} + OH^- + OH^{\cdot} \quad (1)$$

$$Fe^{+3} + H_2O_2 \leftrightarrow Fe^{+2} + OOH^{\cdot} + H^+ \quad (2)$$

$$Fe^{+2} + H_2O_2 \rightarrow (Fe-OH)^{\cdot} + OH^- \quad (1a)$$

$$Fe^{+2} + H_2O_2 \rightarrow Fe(IV)O^{+2\cdot} + H_2O \quad (1b)$$

As mentioned in chapter 1, selenium is an essential trace element involved in many aspects of cellular defenses, homeostasis, and cell cycle progression. Selenium serves as a redox center for several classes of enzymes, many of which play critical antioxidant roles in carrying out reduction of cellular oxidants and regeneration of cellular reductants. In epidemiological studies, a low concentration of selenium in plasma has been identified as a risk factor for many diseases associated with oxidative stress.[23-28] In response to these findings, many organoselenium compounds have been synthesized and several have been shown to possess antioxidant, antihypertensive, and anti-cancer properties.[29-45]

The phenylaminoalkyl selenides developed in our laboratory have been shown to

possess antioxidant and antihypertensive properties. Phenylaminoalkyl selenides are readily taken up into cells and have low toxicity *in vivo* (mice and rats) [34, 36, 38]. Moreover, the selenoxide products generated from the antioxidant activity of these selenides is readily recycled back to the selenide form by cellular reductants such as glutathione (GSH).[37, 38, 40, 41, 44, 46, 47]. We have also shown that as a consequence of this selenium redox cycling, our compounds protect DNA against damage caused by the reactive cellular oxidant, peroxynitrite [31].

Substantial effort has been dedicated to developing "nanomedicines" as methods of delivering low molecular weight molecules and macromolecules. Nanoparticles, micelles, dendrimers, liposomes, etc. are examples of nanocomposite materials currently being investigated, undergoing preclinical development or used in prescription pharmaceutics. [48-52] The utilization of nanomedicines provide a variety of desirable advantages, including improved oral bioavailability, increased drug solubility and stability, prolonged exposure, targeted delivery, controlled release, and overcoming resistance, while limiting unwanted side effects. For example, Pandey and Khuller demonstrated that upon encapsulation into poly(lactic-*co*-glycolic) acid (PLGA) nanoparticles, the oral bioavailability of streptomycin was increased 21-fold compared to intramuscular free drug.[53] Murthy et al. were able to significantly prolong the antipsychotic effect of risperidone, while reducing the extrapryamidal side effects with PLGA encapsulation.[54]

When choosing a polymer for pharmaceutical applications, it is important to investigate both biodegradability and biocompatibility. Together, these properties allow for the degradation of the polymer either by hydrolysis or enzymatic means resulting in

nontoxic products. FDA approved polymers for drug delivery systems include poly(ε-caprolactone) (PCL), poly(lactic acid) (PLA), and PLGA. Upon cell implantation, PLGA nanoparticles undergo hydrolysis and enzymatic degradation to biocompatible substances (lactic and glycolic acid), making them biodegradable, biocompatible, and non-cytotoxic to cells. Semete et al demonstrated that PLGA nanoparticles have a wide biodistribution, with the highest percentage of accumulation being found in the liver, and substantial amounts found in the kidney, brain, confirming their ability to cross cellular barriers and reach hard-to-target tissues.[55-57] Because of these properties, PLGA is the most commonly used polymer for drug delivery systems and is currently used in several commercially available pharmaceutics.[58-62]

Here we report the utilization of hydrogen peroxide specific peroxalate nanoparticles to demonstrate the phenylaminoalkyl selenide redox cycle involving hydrogen peroxide and glutathione, a common cellular oxidant and reductant, respectively. We report the ability of both fluorophenylaminoethyl selenide (FPAESe) and its *N*-acetyl derivative (Nac-FPAESe) to decrease lipopolysaccharide (LPS)-induced oxidative stress in human embryonic kidney cells (HEK293T). Lastly, to increase the attractiveness of phenylaminoalkyl selenides as therapeutic agents, we report the successful encapsulation of Nac-FPAESe in PLGA nanoparticles and have carried out preliminary studies investigating the effects of these encapsulated nanoparticles on LPS-induced oxidative stress in a mammalian cell line.

3.2 METHODS AND MATERIALS

3.2.1 Cells All cell types were maintained at 37ºC in humidified air with 5% CO_2. Human embryonic kidney cells, HEK293T, (ATCC, Manassas, VA) were cultured in Dulbecco's Modified Eagle Medium supplemented with 10% fetal bovine serum and 1% penicillin/streptomycin.

3.2.2 Peroxalate Nanoparticles Peroxalate nanoparticles were made as reported by Murthy et al.[63] Peroxalate esters were provided by the Murthy laboratory (Georgia Institute of Technology, Atlanta, Ga). Peroxalate polymer (20mg) dissolved in 1.5mL dichloromethane and perylene dye (1mg) dissolved in 200µL were mixed and added slowly to a polyvinyl alcohol solution (5.0% in phosphate buffer pH 7.4, made fresh and filtered with a 0.45 µM filter). The mixture is homogenized (Power Gen 500, Fisher Scientific) and sonicated (Branson Sonifier 250) to a fine emulsion. Evaporation of dichloromethane resulted in a nanoparticle suspension. Peroxalate nanoparticles were characterized by dynamic light scattering using a 90X Particle Sizer (Brookhaven Instruments Corporation, Holtsville, NY)

3.2.3 Chemiluminescence Measurements Peroxalate nanoparticles were diluted in sodium phosphate buffer (pH 7.4, 0.1M) to a concentration of 1mg mL^{-1}. In a 90-well, 50µL peroxalate nanoparticle solution was added to various concentrations of H_2O_2 and chemiluminescence measurements were taken using a MLX Microplate Luminometer (Dynex Technologies, Chantilly, VA). An endpoint assay with a 10 sec acquisition time was used. Experiments were repeated in triplicate.

For experiments investigating the effect of phenylaminoalkyl selenide on H_2O_2, H_2O_2 (5mM) was incubated with varying concentrations of FPAESe or Nac-FPAESe for

40 minutes, 50µL peroxalate nanoparticle solution was added to the reaction mixture with mixing, by shaking of the plate, and chemiluminescence measurements were taken. Incubation time was decided by incubation of H_2O_2 (5mM) with FPAESe or Nac-FPAESe (5mM) for varying amounts of time. Experiments were done in triplicate.

For experiments demonstrating the phenylaminoalkyl selenide redox cycle, H_2O_2 (2.5 µM) was incubated selenide (FPAESe or Nac-FPAESe (2.5 µM)) in a 1:1 molar ratio, or with selenide and GSH (2.5 µM) for 40 minutes at room temperature. peroxalate nanoparticle solution was added to the reaction mixture with mixing, by shaking of the plate, and chemiluminescence measurements were taken. Experiments were done in triplicate.

3.2.4 PLGA Nanoparticles Selenide loaded PLGA nanoparticles were made by nanoprecipitation as reported by Barichello et al.[64] Selenide and PLGA were dissolved in acetone and added drop wise to PBS pH7.4 with magnetic stirring. Organic solvent is removed by rotary evaporation or magnet stirring for approx. 3hr. Unencapsulated selenide compound is removed through washing/ centrifugation cycles using PBS pH 7.4 as a rinsing solvent. 100µL of final suspension was removed for Scanning Electron Microscopy imaging. Final suspension is frozen and lyophilized to a fluffy powder. Empty PLGA nanoparticles were made using the same procedure.

PLGA nanoparticle loading is measured by autopsy of weighed amount of PLGA nanoparticles with acetone and analyzed using liquid-chromatography mass spectrometry on a triple quad tandem mass spectrometer (Micromass Quattro LC) coupled with an Agilent 1100 binary HPLC pump. 10µL injections were made onto a Phenomenex Synergi C18 (250 X 2mm, 4µm) HPLC column with the following mobile phase: A) 5:95

acetonitrile: water, 0.1% trifluoroacteic acid; b) 95:5 acetonitrile: water, 0.1% trifluoroacetic acid, 0.250 ml/min flow rate. Gradient was as follows: 20% B ramp to 100% B in 20 minutes hold at 100% B for 10 minutes, return to 20% B and hold for 10 minutes. Mass spectrometer parameters were as follows: capillary voltage, 3.50; cone voltage, 20; source block temperature, 100; desolvation temperature, 250.

3.2.5 Fluorescent Measurements HEK293T cells were allowed to grow to confluence in 24-well black with clear bottom cell culture plates. Cells were washed with PBS pH 7.4, incubated with LPS (2µg/mL, 2hr), varying concentrations of selenide (FPAESe or Nac-FPAESe, 1hr), and CM-H_2DCFDA (20µM, 30 min in dark environment). Fluorescence intensity was measured on a SpectraMax M5 microplate reader (Molecular Devices, Sunnyvale CA), using a well-scan top read assay (λ_{ex}483 and λ_{em} 535).

For experiments investigating the effect of Nac-FPAESe loaded PLGA nanoparticles on LPS-induced oxidative stress, HEK293T cells were pre-incubated on 24-well black with clear bottom cell culture plates with Nac-FPAESe PLGA nanoparticles. After 24hr cells were imaged under microscope to ensure cells were still alive, then incubated with LPS (2µg/mL, 2hr) and CM-H_2DCFDA (20µM, 30 min in dark environment) and fluorescence emission measured.

3.3 RESULTS

Chemiluminescence and fluorescence experiments were conducted to demonstrate the phenylaminoalkyl selenide/ selenoxide redox cycle using a common cellular oxidant and reductant *in vitro* and the response of these compounds to LPS-induced oxidative stress in human embryonic kidney cells (HEK293T). "Peroxalate nanoparticles", a chemiluminescent detection system for hydrogen peroxide developed by Murthy and coworkers have been shown to be H_2O_2 specific and have a linear correlation with hydrogen peroxide in the micromolar concentration range [63]. Peroxalate nanoparticles generate a chemiluminescence response to H_2O_2 via a three component reaction involving H_2O_2, peroxalate esters and fluorescent dyes. As illustrated in Figure 3.1, H_2O_2 diffuses into the nanoparticles and reacts with the peroxalate ester groups, resulting in a highly reactive dioxetanedione. Through chemically initiated electron-exchange, the dioxetanedione excites the encapsulated fluorescent dye, generating a corresponding fluorescent response.

We synthesized peroxalate nanoparticles following the procedure of Lee et al. The nanoparticles were found to be spherical, homogenous nanoparticles using a 90X Plus Particle Sizer (Brookhaven Instruments Corporation) with a diameter of 234nm and polydispersity index (PDI) of 0.187. Figure 3.2 demonstrates the linear correlation between H_2O_2 concentration and the chemiluminescence response of peroxalate nanoparticles.

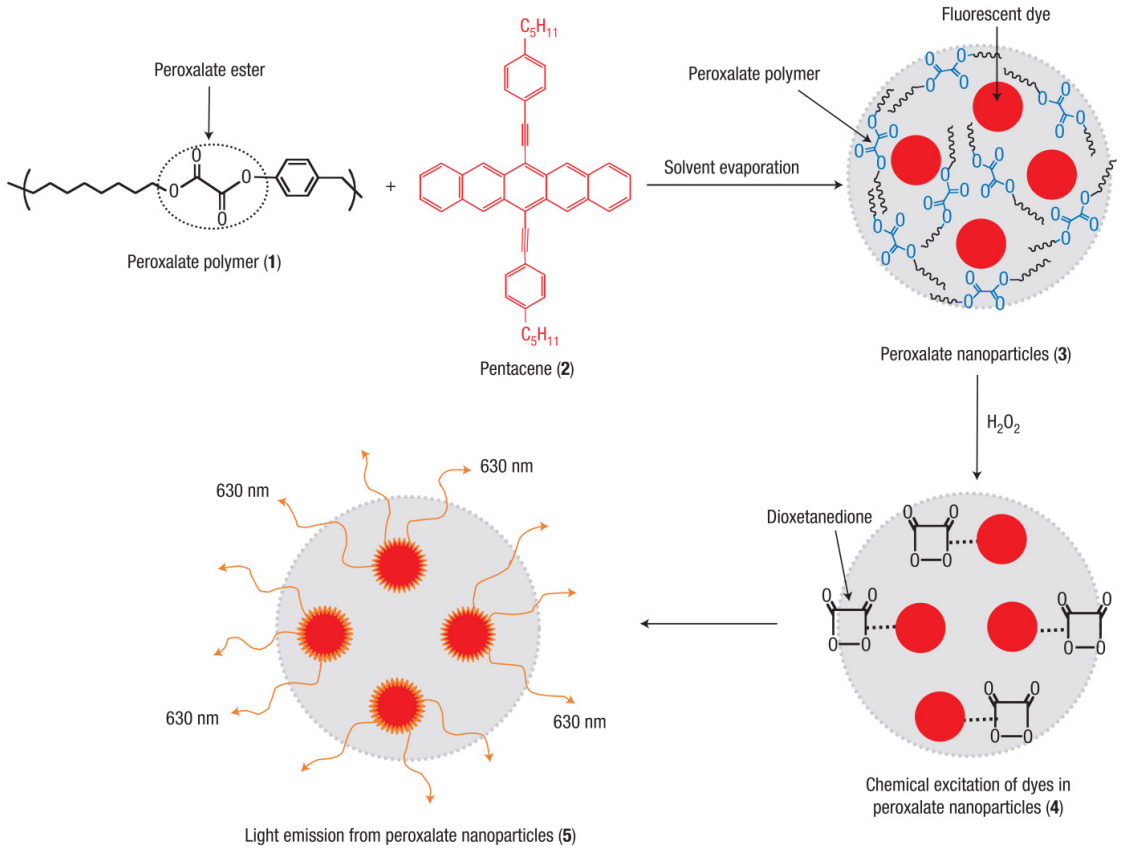

Figure 3.1. Activation of Peroxalate nanoparticles. Lee et al.[63]

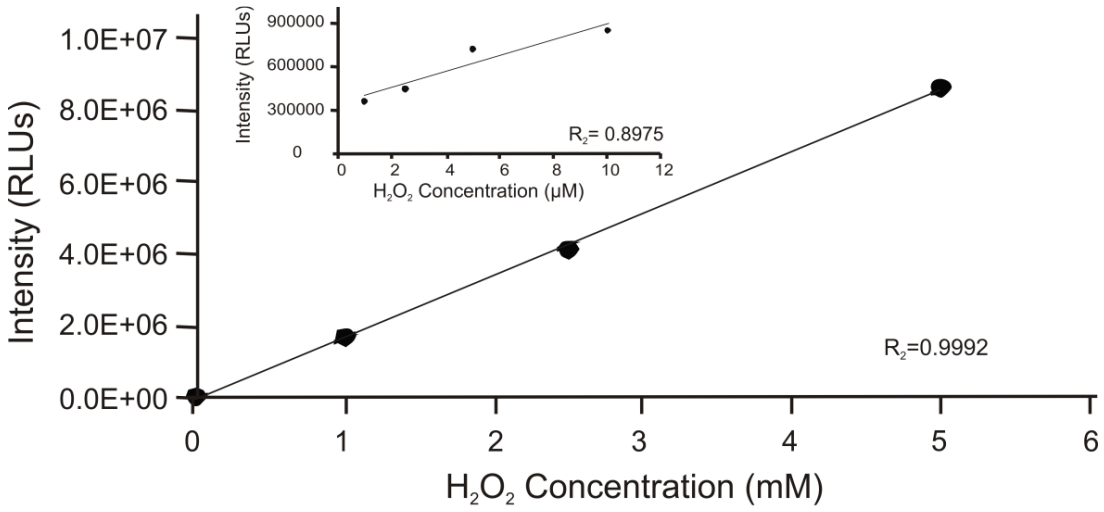

Figure 3.2. Correlation between H_2O_2 and peroxalate nanoparticle chemiluminescence response. n=3

Further chemiluminescence experiments concluded that both fluorophenylaminoethyl selenide (FPAESe) and its *N*-acetyl derivative (Nac-FPAESe) generated a decrease in chemiluminescence due to the depletion of H_2O_2. In a 90-well plate, H_2O_2 (5 mM) was incubated with varying concentrations of FPAESe or Nac-FPAESe for 40 minutes. An incubation time of 40 minutes was determined to an optimal incubation time in preliminary studies in which H_2O_2 and FPAESe or Nac-FPAESe were incubated in a 1:1 molar ratio for varying times (data not shown). After incubation, peroxalate nanoparticle solution (1 mg/mL, in PBS pH 7.4) was added to the reaction mixture with shaking and chemiluminescence measurements taken immediately on a MLX Microplate Luminometer (Dynex Technologies). As shown in Figure 3.3, incubation of H_2O_2 with FPAESe or Nac-FPAESe resulted in a linear decrease in chemiluminescence due to a decrease in remaining H_2O_2 concentration.

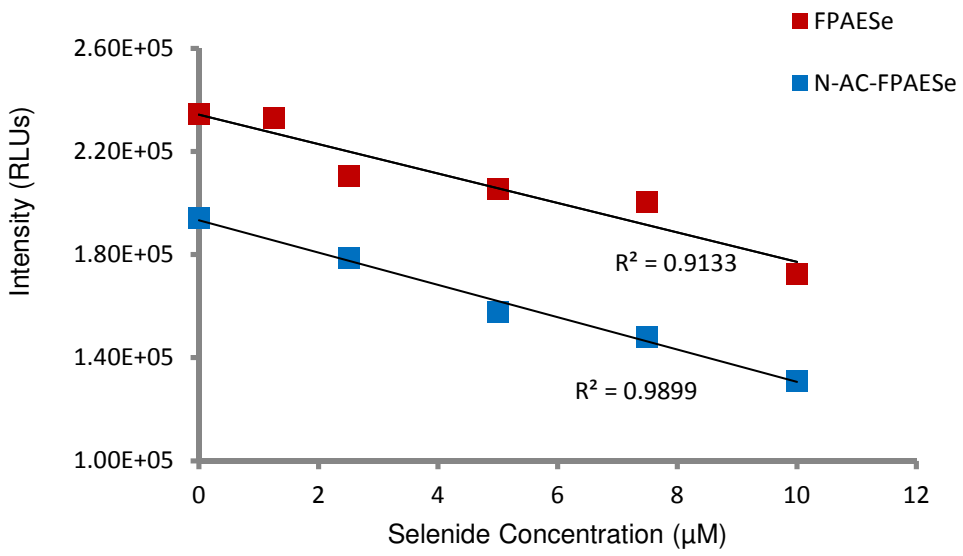

Figure 3.3. Effect of phenylaminoalkyl selenides on H_2O_2 concentration. n=3

These initial results lead to the investigation of the phenylaminoalkyl selenide/selenoxide redox cycle using hydrogen peroxide as the oxidant and glutathione as the reductant. H_2O_2 was incubated alone, with selenide (FPAESe or Nac-FPAESe), or with selenide and GSH for 40 minutes, after which peroxalate nanoparticles were added to the reaction mixture with shaking and chemiluminescence measurements taken immediately. As shown in Figure 3.4, a statistically significant decrease in hydrogen peroxide concentration is observed in the reaction mixture containing H_2O_2 and selenide, compared to H_2O_2 alone. A second statistically significant decrease is observed in the reaction mixture with H_2O_2, selenide and GSH, compared to that containing H_2O_2 and selenide. Control reaction mixtures including H_2O_2 and glutathione, H_2O_2 and selenoxide, etc. were monitored and did not result in a change of H_2O_2 concentration. This decreasing pattern was only observed in the presence of H_2O_2, selenide and GSH,

indicating that the inclusion of a reductant such as GSH in the reaction mixture allowed for the regeneration of the selenide moiety; creating a selenium-based redox cycle and therefore resulting in a greater consumption of H_2O_2 molecules, than observed in the presence of only an oxidant.

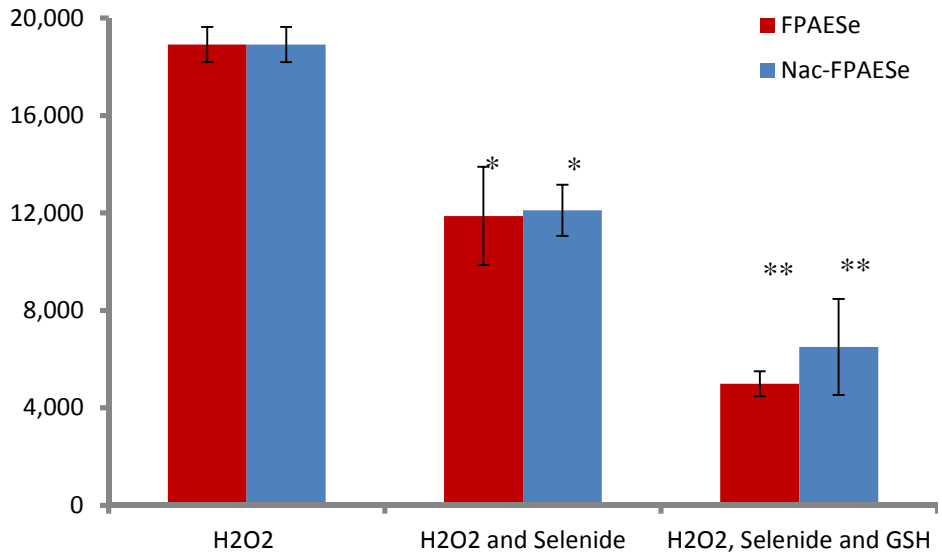

Figure 3.4. Phenylaminoalkyl selenide redox cycle demonstrated through residual H_2O_2 concentration. *=p<0.05 with respect to H_2O_2 group; **=p<0.05 with respect to H_2O_2 and Selenide group, n=3

These *in vitro* results were then followed by the investigation of the reaction between fluorophenylaminoethyl selenides and lipopolysaccharide (LPS)-induced oxidative stress in cells using a common fluorescent dye commonly used in the detection of cellular H_2O_2. LPS binds to multiple cellular receptors including lipid binding protein and CD14, causing the production of pro-inflammatory cytokines and the stimulation of signaling cascades in immune cells, resulting in the production of ROS and creating a state of cellular oxidative stress. CM-H_2DCFDA, a cell permanent dye oxidized

predominantly by H_2O_2, but also shown to be oxidized by peroxynitrite, and hydroxyl radicals, is commonly used as a cellular probe for oxidative stress.[65-69] Human kidney embryonic cells (HEK293T) were washed and sequentially incubated with LPS (2 µg/mL, 2hr), varying concentrations of FPAESe or Nac-FPAESe (1hr) and CM-H_2DCFDA (20µM, 30 minutes in dark environment), and fluorescence measurements (485 and 538 excitation and emission) were taken on a SpetraMax M5 microplate reader (Molecular Devices). A statistically significant dose dependent decrease in ROS-generated fluorescence was observed with increasing selenide (FPAESe and Nac-FPAESe) concentrations (Figure 3.5); thus, demonstrating the ability of phenylaminoalkyl selenides to reduce cellular oxidative stress in mammalian cell culture.

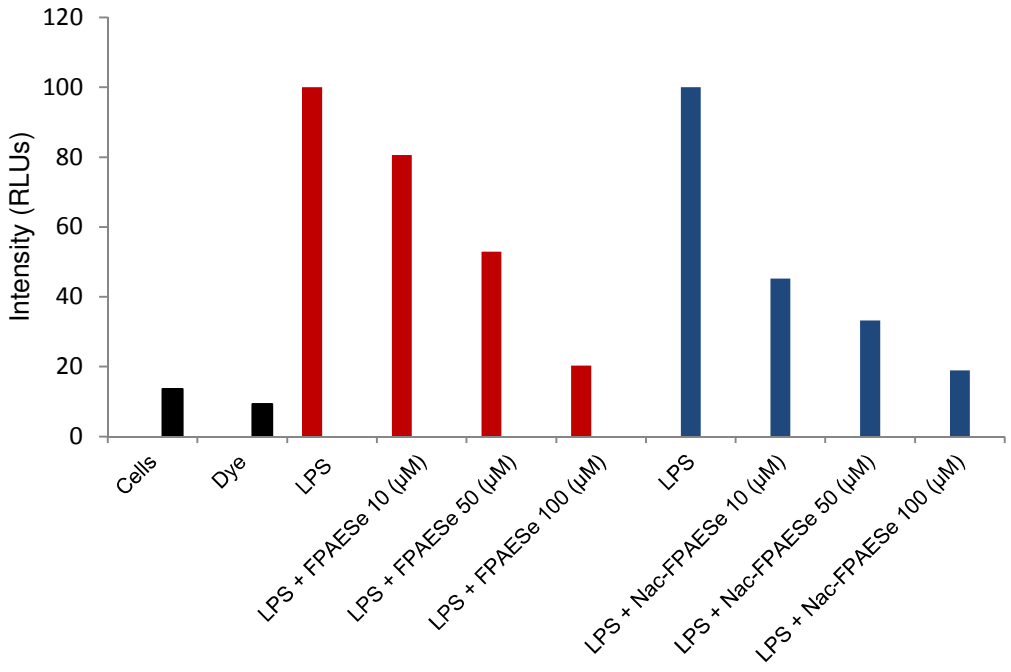

Figure 3.5. Effect of phenylaminoalkyl selenides on LPS-induced oxidative stress in HEK239T cells.

Systems such as micelles, liposomes, nanoparticles, etc. have been investigated for the delivery of therapeutic agents. PLGA nanoparticles are one of the most well-studied drug delivery technologies, mainly due to the excellent biodegradable and biocompatible properties of the PLGA co-block polymer. We have successfully encapsulated *N*-acetyl fluorophenylaminoethyl selenide in PLGA nanoparticles using the commonly used nanoprecipitation technique, and have conducted preliminary studies demonstrating the ability of these selenide loaded nanoparticles to decrease LPS-induced oxidative stress in HEK293T cells.

The nanoprecipitation technique entails mixing of PLGA and drug, dissolved in organic solvent, to be added to an aqueous layer under stirring. The organic solvent is removed by stirring or rotary evaporization and the resulting nanoparticle suspension is washed with fresh aqueous phase and lyophilized to give an airy powder. The hydrophilic nature of the free amine of FPAESe allowed for the diffusion of the drug into the aqueous layer during solvent evaporization, reducing the loading of FPAESe; therefore, Nac-FPAESe was chosen as the selenide drug of choice for encapsulation optimization and nanoparticles experiments. Conditions resulting is maximum loading consisted of a 2:1 selenide: PLGA mass ratio, a 2:1 aqueous: organic phase ratio, and solvent removal by magnetic stirring. Nac-FPAESe-loaded nanoparticles were confirmed to be 113nm in diameter, homogenous with a PI of 0.087 by DLS, shown in Figure 3.6. Maximum loading was found to be 3% wt/wt upon acidic autopsy and analysis by liquid chromatography mass spectrometry.

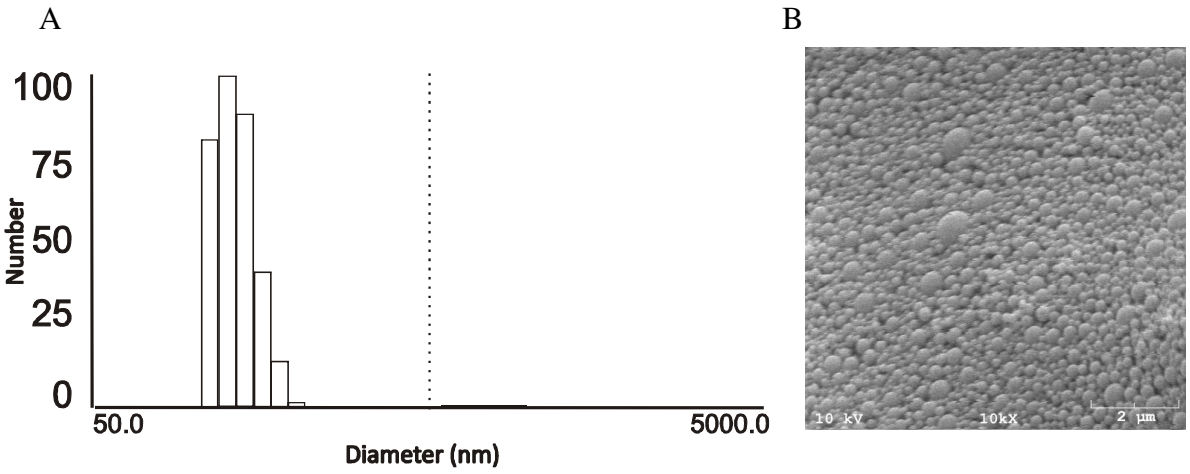

Figure 3.6. Characterization of *N*ac-FPAESe-loaded PLGA nanoparticles. A) Dynamic light scattering B) Scanning electron micrograph

HEK293T cells were pre-incubated with Nac-FPAESe loaded PLGA nanoparticles for 24 hour, incubated with LPS (2ug/mL, 2hr) and H_2-DCFDA (20 µM, 30 minutes, in dark environment). Cells were washed with PBS pH 7.4 between incubations. As shown in Figure 3.7, Nac-FPAESe nanoparticles exhibited a dose-dependent decrease of fluorescence response generated from LPS-induced ROS. Empty PLGA nanoparticles did not demonstrate the same pattern, while actually exhibiting an increase in response as dosage increased. These results were obtained in duplicate experiments. The same selenide dose dependent response was observed with both free FPAESe and Nac-FPAESe drugs, indicating encapsulation in PLGA nanoparticles has no effect on the pharmaceutical, antioxidant characteristics of the drugs. This is most likely explained by the added stress of nanoparticle endocytosis and the lack of stress attenuation provided by the selenide drugs. It is obvious from these preliminary results that further studies are needed.

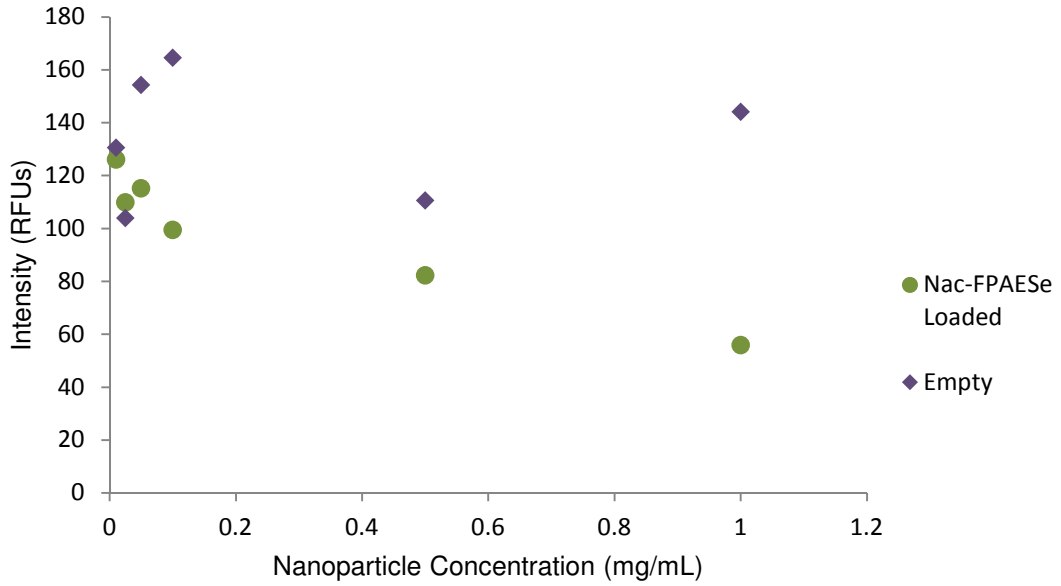

Figure 3.7. Effect of *N*ac-FPAESe and Empty PLGA nanoparticles on LPS-induced oxidative stress.

3.4 FUTURE WORK

The purpose of this work was to strengthen the pharmaceutical potential of phenylaminoalkyl selenides by demonstrating their ability to decrease ROS concentration *in vitro* and oxidative stress in cells. We demonstrated that the redox cycle responsible for the potent antioxidant property of these compounds works in the presence of the well known cellular oxidant H_2O_2. Phenylaminoalkyl selenides were demonstrated to attenuate LPS-induced oxidative stress in human embryonic cells in a dose-dependent manner. We have encapsulated Nac-FPAESe in PLGA nanoparticles using the nanoprecipitation technique and showed initial results for the attenuation of LPS-induced cellular oxidative stress in HEK293T cells with these selenide-loaded nanoparticles.

There are many techniques of drug encapsulation into nanocarriers, depending on the solubility and stability properties of the drug of interest. There are four main types of encapsulation: nanoprecipitation, emulsification solvent evaporation, emulsification solvent diffusion, and double emulsification solvent evaporation. Nanoprecipitation is a common technique used in the encapsulation of PLGA nanoparticles with a low level of difficulty, and for these reasons it was chosen as the method of encapsulation. Although the nanoprecipitation method yields the best results with lipophilic drugs, several investigators have reported the encapsulation of hydrophilic drugs in PLGA nanoparticles using this method.[64, 70-72] Future studies investigating different solvents and non-solvents in the nanoprecipitation procedure and even the investigation of different methods may prove to yield higher encapsulation percentages. With an increase in selenide encapsulation, it is possible that a greater effect of oxidative stress attenuation will be observed compared to empty nanoparticles, demonstrating the potential of these

compounds to be loaded into nanocarriers, improving their potential as therapeutic agents or supplements.

3.5 REFERENCES

1. Rhee, S. G.; Chang, T.-S.; Bae, Y. S.; Lee, S.-R.; Kang, S. W., Cellular regulation by hydrogen peroxide. *Journal of the American Society of Nephrology* **2003,** 14, (S211-S215), S211.

2. Niethammer, P.; Grabher, C.; Look, A. T.; Mitchinson, T., A tissue-scale gradient of hydrogen peroxide mediates rapid wound detection in zeba fish. *Nature* **2009,** 459, 996-1000.

3. Grant, C. M., Regulation of translation by hydrogen peroxide. *Antioxidants & Redox Signaling* **2011,** 15, (1), 191-203.

4. Freinbichler, W.; Colivicchi, M. A.; Stefanini, C.; Bianchi, L.; Ballini, C.; Misini, B.; Weinberger, P.; Linert, W.; Vareslija, D.; Tipton, K. F.; Corte, L. D., Highly reactive oxygen species: detection, formation and possible functions. *Cellular and Molecular Life Sciences* **2011,** 68, 2067-2079.

5. Rhee, S. G., H_2O_2, a necessary evil for cell signaling. *Science* **2006,** 312, 1882-1883.

6. Groeger, G.; Quiney, C.; Cotter, T. G., Hydrogen peroxide as a cell-survival signaling molecule. *Antioxidants & Redox Signaling* **2009,** 11, (11), 2655-2670.

7. Bae, J.-Y.; Ahn, S.-J.; Han, W.; Noh, D.-Y., Peroxiredoxin I and II inhibit H2O2-induced cell death in MCF-7 cell lines. *Journal of Cellular Biochemistry* **2007,** 101, 1038-1045.

8. Woo, H. A.; Yim, S. H.; Shin, D. H.; Kang, D.; Yu, D.-Y.; Rhee, S. G., Inactivation of Peroxiredoxin I by phosphorylation allows localized H_2O_2 accumulation for cell signaling. *Cell* **2010,** 140, 517-528.

9. Finkel, T., Oxidant signals and oxidative stress. *Current Opinion in Cell Biology* **2003,** 15, 247-254.

10. Imlay, J.; Chin, S., S, Toxic DNA damage by hydrogen peroxide through the Fenton reaction in vivo and in vitro. *Science* **1988,** 240, (4852), 640-642.

11. Mello Filho, A. C.; Hoffmann, M. E.; Meneghini, R., Cell killing and DNA damage by hydrogen peroxide are mediated by intracellular iron. *Biochemical Journal* **1984,** 218, 273-275.

12. Fridovich, I., Oxygen toxicity: a radical explanation *The Journal of Experimental Biology* **1998,** 201, 1203-1209.

13. LLoyd, R. V.; Hanna, P. M.; Mason, R. P., The origin of the hydroxyl radical oxygen in the Fenton reaction
Free Radical Biology & Medicine **1997,** 22, (5), 885-888.

14. Merkofer, M.; Kissner, R.; Hider, R. C.; Brunk, U. T.; Koppenol, W. H., Fenton chemitry and iron chelation under phsiologically relevant conditions: Electrochemistry and kinetics. *Chemical Research in Toxicology* **2006,** 19, 1263-1269.

15. Walling, C., Fenton's reagent revisited. *Accounts of Chemical Research* **1975,** 8, (4), 125-131.

16. Wink, D. A.; Wink, C. B.; Nims, R. W.; Ford, P. C., Oxidizing intermediates generated in the Fenton Reagent: Kinetic arguments against the intermediacy of the hydroxyl radical. *Environmental Health Perspectives* **1994,** 102, (Suppl 3), 11-15.

17. Rigg, T.; Taylor, W.; Weiss, J., The rate constant of the reaction between Hydrogen Peroxide and Ferrous Ions. *The Journal of Chemical Physics* **1954,** 22, (4), 575-577.

18. Wu, D.; Cederbaum, A. I., Alcohol, oxidative stress, and free radical damage. *Alcohol Research and Health* **2003,** 27, (4), 277-284.

19. Spector, A., Review: oxidative stress and disease. *Journal of Ocular Phamracology* **2000,** 16, (2), 193-199.

20. Sies, H.; Cadenas, E., Oxidative stress: damage to intact cells and organs. *Philosophical translations of the Royal Society of London B* **1985,** 311, 617-631.

21. Pace, G. W.; Leaf, C. D., The role of oxidative stress in HIV disease. *Free Radical Biology and Medicine* **1995,** 19, 523-528.

22. Finkel, T.; Holbrook, N., Oxidants, oxidative stress and the biology of aging. *Nature* **2000,** 408, 239-247.

23. Baum, M. K.; Shor-Posner, G.; Lai, S. H.; Zhang, G. Y.; Fletcher, M. A.; Sauberlich, H.; Page, J. B., High risk of HIV-related mortality is associated with selenium deficiency. *Journal of Acquired Immune Deficiency Syndromes and Human Retrovirology* **1997,** 15, 370-374.

24. Beck, M. A.; Shi, Q.; Morris, V. C.; Levander, O. A., Rapid genomic evolution of a non-virulent Coxsackievirus B3 in selenium-deficient mice results in selection of identical virulent isolates. *Nature Medicine* **1995,** 1, 433-436.

25. Brenneisen, P.; Steinbrenner, H.; Sies, H., Selenium, oxidative stress, and health aspects. *Molecular Aspects of Medicine* **2005,** 26, (4-5), 256-267.

26. Clark, L. C.; Combs, G. F.; Turnbull, B. W.; Slate, E. H.; Chalker, D. K.; Chow, J.; Davis, L. S.; Glover, R. A.; Graham, G. F.; Gross, E. G.; Krongrad, A.; Lesher, J. L.; Park, K.; Sanders, B. B.; Smith, C. L.; J., T. R., Effects of selenium supplementation for cancer prevention in patients with carcinoma of the skin. *Journal of the American Medical Association* **1996,** 276, 1957-1963.

27. Duntas, L. H., Selenium and inflammation: underlying anti-inflammatory mechanisms. *Hormone and Metabolic Research* **2009,** 41, 443-447.

28. Micke, O.; Schomburg, L.; Buentzel, J.; Kisters, K.; Meuecke, R., Selenium in oncology: from chemistry to clinics. *Molecules* **2009,** 14, 3975-3988.

29. Alberto, E. E.; Soares, L. C.; Sudati, J. H.; Borges, A. C. A.; Rocha, J. B. T.; Braga, A. L., Efficient synthesis of modular amino acid derivatives containing selenium with pronounced GPx-like activity. *European Journal of Organic Chemistry* **2009**, 4211-4214.

30. Back, T. G.; Moussa, Z.; Parvez, M., The exceptional glutathione peroxidase-like activity of di(3-hydroxypropyl) selenide and the unexpected role of a novel spirodioxaselenanonane intermediate in the catalytic cycle. *Angewandte Chemie International Edition* **2004,** 43, 1268-1270.

31. De Silva, V.; Woznichak, M. M.; Burns, K. L.; Grant, K. B.; May, S. W., Selenium redox cycling in the protective effects of organoselenides against oxidant-induced DNA damage. *Journal of the American Chemical Society* **2004,** 126, 2409-2413.

32. Klotz, L. O.; Sies, H., Defenses against peroxynitrite: selenocompounds and flavonoids. *Toxicology Letters* **2003,** 140-141, (125-132), 125.

33. Kunwar, A.; Mishra, B.; Barik, A.; Kumbhare, L. B.; Pandey, R.; Jain, V. K.; Priyadarsini, K. I., 3,3'-Diselenodipropionic acid, an efficient peroxyl radical scavenger and a GPx mimic, protects erythrocytes (RBCs) from AAPH-induced hemolysis. *Chemical Research in Toxicology* **2007,** 20, 1482-1487.

34. May, S. W., Selenium-based drug design: rationale and therapeutic potential. *Expert Opinion on Investigational Drugs* **1999,** 8, 1017-1030.

35. May, S. W., Selenium-based pharmacological agents: an update. *Expert Opinion on Investigational Drugs* **2002,** 11, 1261-1269.

36. May, S. W.; Herman, H. H.; Pollock, S., H.; Fowler, L. C.; Wimalasena, K.; Ciccarello, M. C., Antihypertensive activity and ascorbate depletion via product recycling by DBM-targeted selenides. *Federation Proceedings* **1987,** 46, 1940-1940.

37. May, S. W.; Pollock, S. H., Selenium-based antihypertensives. Rationale and potential. *Drugs* **1998,** 56, 959-964.

38. May, S. W.; Wang, L. Q.; Gill-Woznichak, M. M.; Browner, R. F.; Ogonowski, A. A.; Smith, J. B.; Pollock, S. H., An orally active selenium-based antihypertensive agent with restricted CNS permeability. *Journal of Pharmacology and Experimental Therapeutics* **1997,** 283, 470-477.

39. Mugesh, G.; Panda, A.; Singh, H. B.; Punekar, N. S.; Butcher, R. J., Glutathione peroxidase-like antioxidant activity of diaryl diselenides: a mechanistic study. *Journal of the American Chemical Society* **2001,** 123, 839-850.

40. Overcast, J. D.; Ensley, A. E.; Buccafusco, C. J.; Cundy, C.; Broadnax, R. A.; He, S. Q.; Yoganathan, A. P.; Pollock, S. H.; Hartley, C. J.; May, S. W., Evaluation of cardiovascular parameters of a selenium-based antihypertensive using pulsed Doppler ultrasound. *Journal of Cardiovascular Pharmacology* **2001,** 38, 337-346.

41. Pollock, S. H.; Herman, H. H.; Fowler, L. C.; Edwards, A. S.; Evans, C. O.; May, S. W., Demonstration of the antihypertensive activity of phenyl-2-aminoethyl selenide. *Journal of Pharmacology and Experimental Therapeutics* **1988,** 246, 227-234.

42. Sarma, B. K.; Mugesh, G., Glutathione peroxidase (GPx)-like antioxidant activity of the organoselenium drug Ebselen: Unexpected complications with thiol exchange reactions. *Journal of the American Chemical Society* **2005,** 127, 11477-11485.

43. Wilson, S. R.; Zucker, P. A.; Huang, R.-R. C.; Spector, A., Development of synthetic compounds with glutathione peroxidase activity. *Journal of the American Chemical Society* **1989,** 111, 5936-5939.

44. Woznichak, M. M.; Ogonowski, A. A.; Wang, L.; Overcast, J. D.; Smith, J. B.; Browner, R. F.; Pollock, S. H.; May, S. W., Biochemistry and pharmacology of novel selenium compounds. *FASEB Journal* **1997,** 11, A1153-A1153.

45. Zhao, R.; Holmgren, A., A novel antioxidant mechanism of Ebselen involving Ebselen diselenide, a substrate of mammalian thioredoxin and thioredoxin reductase. *Journal of Biological Chemistry* **2002,** 277, 39456-39462.

46. May, S. W.; Herman, H. H.; Roberts, S. F.; Ciccarello, M. C., Ascorbate depletion as a consequence of product recycling during dopamine beta-monooxygenase catalyzed selenoxidation. *Biochemistry* **1987,** 26, 1626-1633.

47. Woznichak, M. M.; Overcast, J. D.; Robertson, K.; Neumann, H. M.; May, S. W., Reaction of phenylaminoethyl selenides with peroxynitrite and hydrogen peroxide. *Archives of Biochemistry and Biophysics* **2000,** 379, 314-320.

48. Cho, K.; Wang, X.; Nie, S.; Chen, Z. G.; Shin, D. M., Therapeutic nanoparticles for drug delevery in cancer. *Clinical Caner Research* **2008,** 14, 1310-1316.

49. Davis, M. E.; Chen, Z. G.; Shin, D. M., Nanoparticle therapeutics: an emerging treatment modality for cancer. *Nature Reviews Drug Delivery* **2008,** 7, 771-782.

50. Duncan, R., The dawning era of polymer therapeutics. *Nature Reviews Drug Discovery* **2003,** 2, 347-360.

51. Lammers, T.; Hennink, W. E.; Storm, G., Tumour-targeted nanomedicines: principles and practice. *British Journal of Cancer* **2008,** 99, 392-397.

52. Park, J. H.; Lee, S.; Kim, J.-H.; Park, K.; Kim, K.; Kwon, I. C., Polymeric nanomedicince for cancer therapy. *Progress in Polymer Science* **2007,** 33, (1), 113-117.

53. Pandey, R.; Khuller, G. K., Nanoparticle-based oral drug delivery system for an injectable antiobiotic- Strptomycin. *Chemotherapy* **2007,** 53, 437-441.

54. Muthu, M. S.; Rawat, M. K.; Mishra, A.; Singh, S., PLGA nanoparticle formulations of risperidone: preparation and neuropharmacological evaluation. *Nanomedicine: Nanotechnology, Biology and Medicine* **2009,** 5, 323-333.

55. Semete, B.; Booysen, L.; Lemmer, Y.; Kalombo, L.; Katata, L.; Verschoor, J.; Swai, H. S., In vivo evaluation of the biodistribution and safety of PLGA nanoparticles as drug delivery systems. *Nanomedicine, Nanotechnology, Biology, and Medicine* **2010,** 6, 662-671.

56. Koziara, J. M.; Lockman, P. R.; Allen, D. D.; Mumper, R. J., *In Situ* blood-brain barrier transport of nanoparticles. *Pharmaceutical Research* **2003,** 20, (11), 1772-1778.

57. Lockman, P. R.; Mumper, R. J.; Khan, M. A.; Allen, D. D., Nanoparticle technology for drug delivery across the blood-brain barrier. *Drug Development and Industrial Pharmacy* **2002,** 28, (1), 1-12.

58. Zamboni, W. C., Liposomal, nanoparticles, and conjugated formulations of anticancer agents. *Clinical Cancer Research* **2005,** 11, (23), 8230-8234.

59. Sahay, G.; Alakhova, D. Y.; Kabanov, A. V., Endocytosis of nanomedicines. *Journal of Controlled Release* **2010,** 145, 182-195.

60. Reddy, M. K.; Wu, L.; Kou, W.; Ghorpade, A.; Labhasetwar, V., Superoxide dismutase-loaded PLGA nanoparticles protect cultured human neurons under oxidative stress. *Applied Biochemical and Biotechnology* **2008,** 151, 565-577.

61. Mansour, H. M.; Sohn, M.; Al-Ghananeem, A.; DeLuca, P. P., Materials for pharmaceutical dosage forms: Molecular pharmaceutics and controlled release drug delivery aspects. *International Journal of Molecular Science* **2010,** 11, 3298-3322.

62. Javadzadeh, Y.; Ahadi, F.; Davaran, S.; Mohammadi, G.; Sabzevari, A.; Adibkia, K., Preparation and physicochemical characterization of naproxen-PLGA nanoparticles. *Colloids and Surfaces B: Biointerfaces* **2010,** 81, 498-502.

63. Lee, D.; Khaja, S.; Velasquez-Castano, J. C.; Dasari, M.; Sun, C.; Petros, J.; Taylor, R. W.; Murthy, N., *In vivo* imaging og hydrogen peroxide with chemiluminescent nanoparticles. *Nature Materials* **2007,** 6, 765-768.

64. Barichello, J. M.; Morishita, M.; Takayama, K.; Nagai, T., Encapsulation of hydrophilic and lipphilic drugs in PLGA nanoparticles by the nanoprecipitation method. *Drug Development and Industrial Pharmacy* **1999,** 25, (4), 471-476.

65. Carter, W. O.; Narayanan, P. K.; Robinson, J. P., Intracellular hydrogen peroxide and superoxide anion detection in endothelian cells. *Journal of Leukocyte Biology* **1994,** 55, 235-258.

66. Garcia-Ruiz, C.; Colell, A.; Mari, M.; Morales, A., Direct effect of ceramide on the mitochondrial elecron transport chain leads to generation of reactive oxygen species. *The Journal of Biological Chemistry* **1997,** 272, (17), 11369-11377.

67. Hempel, S. L.; Buettner, G. R.; O'Malley, Y. Q.; Wessels, D. A.; Flaherty, D. M., Dihydrofluorescein diacetate is superior for deteecting intracellular oxidants: Comparison with 2',7'-dichlorodihydrofluorescein diacetate, 5(and 6)-carboxy-2',7'-dichlorodihydrofluorescein diacetate, and dihydrorhodamine 123. *Free Radical Biology & Medicine* **1999,** 27, 146-199.

68. Mahadev, K.; Zilbering, A.; Zhu, L.; Goldstein, B. J., Insulin-stimulated hydrogen peroxide reversibly inhibits protein-tyrosine phosphatase 1B *in vivo* and enhances the early insulin action cascade. *The Journal of Biological Chemistry* **2001,** 276, (24), 21938-21942.

69. Shanker, G.; Aschner, J. L.; Syversen, T.; Aschner, M., Free radical formation in cerebral cortical astrocytes in culture induced by mthylmercury. *Molecular Brain Research* **2004,** 128, 48-57.

70. Bilati, U.; Allemann, E.; Doelker, E., Development of nanoprecipitation method intended for the entrapment of hydrophilic drugs into nanoparticles. *European Journal of Pharmaceutical Sciences* **2005,** 24, 67-75.

71. Govender, T.; Stolnik, S.; Garnett, M. C.; Illum, L.; Davis, S. S., PLGA nanoparticles prepared by nanoprecipitation: drug loading and release studies of a water soluble drug. *Journal of Controlled Release* **1999,** 57, 171-185.

72. Cohen-Sela, E.; Chorny, M.; Koroukhov, N.; Danenberg, h. D.; Golomb, G., A new double emulsion solvent diffusion technique for encapsulation hydrophilic molecules in PLGA nanoparticles. *Journal of Controlled Release* **2009,** 133, 90-95.

CHAPTER 4

THE ANTIOXIDANT PHENYLAMINOETHYL SELENIDE REDUCES DOXORUBICIN-INDUCED CARDIOTOXICITY IN A XENOGRAFT MODEL OF HUMAN PROSTATE CANCER

4.1 Introduction

Anthracyclines are common, highly successful antibiotic chemotherapy agents used to treat a variety of cancers including luekemias, lymphomas, breast, uterine, and lung cancers.[1] Adriamycin, better known as Doxorubicin (DOX), is the most commonly prescribed anthracycline in the US (Figure 4.1). Doxorubicin binds tightly to DNA, interrupting many DNA activities. For instances, the primary mode of doxorubicin anticancer activity is the inhibition of topoisomerase II, an enzyme responsible for the cleaving of the DNA double helix for the purpose of untangling DNA supercoils in DNA replication, segregation of sister chromosomes, and gene transcription.[1, 2] Secondary modes of activity include DNA intercalation and inhibition of nuclear helicases, the enzymes responsible for separation of nucleic acid strands and oxidative DNA damage.[3, 4]

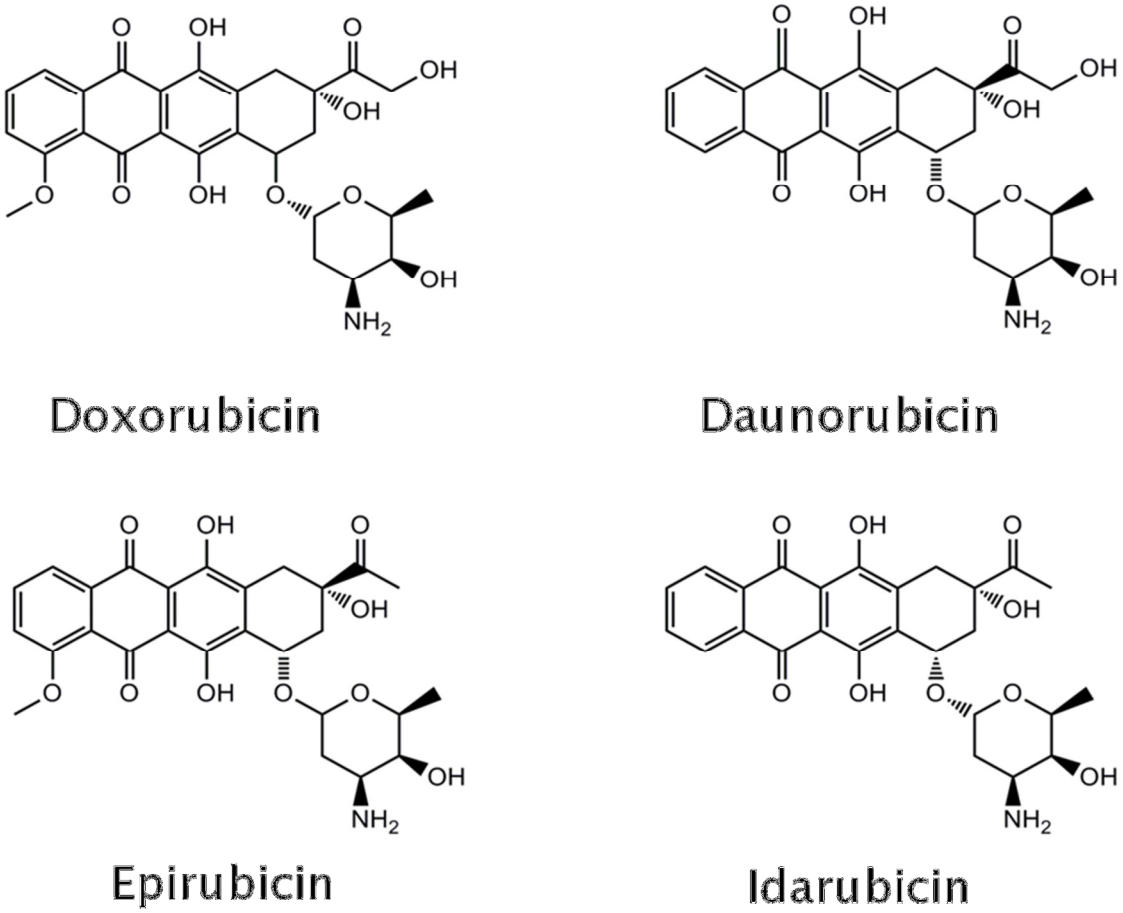

Figure 4.1. Anthracyclines commonly prescribed in the United States

The advantages of DOX and other anthracyclines do not come without a cost; as a side effect, this class of anticancer agents produces ROS and induces oxidative stress in nontargeted tissues, leading to 'normal tissue injury'.[5] Heart, kidney and brain tissues have been reported as areas of 'normal tissue injury'.[5] DOX treatment has been shown to dysregulate blood pressure and flow as well as decrease heart contractility.[6] In addition, DOX toxicity has been shown to cause myofibrillar loss, sarcoplasmic reticulum disruption, mitochondria and swelling and lesions.[7] These characteristics eventually lead to cardio-toxicities, such as cardiomyopathy and congestive heart failure.[1, 8] While the cardiotoxic effect has been known to occur after a single dose of DOX (240mg/m^2) and as late as seven years after termination of dosing, the cardiotoxicity of DOX has consistently been shown to be dose-dependent.[9, 10] Current recommendations suggest that the total cumulative dose of anthracycline should not exceed 550mg/m^2 body surface area.[1, 8, 11]

There are several proposed mechanisms for anthracycline-mediated cardiotoxicity including free radical formation, oxidative damage to membrane lipids and cellular components, inhibition of DNA synthesis, release of vasoactive substances such as histamine and catecholamine, increased intracellular calcium (Ca^{2+}) concentrations, changes in cardiac β-adrenergic receptors, and lower glutathione peroxidase activities in the heart.[12-14] Among these, the primary cause of myocardial damage has been correlated to the formation of free oxygen radicals.[15] Supporting this view, Wang *et.al*. have shown the toxic effect of DOX on tumor and normal (bovine aortic endothelial and adult rat cardiomyocytes) cells is caused by different pathways.[16] Apoptosis in normal cells was found to be H_2O_2 dependent, while that in tumor cells was found to be p53 dependent.

The heart an organ that is a particularly vulnerable to free radical damage induced by DOX for several reasons; *i*) cardiolipin, a phospholipid in cardiomyocytes, has a high affinity for DOX, *ii*) there are limited antioxidants in the heart, and *iii*) oxidative metabolism is activated highly so that the reaction with free radicals is enhanced.[15] DOX has a high affinity for the negatively charged phopholipid, cardiolipin, found in the mitochondrial inner membrane. This affinity and the high concentration of mitochondrion found in cardiomyocytes, results in a cardiac accumulation of DOX. Once accumulated in the mitochondrial membrane, the catalysis of the redox cycling of DOX between the quinone and the semiquinone forms, produces high concentrations of $O_2^{-\cdot}$, eventually being converted to other ROS, Figure 4.2.[1, 17]

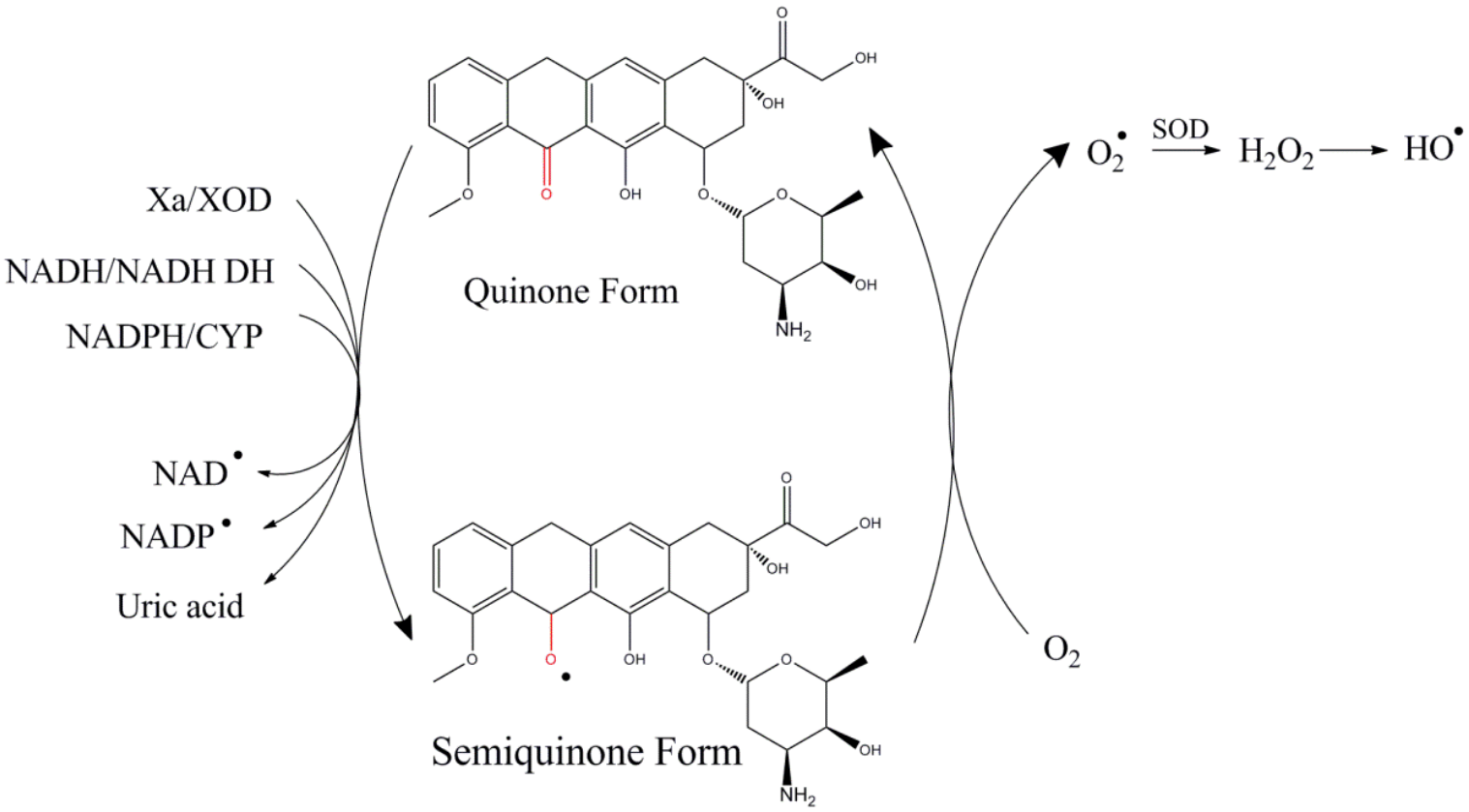

Figure 4.2. The redox cycle of anthracyclines between the quinine and semiquinone forms.

These oxygen-derived toxic species can be detoxified by antioxidant enzymes such as superoxide dismutase, catalase, and selenium-dependent glutathione peroxidase under normal physiological conditions. However, DOX metabolism could interrupt this balance with high free radical formation and oxidative stress so that lipid peroxidation is induced and cellular homeostasis is changed.[18, 19] Evidence suggests that DOX treatment reduces selenium-dependent glutathione peroxidase in myocardial cells [20], resulting in an increase in the formation of free radicals and a decrease in the ability to detoxify them.

The first incidence of fatal cardiotoxicity from prolonged use of an anthracycline was reported in 1967, by Marcez *et al.*[21] Since this discovery, thousands of DOX analogues have been synthesized, but none of these are as effective anticancer agents as DOX.[22] Another approach to mediate anthracycline-induced cardiotoxicity without losing the anticancer effectiveness is co-administration with other pharmaceuticals. Antioxidants have been shown to be effective against DOX-mediated cardiac toxicity. Many studies have examined the ability of antioxidants to protect the heart from DOX-induced oxidative damage.[15, 23] The concomitant administration of antioxidants, *e.g.,* vitamin C or α-tocopherol (vitamin E), with DOX has been studied using *in vivo* model systems and accessed clinically.[24, 25]

Dexrazoxane is a drug approved by the U.S. Food and Drug Administration (FDA) to reduce toxicity associated with extravasation of anthracyclines, and is used to reduce anthracycline-mediated cardiotoxicity. Dexrazoxane is a derivative of EDTA and potently chelates iron, thereby interfering with the formation of anthracycline-iron mediated free radicals.[26] Although dexrazoxane has been shown to reduce anthracycline mediated cardiotoxicity, it also causes myelosuppression, and recent studies suggest it

may lead to acute myeloid leukemia and myelodysplastic syndrome.[26, 27] Although the mechanism responsible for the observed toxicity is not fully understood, it is believed that its ability to reversibly antagonize topoisomerase II, leading to direct cytotoxic effects or schedule dependent synergistic effects. The FDA and the European Medicines Agency has recommended restricting dexrazoxane usage to adult patients with advanced or metastatic breast cancer who have received greater than 300 mg/m^2 dose of doxorubicin or 540 mg/m^2 of epirubicin due to concerns over toxicity.[27]

Amifostine, another antioxidant drug approved by the FDA, has been shown to lessen cisplatin-mediated toxicity on the kidney and salivary glands. Although its complete mechanism of action is not known, it is a prodrug that is dephosphorylated in tissue by alkaline phosphatase to a pharmacologically active free thiol metabolite.[28] This metabolite is believed to be a potent scavenger of cisplatin generated free radicals. However, in hypertensive rats, amifostine was less cardio protective than dexrazoxane and did not prevent doxorubicin weight loss or alter mortality.[28]

Other cardiovascular drugs, such as probucol, a lipid lowering drug, are also being used to limit cardiotoxicity by decreasing oxidative stress. Although there are a number of compounds that are in clinical use, there is concern related to off-target activity and potential interactions with primary chemotherapeutic agents.

Phenylaminoethyl selenide (PAESe) is a novel antioxidant, developed in the May laboratory to treat cardiovascular disease.[29-32] PAESe has been shown to exhibit potent antioxidant activity, reacting rapidly with many metabolic oxidants such as peroxide, peroxynitrite anion, and hydroperoxides. The selenoxide product generated from this antioxidant activity, phenylaminoethyl selenoxide (PAESeO), is then recycled back

readily to the selenide form by cellular reductants such as ascorbate and glutathione, with no complex side reactions.[19, 29, 33-37] Metabolic oxidants are known to react readily with DNA, resulting in base modifications and induction of double- and single-strand breaks.[19, 38] It has been demonstrated that GSH-mediated redox cycling of PAESe results in protection of DNA against oxidant-induced damage.[19]

In collaboration with Dr. Robert Arnold's research group at the University of Georgia, we have investigated the effect of phenylaminoalkyl selenides on cellular oxidative stress and anthracycline-induced cardiotoxicity without hindering the desirable anticancer properties. We have shown that PAESe has no effect on the antitumor activities of DOX, that free radical accumulation is decreased significantly when DOX or tert-buytlhydroperoxide (TBHP), a known oxidant, are codosed with PAESe, and that co-administration of PAESe shows noteworthy myocardium protection from DOX-induced cardiotoxicity.

4.2 METHODS AND MATERIALS

4.2.1 Materials PAESe was synthesized, purified and fully characterized as described previously [30, 34]. Vincristine was obtained from Calbiochem (La Jolla, CA), and F-12K Nutrient Mixture (Kaighn's Mod.) was obtained from Mediatech (Manassas, VA). CM-H_2DCFDA (5-(and-6)-chloromethyl-2',7'-dichlorodihydrofluorescein diacetate acetyl ester) was purchased from Invitrogen (Carlsbad, CA). Doxorubicin hydrochloride, *tert*-butylhydroperoxide (TBHP) and 3-(4,5-Dimethylthiazol-2-yl)-2,5-diphenyltetrazolium bromide (MTT) were obtained from Sigma-Aldrich Inc (St. Louis, MO). Acetic acid, dimethyl sulfoxide (DMSO), sulforhodamine B (SRB), trichloroacetic acid (TCA), tris(hydroxymethyl)aminomethane (TRIS), Fetal bovine serum and trypsin (0.25% w/v) were purchased from Thermo Fisher Scientific Inc. (Rockford, IL).

4.2.2 Cell lines Androgen-independent human prostate epithelial cells (PC-3) were obtained from American Type Culture Collection (ATCC) (Rockville, MD) and were cultured in F-12K media supplemented with 10% (v/v) FBS in a humidified cell culture chamber (NuAire Inc. Plymouth, MN) at 37˚C, 5% CO_2. Cells were passaged when they reached approximately 80-90% confluency.

4.2.3 Cytotoxicity of PAESe The cytotoxicity of PAESe on PC-3 growth inhibition was determined at 24, 48 and 72 h. PC-3 cells were seeded at 2×10^3 cells/well in 96 well plates with F-12K media supplemented with 10% (v/v) FBS and 100 U/mL of penicillin. Plates were incubated for 24 h prior to media change and replacement with serum supplemented media containing PAESe (0.1 to 10,000 nM). Plates were then incubated at 37˚C, 5% carbon dioxide for an additional 24, 48 or 72 h. Three independent studies were performed with 5 replicates at each concentration of PAESe. The growth inhibitory

effect was assessed at each time point using a mitochondrial enzymatic assay (MTT) and a protein binding assay (SRB), described below.

4.2.4 Growth inhibition of PAESe and DOX, Vincristine or TBHP The effect of PAESe on the cytotoxic effects of conventional anticancer agents, such as DOX (a topoisomerase II antagonist and known to cause free radical mediated cardiotoxicity) and vincristine (a tubulin binding drug), and a known oxidant, TBHP, was determined at or near their IC_{50}'s. PC-3 cells were seeded as described above, *Cytotoxicity of PAESe*. Twenty four hours after seeding, the media was withdrawn and replaced with serial dilutions of PAESe (100 to 10,000 nM in DMSO) and DOX (100 or 500 nM in DMSO) or vincristine (5 to 25 nM in DMSO) or TBHP (3 to 3,000 μM in PBS) to a final volume of 200 μL. Three independent studies were performed with 5 replicates for each concentration of PAESe. MTT and SRB assays were performed after 24, 48 and 72 h incubation time to determine effect on growth.

The effect of PAESe on the growth inhibition of DOX and TBHP in PC-3 cells was also determined under continuous exposure of PAESe. Serial concentrations of PAESe (10 to 10,000 nM) were treated to the PC-3 cells in combination with DOX (100 to 1,000 nM) or TBHP (3 to 300 μM) 24 h after seeding. To maintain PAESe concentration over study, concentrated PAESe (10 to 10,000 nM) was spiked into each well every 24 h after initial drug treatment. A second independent study was conducted where the media was replaced with fresh media and PAESe (10 to 10,000 nM) every 24 h (*i.e.,* at 24 and 48 h after initial drug exposure) after initial concomitant treatment to provide continuous antioxidant effect. The growth inhibitory effect was also determined by MTT and SRB assays after 72 h.

4.2.5 Assessment of cell growth and viability The cytotoxic effects of PAESe and/or DOX, vincristine, TBHP were tested using conventional MTT and SRB staining. MTT and SRB staining were performed as described previously.[39, 40] Briefly, 10 μL of MTT reagent were added to each well and plates were placed to the same conditions for 2 h. The resultant insoluble formazan was dissolved in 200 μL DMSO and absorbance was measured at 550 nm using Synergy H/T multi-mode microplate reader (BioTek Instruments, Inc., Winooski, VT). SRB staining was performed by fixing viable cells with 10% (w/v) TCA for 1 h at 4˚C. Fixed cells were stained with SRB dye for 5 min, and excess SRB was removed by washing plates with 1% (v/v) acetic acid. The absorbance of cellular protein-bound dye extracted by 10 mM TRIS buffer (pH 7.5) was determined at 490 nm using Synergy H/T multi-mode microplate reader. Mean ± standard error of the mean (SEM) was calculated and described as percent (%) of control.

4.2.6 ROS Generation Intracellular formation of ROS was determined by quantifying the oxidation of a non-fluorescent marker to its fluorescent product (DCF, 2',7'-dichlorofluorescein). Cell-permanent indicator CM-H_2DCFDA is known to detect several ROS such as hydrogen peroxide, hydroxyl radical, peroxynitrite anion$^-$ and peroxyl radical. Briefly, cells (2 x 10^5) were plated in 96 well plates and incubated for 24 h in 37˚C at 5% CO_2. CM-H_2DCFDA was dissolved in DMSO to make a concentrated stock solution and added to each well to final working concentration of 5 μM. After incubating cells at 37˚C for 30 min, the loading media was replaced with pre-warmed serum free media, and incubated at 37˚C for 10 min to allow the deacetylation and oxidation of the dye. Cells were then treated with different concentration of PAESe (0 to 1000 nM) and DOX (0 to 500 nM) or TBHP (0 to 300 μM), and were incubated at 37˚C

in darkness. Cells in the absence of drugs were used as controls. After 2 h, media was aspirated and 0.5% Triton X-100 (pH 7.4) in 0.01 M Tris-HCl (200 μL) was added to each wells for 5 min to detach the cells. Fluorescence intensity of the cell lysates (100 μL) was measured with a FLUOstar OPTIMA plate reader (BMG Labtech, Offenburg, Germany) at an excitation wavelength of 485 nm and an emission wavelength of 520 nm.

4.2.7 Tumor growth inhibition effect of PAESe Animal model Nude (NCr) mice (body weight, approx. 25 g) at 6-8 weeks of age were obtained from Taconic Farms, Inc., (Germantown, NY). Mice were maintained according to an approved Institutional Animal Care and Use Committee protocol at the University of Georgia and the U.S. Public Health Service Policy on Humane Care and Use of Laboratory Animals, updated 1996. Mice were kept in pathogen-free cages in a light and temperature-controlled isolated room and provided with standard rodent chow and sterile water *ad libitum* during the experimental periods. PC-3 cell suspension in serum free media (1×10^7 cells/mL) was mixed with ice-cold Matrigel (BD Biosciences, Franklin Lakes, NJ) in 1:1 (v/v), and 100 μL of the mixture was injected subcutaneously into the flank of nude mice to establish tumor xenograft. Tumor growth and body weight were monitored every other day. Tumor volume was assessed using digital calipers as described previously where the volume was the product of largest dimension and $(\text{smallest dimension})^2 \times 0.52$ [41]. When tumor volume reached approximately 200 mm^3, DOX and PAESe treatment were initiated, as described below. Mice were observed every other day until 1 week after the last injection for their general appearance as well as the treatment-mediated toxicities such as weight change, blood in stool, and decreased activity.

4.2.8 Effect of PAESe on antitumor activity of DOX Mice were divided into four treatment groups, control, DOX, PAESe and DOX+PAESe treated, n = 5 to 8 animals/group. DOX and PAESe were administered weekly by tail vein injections (each containing 5 mg/kg DOX and 10 mg/kg PAESe) over four weeks for a total of five injections and a total cumulative dose of 25 mg DOX/kg, and 50 mg PAESe/kg. Control animals were injected with the vehicle alone (saline-control) following the same dosing schedule. Two weeks after the last injection, mice were sacrificed by cervical dislocation under isoflurane anesthesia. The heart and tumor were excised rapidly, and stored in formalin solution at 4°C until paraffin embedding. The heart tissues were examined for histopathological evidence of cardiotoxicity. Tumor volume and body weight (mean ± SEM) for each group was plotted against time versus and normalized to tumor volume or body weight on day 0 (start of treatment).

4.2.9 Histological Examination For histological evaluation, four hearts from each treatment group were fixed in formalin solutions (10%, v/v) for 24 h, bisected longitudinally and embedded in paraffin. Serial sections were collected and stained with hematoxylin and eosin (H&E). A total of four sections from each heart were examined under a Nikon AZ100 stereo-fluorescent microscope mounted with a Nikon *DS-Qi1Mc color* camera. NIS-Elements image analysis software was used for processing. Micrographs were examined microscopically and evaluated for signs of anthracycline-mediated cardiotoxicity [42] by a pathologist who was initially blinded to their identity.

4.2.10 Statistical analysis Data from *in vitro* and *in vivo* studies were analyzed using one-way ANOVA followed by a post-hoc analysis (Dunnett's t-test), Sigma Stat (v3.1,

Systat Software Inc., San Jose, CA). Differences with a p-value ≤ 0.05 were regarded as statistically significant.

4.3 RESULTS AND DISCUSSION

The cytotoxic effects of PAESe on prostate cancer cells (PC-3) were assessed by measurement of MTT and SRB absorbance after 24, 48 and 72 h. MTT and SRB assays are colormetric indicators of cell viability that monitor active reductase enzymes and cellular protein density, respectively. As seen in Figure 4.3, PAESe did not inhibit *in vitro* growth significantly at 0.1 to 1,000 nM concentrations, but some growth inhibition was observed above 10 μM at 72 h.

The growth inhibition activity of PAESe in combination with DOX, vincristine and TBHP was determined in PC-3 cells. After 24 h seeding, PAESe and DOX or vincristine or TBHP were added into the each well, and then MTT and SRB assays were performed after 72 h exposure. As seen Figure 4.4 A, the cytotoxic activity of vincristine on PC-3 cells was not altered by the presence of PAESe, as expected. TBHP, which is a well-known potent oxidizing agent, was used as a positive control to determine the antioxidant activity of PAESe. TBHP exerted oxidative-mediated cytotoxicity on PC-3 cells when used alone. However, PAESe significantly (p-value <0.05) decreased this cytotoxic effect of TBHP when used in combination in a dose-dependent manner up to 300 μM, as expected (Figure 4.4B). In contrast, PAESe had limited effect on DOX's ability to decrease MTT and SRB staining of PC-3 cells when used in combination (Figure 4.4C). The same growth inbition pattersn were observed in continuous exposure studies, in which cells were either spiked with PAESe or media was replaced with fresh media and PAESe at 24 and 48 h after initial exposure. Additionally, it was observed that this additional exposure did not interfere with the cytotoxic activity of DOX or TBHP in PC-3 cells.

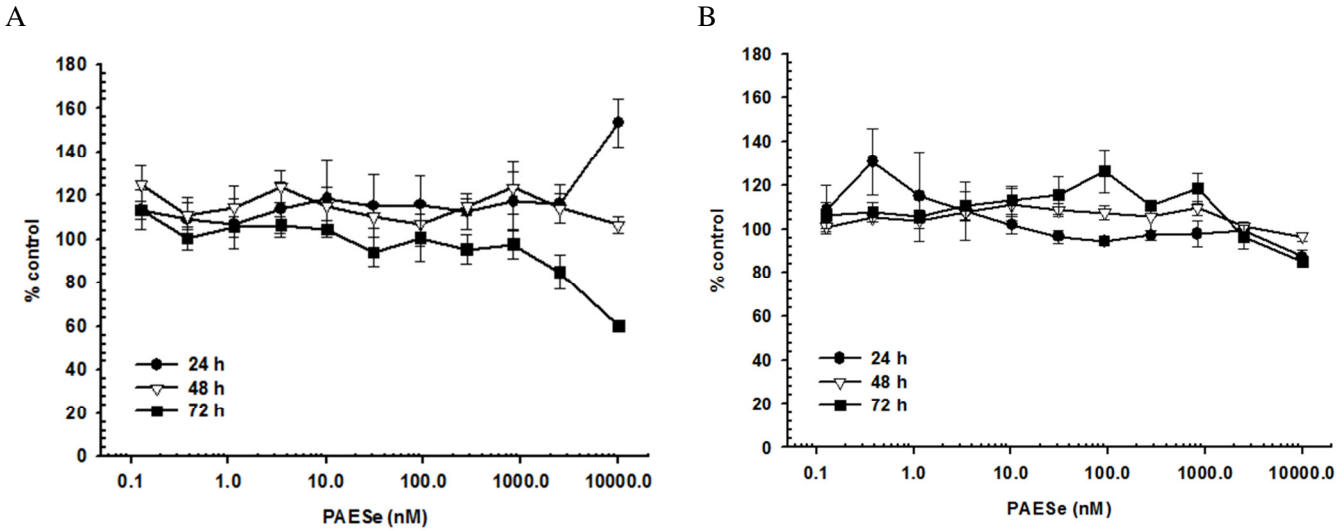

Figure 4.3. Effect of PAESe on the growth of PC-3 cells determined by A) MTT and B) SRB assay results. n=5

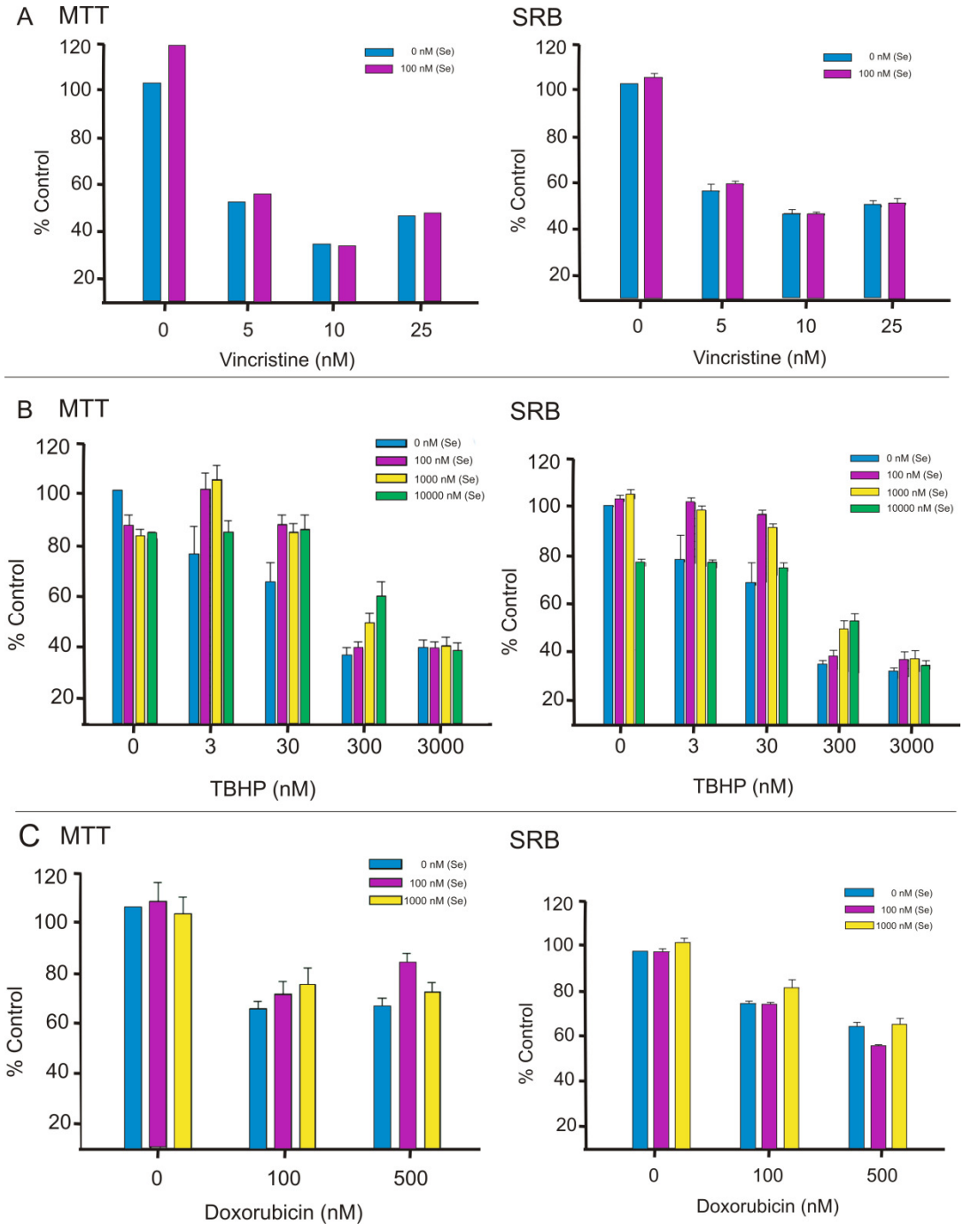

Figure 4.4. Effect of PAESe on the growth inhibition of vincristine (A), TBHP (B), and DOX (C) in PC-3 cells determined by MTT and SRB assays. n=5

We next investigated the effect of PAESe on DOX-mediated generation of intracellular oxidants using cell-permanent indicator, CM-H_2DCFDA to quantify production of free radicals. Preliminary studies suggested that ROS generation was maximal at 1 to 2 hours, but not detectable at 24 hours when cells were exposed to TBHP and/or PAESe, relative to control (data not shown). An increase in ROS was observed with increasing concentration of both DOX and TBHP, as expected (Table 4.1). However, generation of free radicals after exposure to TBHP and DOX was decreased significantly ($p < 0.05$) in the presence of PAESe in a dose-dependent manner. PAESe decreased free radicals generated from TBHP and DOX in a dose-dependent manner up to 300 μM and 500 nM, respectively.

Table 4.1. Effect of PAESe on THBP and DOX ROS generation

	TBHP		
	0 μM	30 μM	300 μM
0 nM	100	121 ± 7	193 ± 13
100 nM	103 ± 5	111 ± 5	150 ± 10*
1000 nM	101 ± 3	102 ± 4	142 ± 7*
	DOX		
	0 nM	100 nM	500 nM
0 nM	100	142 ± 9	184 ± 11
50 nM	105 ± 5	118 ± 5*	156 ± 8*
500 nM	191 ± 2	113 ± 5*	142 ± 9*

Mean ± SEM, *$p \leq 0.05$ vs. controls, 3 studies (n=5).

The effect of PAESe on antitumor activity of DOX was determined in an *in vivo* xenograft tumor model of human prostate cancer in NCr nude mice. Thirty two days after initiating treatment, the DOX group (5 mg/kg/week) had significantly smaller tumor volumes (223% ± 55) compared to controls (631% ± 204) (Figure 4.5A). Concomitant administration of DOX and PAESe did not significantly alter the antitumor activity of DOX (256% ± 65) compared to free DOX (223% ± 55), which agreed with the *in vitro* results. Interestingly, administration of PAESe alone also decreased tumor volume (196% ± 77) significantly relative to saline treated controls. There were no significant differences in tumor volume of PAESe alone or in combination with DOX relative to mice treated with free DOX. Body weight, a metric of gross systemic toxicity, was decreased significantly ($p < 0.05$) in DOX group (-8.62% ± 4.06) by day 32 (Figure 4.5B). Treatment with DOX+PAESe did result in an initial decrease in body weight, however, the observed decrease was found to be statistically insignificant when compared to control.

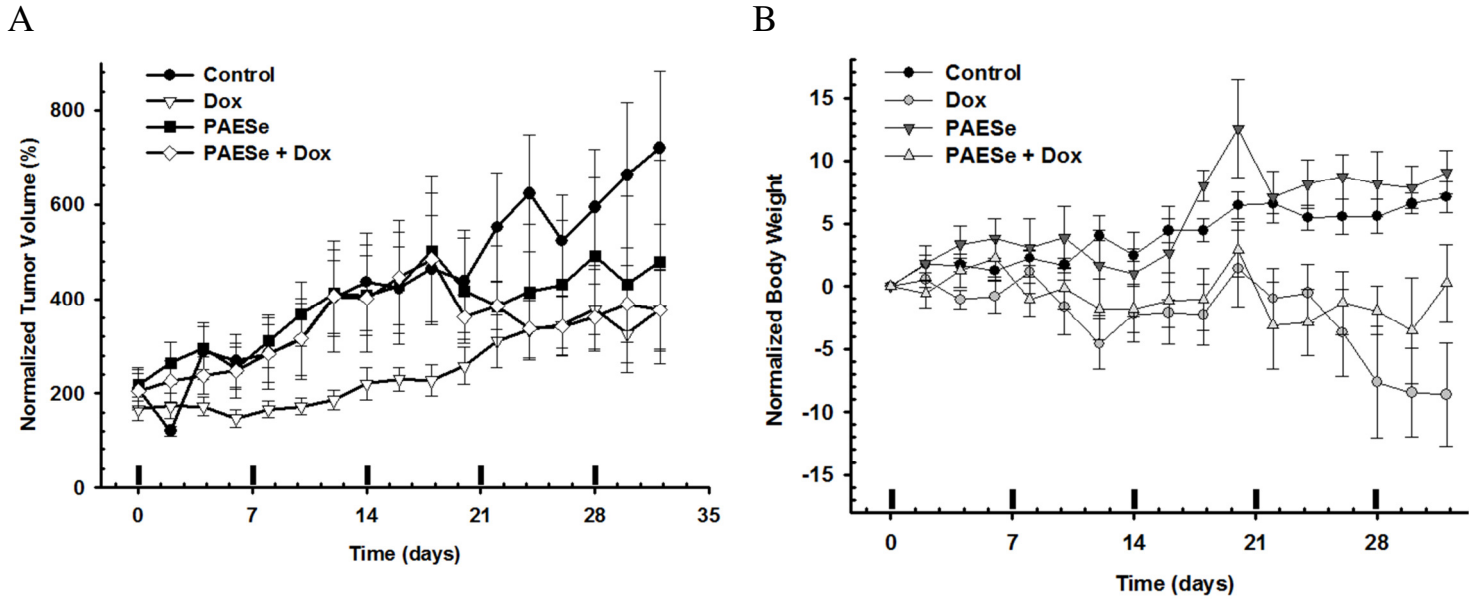

Figure 4.5. Effect of PAESe on antitumor activity of DOX in a PC-3 xenograft model monitored by tumor growth volume (A.) and body weight (B.).

Histopathological examination showed evidence of treatment-mediated differences between control and treatment groups. Micrographs of the myocardium of the left ventricular wall of control (Figure 4.6 A) and PAESe group (Figure 4.6 C) mice showed a histologically normal appearance. The myocardium was intact with faint outlines of cross striation. In contrast, the DOX group (Figure 4.6 B) exhibited evidence of treatment-mediated cardiotoxicity using a modification of the Jaenke (1974) method, where a slight change in scattered, single myocardial fibers and inflammation is evidence of low Grade 1 anthracycline mediated cardiotoxicity. No evidence of Grade 2 (scattered alterations in myocardial fibers throughout the myocardium), Grade 3 (moderate degree of change with disseminated myocardial fiber change throughout the section), or Grade 4 (marked degree of change with most myocardial fibers affected) was observed. In all of the DOX (4/4) treated animals minute inflammatory foci, Grade 1, were observed in each longitudinal section. Further, there was a disruption and fragmentation of the myofibers accompanied by a small focus of inflammatory infiltrate composed of small numbers of neutrophils and macrophages. This is a statistically significant difference from the DOX + PAESe group, in which only one of four hearts showed any signs of toxicity. In the DOX+PAESe group (Figure 4.6 D), one minute inflammatory focus was observed, with disruption and fragmentation of the myofibers. Overall, alterations in myocardial fibers and inflammatory foci were observed in 4/4 of the mice treated with DOX, whereas only 1/4 treated with DOX+PAESe. These data suggest that PAESe decreased myocardial early damage following DOX treatment.

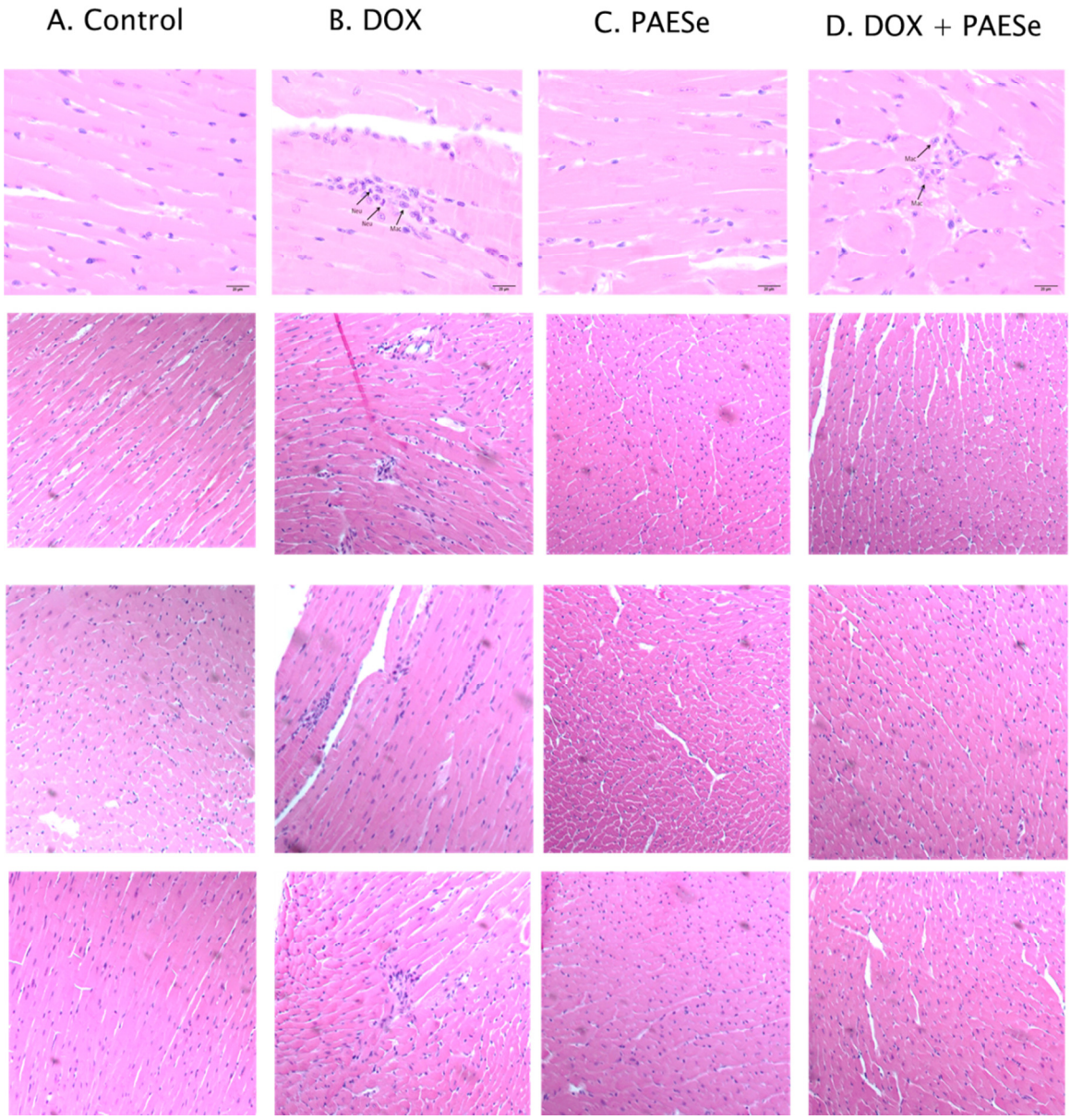

Figure 4.6. Micrographs of myocardium sections of control (A), DOX group (B), PAESe group (C), and DOX + PAESe group (D) stained with H&E.

The use of antioxidants may be a favorable approach to reduce the cardiotoxicity of anthracyclines, thereby improving clinical utility of these promising chemotherapeutic agents. Many studies have explored the use of antioxidants in diminishing DOX-induced cardiotoxicity [15]. A number of FDA approved drugs have been explored as chemoprotectants; however, questions remain over their potential to limit chemotherapeutic activity or synergistic potential to enhance non-cardiac toxicity.

PAESe was developed as potent antioxidant to treat cardiovascular disease. It has been shown that selenium redox cycling increases the free radical scavenging effects of PAESe against oxidant-induced DNA damage.[19] In this redox cycling process, the selenoxide-form of PAESe is produced when this selenide reduces cellular oxidants such as peroxide or peroxynitrite, and the selenoxide is then recycled back to PAESe by cellular reductants such as ascorbate and glutathione.

Up to 1 μM PAESe was found to have little to no cytotoxic effects to PC-3 cells after 72 h exposure. We then examined whether there would be an effect of PAESe on the antitumor activity of DOX. In this combination study, the range of 100 to 1,000 nM DOX were chosen based on the fact that clinically-relevant concentrations (*i.e.,* 1–100 % peak plasma concentration) are represented by 10–1000 nM.[43] We found that PAESe did not affect the antitumor activity with DOX in PC-3 cells at non-toxic or cytotoxic concentrations. The cytotoxicity of DOX has been correlated with antagonism of topoisomerase-2 rather than free radical generation, whereas cardiotoxicity has known to be more related with free radical formation.[44] PAESe did not alter the antitumor activity of vincristine, known to inhibit growth via tubulin polymerization. In contrast, the oxidant-mediated cytotoxicity of TBHP was decreased significantly ($p \leq 0.05$) in the

presence of PAESe in a dose-dependent manner up to 300 μM. These data suggest that PAESe may be useful in combination with DOX to preserve DOX's antitumor activity, but decrease the toxicity of its ROS on cardiomyocytes.

These results were further supported by the effect of PAESe on ROS formation, as estimated by CM-H_2DCFDA, a membrane permeable non-fluorescent reduced derivative of 2,7-dichlorofluorescein. The acetate groups of CM-H_2DCFDA are removed by esterase cleavage intracellularly; followed by oxidation that can be determined using a fluorescence microplate reader or visualized by fluorescence microscopy. CM-H_2DCFDA can detect several ROS including peroxynitrite, hydrogen peroxide, hydroxyl radical, and peroxy radical. Our results showed clearly that the ROS generation after DOX exposure was suppressed significantly in the presence of PAESe. These results further support the ability of PAESe to decrease DOX-mediated generation of a variety of ROS, without altering its antitumor activity.

We then examined whether *in vitro* results in which PAESe decreased ROS generation without altering the antitumor effects of DOX could be related to *in vivo* treatment. In a human prostate xenograft (PC-3) mouse model, concomitant administration of PAESe did not alter the antitumor activity of DOX as compared to DOX alone. These results are in agreement with our *in vitro* data showing PAESe did not alter the cytotoxic effect of DOX. These data also suggest that PAESe was able to reverse weight loss associated with continual doxorubicin treatment. This is in contrast to amifostine that improved cardiac function but didn't reverse weight loss or improve survival.[28]

It is noteworthy that administration of PAESe alone also had significant antitumor effects. The unexpected anticancer activity of PAESe might be associated with altering *in vivo* immune function. Antioxidants have been shown to enhance not only the activity of several immune cells such as lymphocytes, macrophage and mononuclear cells but also the cytotoxicity of natural killer cells, which are known to destroy tumors in a non-specific fashion.[45] Also, immune function has known to be increased by up-regulation of the interleukin-2 receptors expression as well as the responsiveness of T cell to interleukin-2 through antioxidant activity. Unlike *in vitro* studies, tumor cells could be more vulnerable to the activity of chemotherapeutic agents in an *in vivo* system because of the immune-enhancing effect of PAESe to increase the cytotoxic activity of a variety of immune cells as demonstrated in animal and human studies.[45] It should be noted that the NCR mice contain a Fox1n1^{nu} mutation that alters immune function, permitting implantation of tumor xenografts, but does not render the animal completely devoid of immune function. This is a possible explanation for the increase in antitumor activity of PAESe alone, but further studies are needed.

Histological examinations supported the hypothesis that PAESe can reduce DOX-mediated cardiotoxicity. The myocardium of mice treated PAESe alone was intact and similar to the control. Early cardiac damage such as disrupted myocardial fibers, immune cell infiltration, and inflammation [42, 46] were observed in all sections after DOX treatment and only observed in one tissue section of an animal treated concomitantly with DOX with PAESe.

In conclusion, we have successfully demonstrated that PAESe exhibited *in vivo* antitumor activity in the absence of cardiotoxicity and weight loss associated with DOX.

Further, concomitant administration of PAESe did not alter DOX antitumor activity, but did limit DOX-mediated cardiotoxicity and decreased DOX-mediated weight loss. These effects are believed to be related to its potent antioxidant activity, as assessed by *in vitro* growth inhibition assays, alteration in ROS generation, *in vivo* tumor growth inhibition and histopathological examination. The benefits of this study are worthwhile because this is the first to demonstrate the ability of PAESe to reduce DOX-induced cardiotoxicity and weight loss, without altering its antitumor activity, suggesting that concomitant administration of PAESe could be used to improve the clinical utility of DOX.

4.4 FUTURE WORK

The effectiveness of anthracyclines and the lack of positive results from synthetic analogues have sparked interest in other methods of anthracycline-induced cardiotoxicity mediation. One method, the co-administration of an antioxidant supplement pharmaceutical has been discussed in previous sections. The encapsulation of anthracyclines into nanocarriers is a second approach to mediate cardiotoxicity and has been shown in preclinical trials to be effective in attenuating anthracycline-induced-toxicity with as effective or greater antitumor activity.

Liposomes generally extravasate in areas where capillaries are disrupted and in organs lined with fenestrated endothelial barriers and without tight junctions (e.g. liver, spleen, and bone marrow). Because of this behavior, DOX- liposomal formulations would be expected to be directed away from the myocardium, which is supplied by vessels with tight junctions. This solution is problematic; liposomes are susceptible to rapid clearance by phagocytic cells of the reticuloendothelial system, possibly reducing the amount of DOX placed in the tumor.

It has been reported that a polyethylene glycol layer applied to liposomes causes the impairment of uptake by the reticuloendothelial system and mononuclear phagocyte system; therefore, increasing liposomal serum and plasma half-lives. Compared to conventional administration in which DOX enters tissues as a concentrated pulse, pegylated DOX liposomes cause DOX to be slowly released over days, and change the biodistribution to be primarily cancer cells. This results in the portion of bioavailable DOX at the tumor site at any one time is several times higher than in normal tissues. As a result of this conduct, pegylated DOX formulations are able to decrease cardiotoxicity

while still maintain the highly desirable antitumor activity. Papahadjopoulos et al. reported peak drug levels measured in heart muscle were lower for pegylated liposomal DOX than for traditional DOX.[47] For example, in preclinical studies, Working et al. report when comparing myocardium damage in dogs treated with conventional DOX or pegylated liposomal DOX up to a cumulative dose of 10 mg/kg, dogs receiving the conventional DOX showed vacuolization and myofibrillar loss in the myocardium while dogs receiving the pegylated liposomal formulation showed no histological evidence of cardiotoxicity either 1 or 5 weeks after treatment.[48] In a clinical trial, patients treated with pegylated liposomal DOX for AIDS-related Kaposi's sarcoma had lower biopsy scores compared to those of conventional DOX (0.3 compared to 3.0) despite receiving higher cumulative doses of drug.[49]

Some liposomal anthracycline formulations are currently used in clinic, including liposomal daunorubicin (DaunoXome®), liposomal doxorubicin (Myocet®, D-99), and pegylated liposomal DOX (Doxil® and Caelyx®). While the encapsulation of the drug alone has been shown to reduce cardiotoxicity, there is still room for improvement. It is possible that the combination of the two methods of cardiotoxicity mediation would result in the desired decrease in toxicity. The encapsulation of both antitumor drug and antioxidant in the same formulation may be a promising solution.

Our laboratory in collaboration with the Arnold laboratory (University of Georgia, Athens Ga) have been working on encapsulating phenylaminoalkyl selenides in pegylated liposomal formulations used as a nanocarrier for DOX. This continuation of this research and the investigation of the co-encapsulation could possibly demonstrate the ability of the phenylaminoalkyl selenides to be effect supplements for reducing

anthracycline-induced cardiotoxicity and could possibly demonstrate the further reduction of cardiotoxicity by combining pegylated liposomal encapsulation as well as concomitant delivery with an antioxidant.

4.5 REFERENCES

1. Hande, K. R., Clinical applications of anticancer drugs targeted to topoisomerase II. *Biochimica et Biophysica Acta (BBA) - Gene Structure and Expression* 1998, 1400, (1-3), 173-184.

2. Tewey, K. M.; Rowe, T. C.; Yang, L.; Halligan, B. D.; Liu, L. F., Adriamycin-induced DNA damage mediated by mammalian DNA Topoisomerase II. *Science* 1984, 226, 466-468.

3. Bachur, N. R.; Robin, J.; Hickey, R.; Wu, Y.; Malkas, L., Helicase inhibition by anthracycline anticancer agents. *Molecular Pharmacology* 1992, 41, 993-998.

4. Mizutani, H.; Tada-Oikawa, S.; Hiraku, Y.; Kojima, M.; Kawanishi, S., Mechanism of apoptosis induced by doxorubicin through the generation of hydrogen peroxide. *Life Sciences* 2005, 76, 1439-1453.

5. Chen, Y.; Jungsuwadee, P.; Vore, M.; Butterfield, D. A.; Clair, D. K. S., Collateral damage in cancer chemotherapy: Oxidative stress in nontargeted tissues. *Molecular Interventions* 2007, 7, (3), 147-156.

6. Cassidy, S. C.; Chan, D. P.; Rowland, D. G.; Allen, H. D., Effects of doxorubicin on diastolic function, contractile reserve, and ventricular–vascular coupling in piglets. *Pediatric Cardiology* 1998, 19, (6), 450-457.

7. Saeki, K.; Obi, I.; Ogiku, N.; Shigekawa, M.; Imagawa, T.; Matsumoto, T., Doxorubicin directly binds to the cardiac-type ryanodine receptor. *Life Sciences* 2002, 70, (20), 2377-2389.

8. Tokarska-Schlattner, M.; Zaugg, M.; Zuppinger, C.; Wallimann, T.; Schlattner, U., New insights into doxorubicin-induced cardiotoxicity: The critical role of cellular energetics. *Journal of Molecular and Cellular Cardiology* 2006, 41, 389-405.

9. Swain, S. M.; Whaley, F. S.; Ewer, M. S., Congestive heart failure in patients treated with doxorubicin. *Cancer* 2003, 97, (11), 2869-2879.

10. Freter, C. E.; Lee, T., C.; Billingham, M. E.; Chak, L.; Bristow, M. R., Doxorubicin cardiac toxicity manifesting seven years after treatment. Case report and review. *The American Journal of Medicine* 1986, 80, (3), 483-485.

11. Billingham, M. E.; Mason, J. W.; Bristow, M. R.; Daniels, J. R., Anthracycline cardiomyopathy monitored by morphologic changes. *Cancer treatment reports* 1978, 62, (6), 865-72.

12. Gewirtz, D. A., A critical evaluation of the mechanisms of action proposed for the antitumor effects of the anthracycline antibiotics adriamycin and daunorubicin. *Biochemical Pharmacology* 1999, 57, (7), 727-741.

13. Fujita, N.; Hiroe, M.; Ohta, Y.; Horie, T.; Hosoda, S., Chronic Effects of Metoprolol on Myocardial [beta]-Adrenergic Receptors in Doxorubicin-Induced Cardiac Damage in Rats. *Journal of Cardiovascular Pharmacology* 1991, 17, (4), 656-661.

14. Revis, N. W.; Marusic, N., Glutathione peroxidase activity and selenium concentration in the hearts of doxorubicin-treated rabbits. *Journal of Molecular and Cellular Cardiology* 1978, 10, (10), 945-948.

15. Quiles, J. L.; Huertas, J. s. R.; Battino, M.; Mataix, J.; RamÌrez-Tortosa, M. C., Antioxidant nutrients and adriamycin toxicity. *Toxicology* 2002, 180, (1), 79-95.

16. Wang, S.; Konorev, E. A.; Kotamraju, S.; Joseph, J.; Kalivendi, S.; Kalyanaraman, B., Doxorubicin induces apoptosis in normal and tumor cells via distinctly different mechanisms. *The Journal of Biological Chemistry* 2004, 279, (24), 25535-25543.

17. Handa, K.; Sato, S., Generation of free radicals of quinone group-containing anti-cancer chemicals in NADPH-microsome system as evidenced by initiation of sulfite oxidation. *Gann* 1975, 66, (1), 43-7.

18. Zhou, S.; Palmeira, C. M.; Wallace, K. B., Doxorubicin-induced persistent oxidative stress to cardiac myocytes. *Toxicology Letters* 2001, 121, (3), 151-157.

19. De Silva, V.; Woznichak, M. M.; Burns, K. L.; Grant, K. B.; May, S. W., Selenium redox cycling in the protective effects of organoselenides against oxidant-induced DNA damage. *Journal of the American Chemical Society* 2004, 126, 2409-2413.

20. Doroshow, J. H.; Locker, G. Y.; Myers, C. E., Enzymatic Defenses of the Mouse Heart Against Reactive Oxygen Metabolites: Alterations produced by doxorubicin. *The Journal of Clinical Investigation* 1980, 65, (1), 128-135.

21. Tan, C.; Tasaka, H.; Yu, K.-P.; Murphy, L. M.; Karnofsky, D. A., Daunomycin, an antitumor antibiotic, in the treatment of neoplastic disease. *Cancer* 1967, 20, (3), 333-353.

22. Weiss, R. B., The anthracyclines: Will we ever find a better Doxorubicin? *Seminars in Oncology* 1992, 19, (6), 670-686.

23. Yagmurca, M.; Fadillioglu, E.; Erdogan, H.; Ucar, M.; Sogut, S.; Irmak, M. K., Erdosteine prevents doxorubicin-induced cardiotoxicity in rats. *Pharmacological Research* 2003, 48, (4), 377-382.

24. Shimpo, K.; Nagatsu, T.; Yamada, K.; Sato, T.; Niimi, H.; Shamoto, M.; Takeuchi, T.; Umezawa, H.; Fujita, K., Ascorbic acid and adriamycin toxicity. *The American Journal of Clinical Nutrition* 1991, 54, (6), 1298S-1301S.

25. Wahab, M. H.; Akoul, E. S.; Abdel Aziz, A. A., Modulatory effects of melatonin and vitamin E on doxorubicin-induced cardiotoxicity in Ehrlich ascites carcinoma-bearing mice. *Tumori* 2000, 86, (2), 157-62.

26. Pearlman, M.; Jendiroba, D.; Pagliaro, L.; Keyhani, A.; Liu, B.; Freireich, E. J., Dexrazoxane in combination with anthracyclines lead to a synergistic cytotoxic response in acute myelogenous leukemia cell lines. *Leuk Res* 2003, 27, (7), 617-26.

27. Tebbi, C. K.; London, W. B.; Friedman, D.; Villaluna, D.; De Alarcon, P. A.; Constine, L. S.; Mendenhall, N. P.; Sposto, R.; Chauvenet, A.; Schwartz, C. L., Dexrazoxane-associated risk for acute myeloid leukemia/myelodysplastic syndrome and other secondary malignancies in pediatric Hodgkin's disease. *J Clin Oncol* 2007, 25, (5), 493-500.

28. Herman, E. H.; Zhang, J.; Chadwick, D. P.; Ferrans, V. J., Comparison of the protective effects of amifostine and dexrazoxane against the toxicity of doxorubicin in spontaneously hypertensive rats. *Cancer Chemother Pharmacol* 2000, 45, (4), 329-34.

29. May, S. W.; Pollock, S. H., Selenium-based antihypertensives. Rationale and potential. *Drugs* 1998, 56, 959-964.

30. May, S. W.; Wang, L. Q.; Gill-Woznichak, M. M.; Browner, R. F.; Ogonowski, A. A.; Smith, J. B.; Pollock, S. H., An orally active selenium-based antihypertensive agent with restricted CNS permeability. *Journal of Pharmacology and Experimental Therapeutics* 1997, 283, 470-477.

31. May, S. W., Selenium-based drug design: rationale and therapeutic potential. *Expert Opinion on Investigational Drugs* 1999, 8, 1017-1030.

32. May, S. W., Selenium-based pharmacological agents: an update. *Expert Opinion on Investigational Drugs* 2002, 11, 1261-1269.

33. May, S. W.; Herman, H. H.; Roberts, S. F.; Ciccarello, M. C., Ascorbate depletion as a consequence of product recycling during dopamine beta-monooxygenase catalyzed selenoxidation. *Biochemistry* 1987, 26, 1626-1633.

34. Overcast, J. D.; Ensley, A. E.; Buccafusco, C. J.; Cundy, C.; Broadnax, R. A.; He, S.; Yoganathan, A. P.; Pollock, S. H.; Hartley, C. J.; May, S. W., Evaluation of cardiovascular parameters of a selenium-based antihypertensive using pulsed Doppler ultrasound. *J. Cardiovasc. Pharmacol.* 2001, 38, 337-346.

35. Pollock, S. H.; Herman, H. H.; Fowler, L. C.; Edwards, A. S.; Evans, C. O.; May, S. W., Demonstration of the antihypertensive activity of phenyl-2-aminoethyl selenide. *Journal of Pharmacology and Experimental Therapeutics* 1988, 246, 227-234.

36. Woznichak, M. M.; Overcast, J. D.; Robertson, K.; Neumann, H. M.; May, S. W., Reaction of phenylaminoethyl selenides with peroxynitrite and hydrogen peroxide. *Archives of Biochemistry and Biophysics* 2000, 379, 314-320.

37. Cowan, E. A.; Oldham, C. D.; May, S. W., Identification of a thioselenurane intermediate in the reaction between phenylaminoalkyl selenoxides and glutathione. *Archives of Biochemistry and Biophysics* 2011, 506, (2), 201-207.

38. Henle, E. S.; Linn, S., Formation, Prevention, and Repair of DNA Damage by Iron/Hydrogen Peroxide. *Journal of Biological Chemistry* 1997, 272, (31), 19095-19098.

39. Mosmann, T., Rapid colorimetric assay for cellular growth and survival: Application to proliferation and cytotoxicity assays. *Journal of Immunological Methods* 1983, 65, (1-2), 55-63.

40. Skehan, P.; Storeng, R.; Scudiero, D.; Monks, A.; McMahon, J.; Vistica, D.; Warren, J. T.; Bokesch, H.; Kenney, S.; Boyd, M. R., New Colorimetric Cytotoxicity Assay for Anticancer-Drug Screening. *Journal of the National Cancer Institute* 1990, 82, (13), 1107-1112.

41. Davol, P. A.; Frackelton, A. R., Targeting human prostatic carcinoma through basic fibroblast growth factor receptors in an animal model: Characterizing and circumventing mechanisms of tumor resistance. *The Prostate* 1999, 40, (3), 178-191.

42. Jaenke, R. S., An anthracycline antibiotic-induced cardiomyopathy in rabbits. *Lab Invest* 1974, 30, (3), 292-304.

43. Kurbacher, C. M.; Wagner, U.; Kolster, B.; Andreotti, P. E.; Krebs, D.; Bruckner, H. W., Ascorbic acid (vitamin C) improves the antineoplastic activity of doxorubicin, cisplatin, and paclitaxel in human breast carcinoma cells in vitro. *Cancer Letters* 1996, 103, (2), 183-189.

44. Keizer, H. G.; Pinedo, H. M.; Schuurhuis, G. J.; Joenje, H., Doxorubicin (adriamycin): A critical review of free radical-dependent mechanisms of cytotoxicity. *Pharmacology & Therapeutics* 1990, 47, (2), 219-231.

45. Patrick, L., Selenium Biochemistry and Cancer: A Review of the Literature. *Alternative Medicine Review* 2004, 9, (3), 239-258.

46. Weinstein, D. M.; Mihm, M. J.; Bauer, J. A., Cardiac Peroxynitrite Formation and Left Ventricular Dysfunction following Doxorubicin Treatment in Mice. *Journal of Pharmacology and Experimental Therapeutics* 2000, 294, (1), 396-401.

47. Papahadjopoulos, D.; Allen, T. M.; Gabizon, A.; Mayhew, E.; Matthay, K.; Huang, S. K.; Lee, K.-D.; Woodle, M. C.; Lasic, D. D.; Redemann, C.; Martin, F. J., Sterically Stabilized Liposomes: Improvements in Pharmacokinetics and Antitumor Therapeutic Efficacy. *Proc. Natl. Acad. Sci. USA* 1991, 88, 11460-11464.

48. Working, P. K.; Newman, M. S.; Sullivan, T.; Yarrington, J., Reduction of the Cardiotoxicity of Doxorubicin in Rabbits and Dogs by Encapsulation in Long-Circulating, Pegylated Liposomes. *The Journal of Pharmacology and Experimental Therapeutics* 1999, 289, (2), 1128-1133.

49. Berry, G.; Billingham, M.; Alderman, E.; Richardson, P.; Torti, F.; Lum, B.; Patek, A.; Martin, F. J., The Use of Cardiac Biopsy to Demonstrate Reduced Cardiotoxicity in AIDS Kaposi's Sarcoma Patients Treated with Pegylated Liposomal Doxorubicin. *Annals of Oncology* 1998, 9, (7), 711-716.

CHAPTER 5

CIBER: CENTER FOR INNOVATIVE BIOMATERIAL EDUCATION AND RESEARCH

5.1 Introduction

CIBER, The Center for Innovative Biomaterial Education and Research, is a multidisciplinary program focused on developing biomaterials from renewable resources and educating the public, scientists and engineers on the needs, opportunities, benefits, and issues surrounding biomass conversion. Two main goals were set for the CIBER project: 1) The use of chemical and enzymatic polymerizations to create monomers and polymers from compounds originating from cellulose, lignin, and other biomass sources. Lipases and other enzymes were investigated to create novel monomers and biodegradable polymers. 2) The construction of a website to serve as an outreach tool educating students, teachers and the general public on the benefits of investing in biodegradable products, and their sources. This website would also be used as a resource for scientist in the field.

The field of creating usable materials from biomass sources is a large and steadily growing area of research. Today, biomaterials, defined as a material made solely from natural or a combination of natural and chemical components, is used in many industries; a few examples are, medical device, pharmaceutical, carpeting, automotive, plastics and energy. Biodegradable polymers, are polymers that are broken down by the action of living organisms, and constitute a large part of the biomaterial field. Conventional, chemical polymerizations can involve many undesirable attributes, including extreme

temperatures, toxic reactants and solvents, and low yields. Compared to chemical catalysis, enzymes allow reactions to be carried out under mild reaction conditions, provide high selectivity for substrates and reaction modes, eliminate problematic byproducts and are highly effective.

Enzymes have entered the field of organic synthetic chemistry as powerful catalysts for stereo- and regioselective reactions and allowing a strategy for synthesis or polymers, some of which are difficult to produce. The elimination of harsh reaction environments and of the need for toxic chemicals has made enzymatic polymerization an attractive way to achieve "green chemistry'. Lipases, enzymes that catalyze the hydrolysis of fatty acids, are commonly used as polymerization catalyst. Lipases have been shown to be stable in organic solvents and perform a broad spectrum of reactions, including etherification, transesterification, condensation, and Michael addition reactions.

Candida Antarctica Lipase B (CALB) (Figure 5.1), due to its broad range of substrates and its ability to form different types of bonds, is one of the most common enzymes chosen for polymerization.[1-5] First crystallized in 1994, CALB is a 33kDa lipase with 3 disulphide bonds.[6] The catalytic triad, Ser105, His224, and Asp187 lie at the bottom of the catalytic pocket. Two parallel channels lead from the active site serine out to the surface of the molecule. These channels are known as the large, nonselective acyl pocket and the smaller alcohol pocket, responsible for the stereoselectivity of the enzyme.[7] Being one of the few lipases that accept secondary alcohols preferentially, it has been used in research and industry for the synthesis monomers and biodegradable polymers.[8-15] We have been using molecular modeling to investigate the stereoselectivity of CALB towards secondary alcohols and other small molecule substrates. In addition,

we explored the use of CALB as a catalyst for l Michael addition reactions.

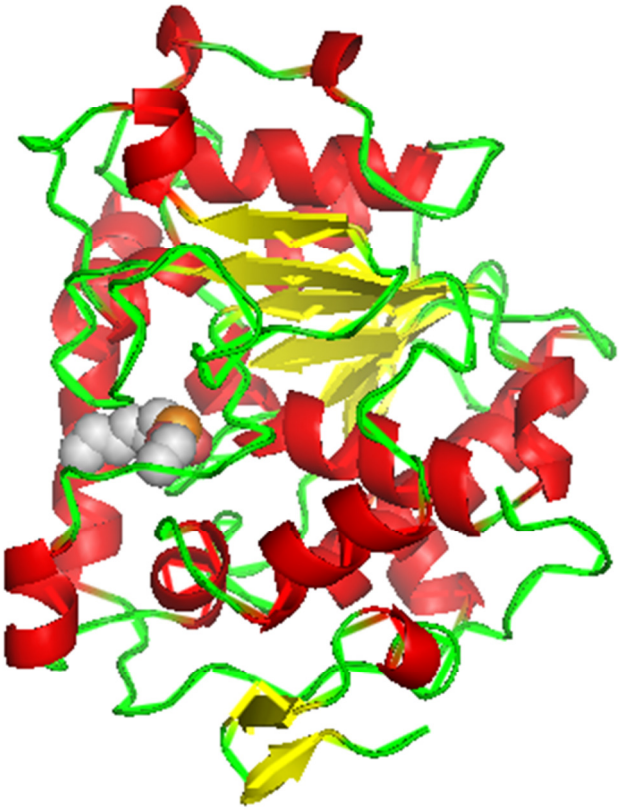

Figure 5.1. *Candida antarctica* Lipase B with bound n-Hexylphosphonate ethyl ester.

5.2 METHODS AND MATERIALS

5.2.1 Molecular Docking Simulations were run using Molecular Operating Environment (MOE) software, Chemical Computing Group, Inc. (Montreal, Canada). Ligands were constructed using MOE builder module. Polar hydrogens were added to the ligands and were minimized using the Engh-Huber force field with default parameters and 'solvation' embedded. The receptor used for molecular docking was the CALB crystal structure reported by Uppenberg *et al.*[7] (PDB ID 1LBS).

5.2.2 CALB catalyzed Michael Additions Michael addition reactions were carried out in bulk, with solvents. To a round bottom flask containing thiol or dithiol and acrylonitrile (1:2 molar ratio), 60mg CALB beads (Novozyme 435) were added. CALB beads were vacuum dried for 24hr prior to use. Reaction mixtures were allowed to reaction at temperatures 25-60°C, with mixing by shaking at 200 rpm for 48 to 96 hr. Reactions were quenched by removal of enzyme beads and diluted with methanol, acetone, or hexane for GC-MA analysis.

5.3 RESULTS

5.3.1 Molecular Modeling Results

Chiral secondary alcohols are building blocks in the preparation of natural products, chemicals and pharmaceuticals. Enzymatic resolution with lipases has become one of the more common methods for preparation of enantiomerically pure alcohols. CALB has been shown to have a high natural enantioselectivity towards secondary alcohols. Adam *et al.* [16] reported that CALB exhibited the best results out of several lipases for the kinetic resolution of α-hydroxy valeric acid. The (*S)*-enantiomer was shown to be the preferred, having an enantiomeric excess of 80% at 55% conversion, while the (*R*)-enantiomer was left unreacted with an enantiomeric excess of 99%. The authors reported results from kinetic analysis, but neglected to give any structural reason for the difference between the preferred (*S*)-enantiomer and the unreactive (*R*)-enantiomer.

Using literature and modeling data, sought to better understand the enantiospecificity of *Candida antarctica* Lipase B (CALB) for secondary alcohols and other small molecule substrates. Modeling software, Molecular Operating Environment (MOE), was used to model the binding of different enantiomers of CALB substrates in the enzyme's active site. Substrates were built individually, energy minimized and docked into an energy-minimized structure derived from the crystal structure shown in Figure 14.[7] The results from the docking simulation were ranked by a combination of 1) the sum of Gaussians over all ligand atom-receptor atom pairs and ligand atom-alpha sphere pairs, 2) the affinity scoring dG function, whose terms address atomic contacts of

specific types, and 3) an estimated self-energy of the ligand. The lowest value of this combination was taken as the best conformation.

The preferred (*S*)- and the unreactive (*R*)-enantiomers of 2-hydroxy valeric acid were docked individually in the CALB active site using MOE. The best result from each docking was then superimposed in the active site of CALB in order to visualize any differences when binding. As shown in Figure 5.2A, the (*R)*-enantiomer is centered in the active site, while the (*S*)-enantiomer is positioned more to the right, closer to the catalytic residues of the active site. As shown in Figure 5.2B, the *(S)*-enantiomer binds in an orientation in which the carbonyl carbon is closer to the catalytic residue, Serine 105, than the (*R*)-enantiomer. Uppenberg *et al.*[7] pointed out the importance of the epsilon amine of histidine 224 in the catalysis of the hydrolysis reaction by CALB. The alcohol oxygen of the substrate must be able to receive a proton from the nitrogen of the enzyme. When examining at the interactions between the enantiomers and the catalytic residues of the active site, it is noticeable that the (*S*)-enantiomer is closer to the histidine, with a distance of 3.91 Å between oxygen of the alcohol and the hydrogen of the histidine (Figure 5.3). The oxygen of the (*R*)-enantiomer is further from the histidine with 5.20Å between the two atoms (Data not shown). When considering this important interaction the only probable reactive enantiomer is the (*S*)-enantiomer.

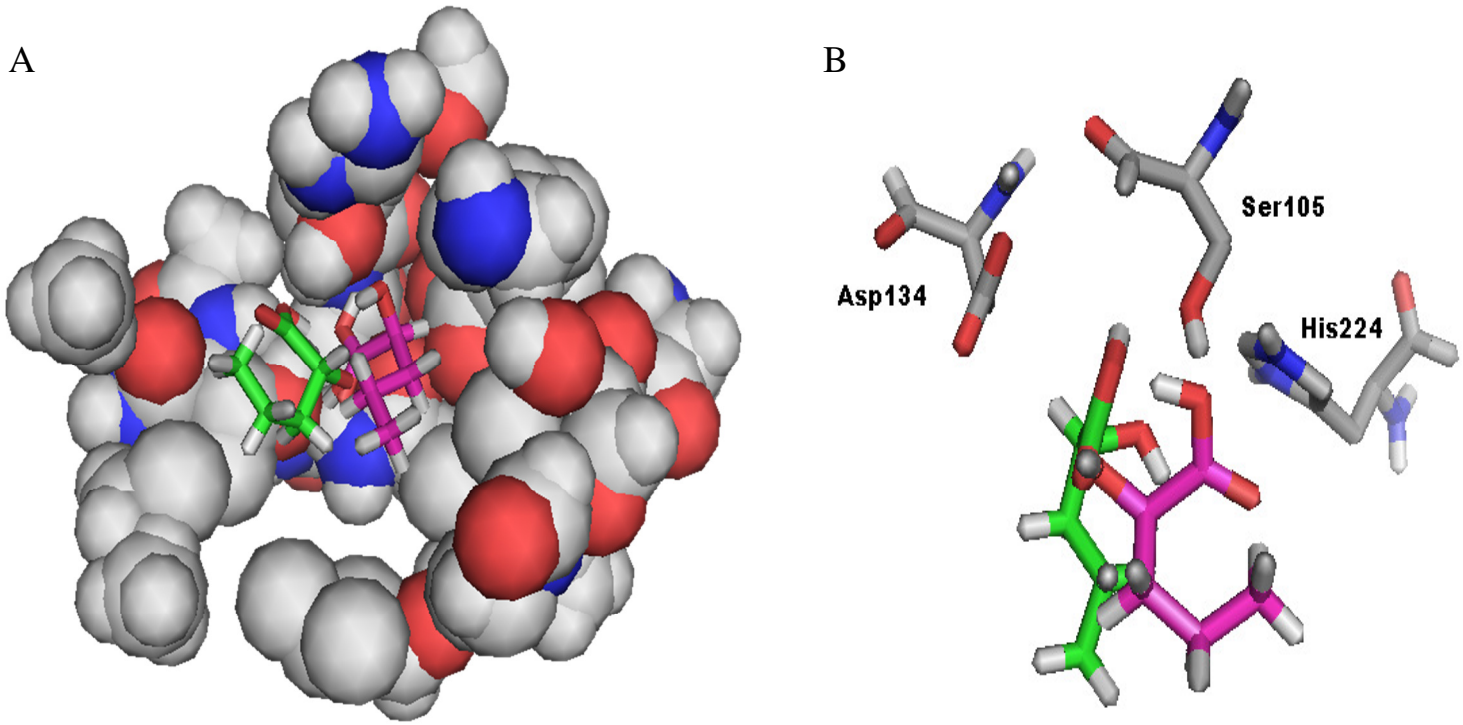

Figure 5.2. (*R*)- and (*S*)-2-hydroxy valeric acid in the active site of CALB. Color scheme CALB: blue- Nitrogen, red- Oxygen, large grey - Carbon, small grey- Hydrogen; A. (*R*) and (*S*)-2-hydroxy valeric acid: red- Oxygen, white- Hydrogen, *(R)*- green- Carbon, (*S*)-purple- Carbon. A. CALB spacefill with (*R*)- and (*S*)-enantiomers in stick form. B. CALB catalytic triad with both enantiomers docked in the same configuration as in A.

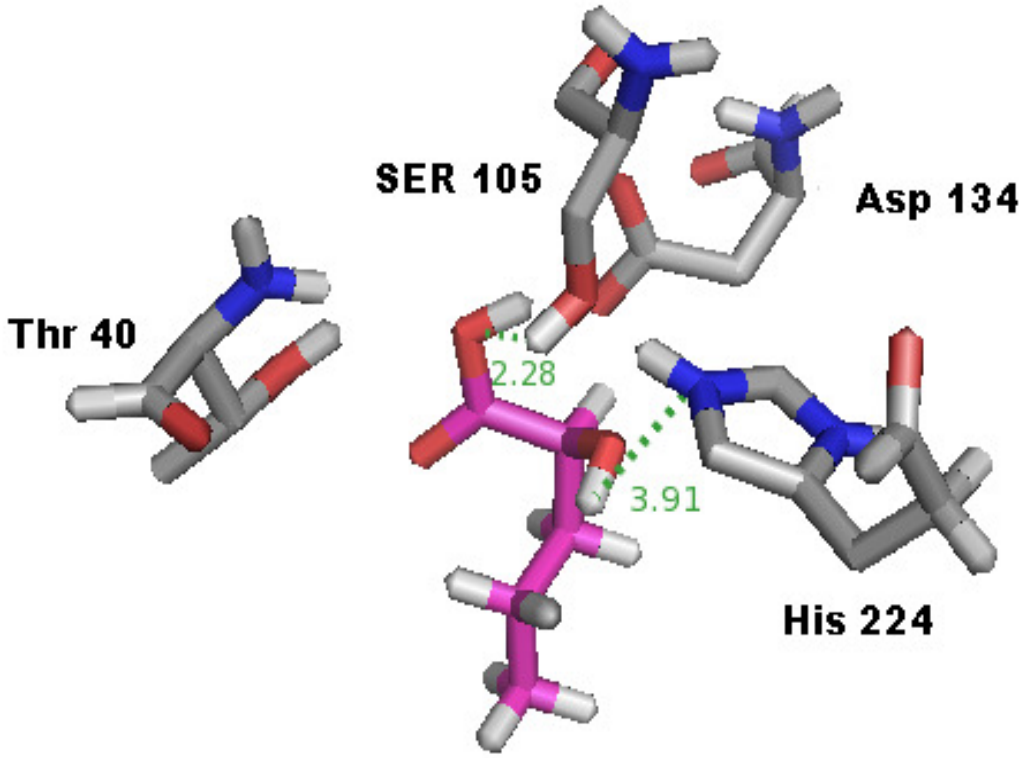

Figure 5.3. Distances of hydrogen bonds detected by MOE between the bound (*S*)-2-hydroxy valeric acid and the CALB active site. The distance from the epsilon amine of His224 to the alcohol oxygen of the α-hydroxy acid is 3.91Å. The color scheme is the same as in Figure 5.2.

5.3.2 CALB catalyzed Michael Adduct Monomers

We successfully used CALB as a catalyst to synthesize, via Michael addition reactions, novel compounds that can further be used as monomers in polymerization reactions via enzymatic and non-enzymatic catalyzed reactions. Primary and secondary amines and thiols were used as nucleophiles. The Michael addition reaction is a common reaction in synthetic organic chemistry between a nucleophile and an α,β-unsaturated carbonyl compound. Recently, the reaction has been employed by polymer chemists for the synthesis of linear, graft, hyperbranched, dendritic, and network polymers.[17] Usually these reactions are catalyzed by strong bases, causing unwanted side reactions with starting materials and products. In the base-catalyzed Michael addition mechanism (Figure 5.4), the Michael acceptor is first deprotonated by the base resulting in a carbanion. The nucleophile then reacts and proton extraction by the enolate leads to the final Michael adduct. Common catalysts for Michael additions in organic chemistry are transition metals and lanthanides.[18]

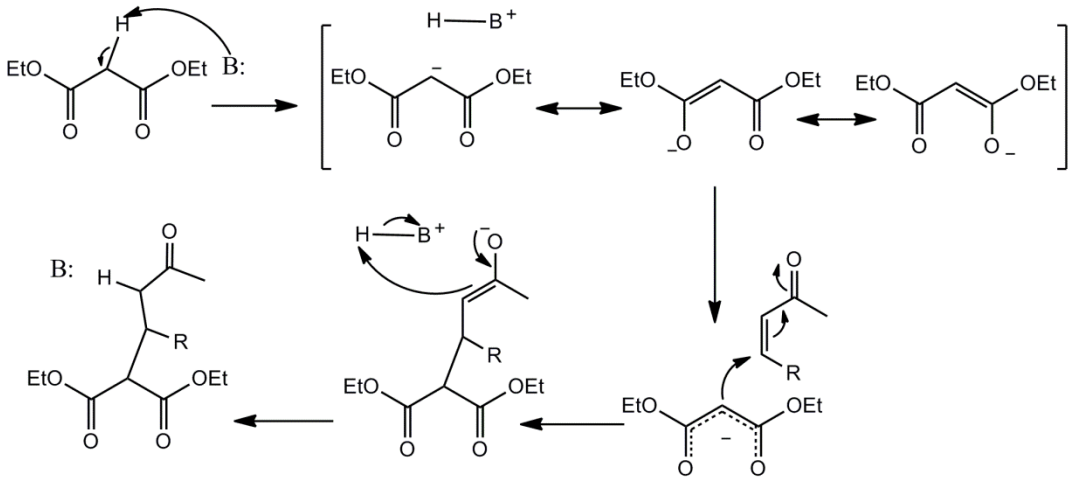

Figure 5.4. Base catalyzed of the Michael addition reaction.

An alternative to base catalysis is the use of enzymes (Figure 5.5). The oxyanion hole of the lipase active site stabilizes the negative charge of the transition state and the His-Asp pair acts as a proton shuttle in the enzymatic mechanism. The carbonyl oxygen of the α,β-unsaturated carbonyl compound is bound in the oxyanion hole formed by Gln106, Ser105, and Thr40. His224 acts as a general base to activate the nucleophile.[19]

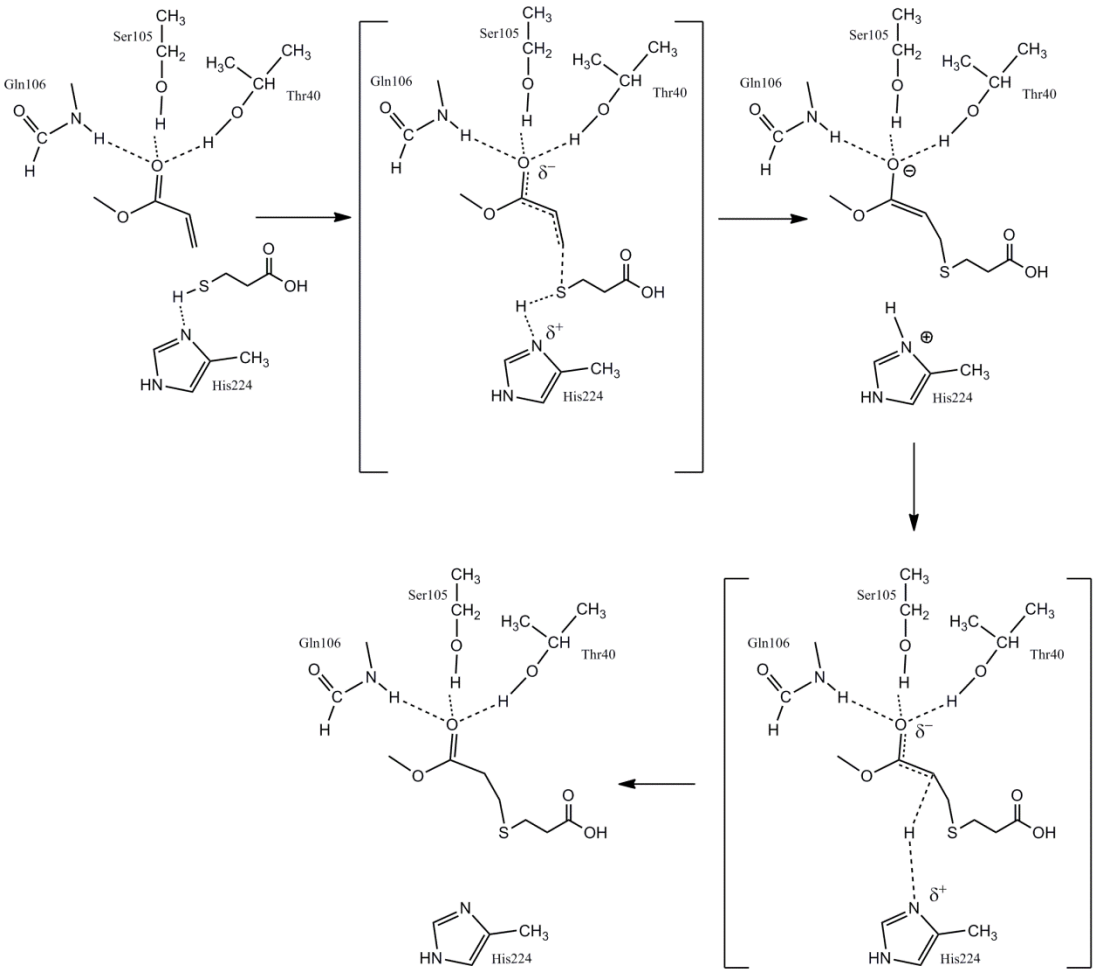

Figure 5.5. Enzymatic catalysis of the Michael addition reaction.

Experimental data has shown that CALB is able to catalyze several Michael additions, resulting in products that can be used as monomers for novel polymers.

Amines and thiols have been shown to be good nucleophiles for lipase catalyzed Michael additions.[20] In a one pot reaction, CALB (Novozyme435, vacuum 24hr) was used to catalyze the Michael addition of 1, 2-ethanedithiol and acrylonitrile (1:2 molar ratio) resulting in the thioether-nitrile mono- and di-Michael adducts. Reactions were quenched by removal of enzyme beads and analyzed by GC-MS. Control reactions in which no enzyme beads were added did not demonstrate the presence of mono or di-Micheal adducts. After the enzyme catalyzed Michael addition, the nitrile group can easily be converted to the free acid through acid hydrolysis and can be further polymerized, chemically or enzymatically, using a variety of monomers resulting in a novel polymer containing thioether functional groups within the backbone. The free sulfide of the mono-Michael adduct can be used as a nucleophile in further polymerizations.

Amines were also used as nucleophiles for CALB catalyzed Michael additions. In a one pot reaction, CALB (87mg) catalyzed Michael addition of methylmethacrylate and N-phenylethane-1,2-diamine (1:1 molar ratio, rm temp, 24hr) resulted in the propoanoate. This product was only observed in the reaction in which CALB enzyme beads were present. Once again, this product is an acceptable monomer for polymerizations having a reactive carboxylic acid group.

5.3.3 CIBER Website

To fulfill an educational objective of the CIBER, a website has been created to provide general and scientific information on biomass sources, biomaterials, polymers, and enzymes, Figure 5.6. The CIBER website is designed to provide information for all

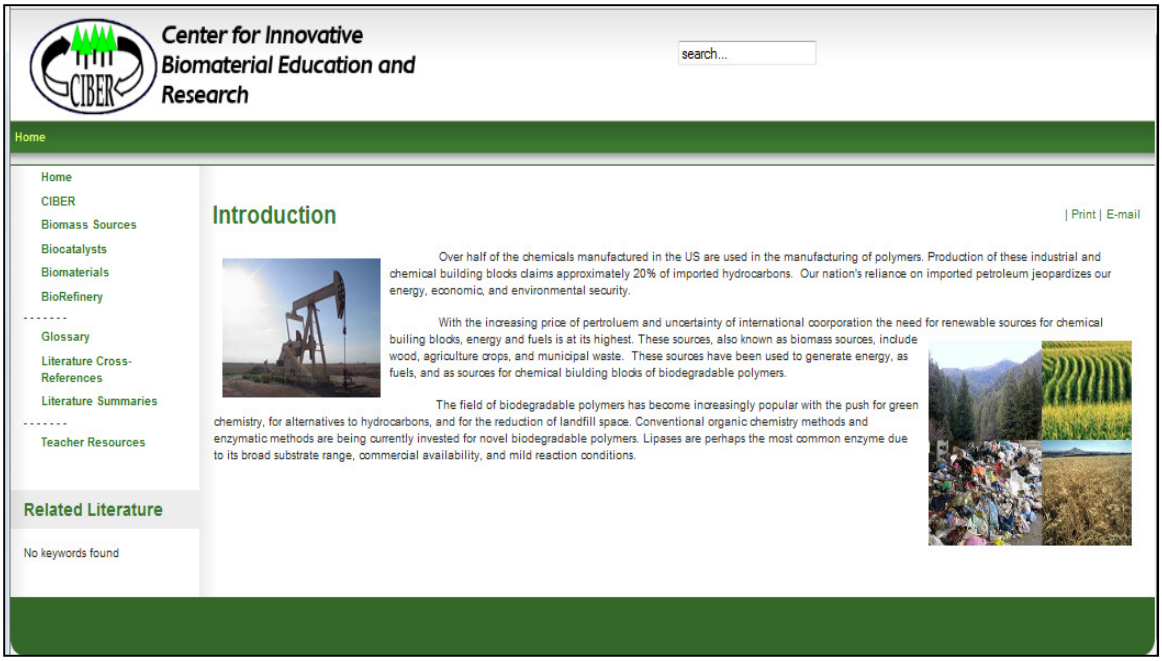

Figure 5.6. Introduction page of the CIBER website

ages and education levels on the importance, uses, and sources of biomaterials. It includes a searchable database of literature and presentations in the field of biomaterials, a glossary of commonly used definitions and formulas, and a page with activities and projects for K-12 students, the website is designed to useful to teachers, students, the general public and scientists in the field. General information is provided through topic and subtopic pages on enzyme commonly used in enzymatic polymerizations, biodegradable polymers, biomass sources, etc. A searchable database of scientific peer-reviewed article summaries provides a more in depth information for those in the field of biomaterials or for students conducting literature reviews or research. An example summary can be seen in Figure 5.7. Presentations given by graduate students and professors on the latest research being conducted in field are included in this section of the website.

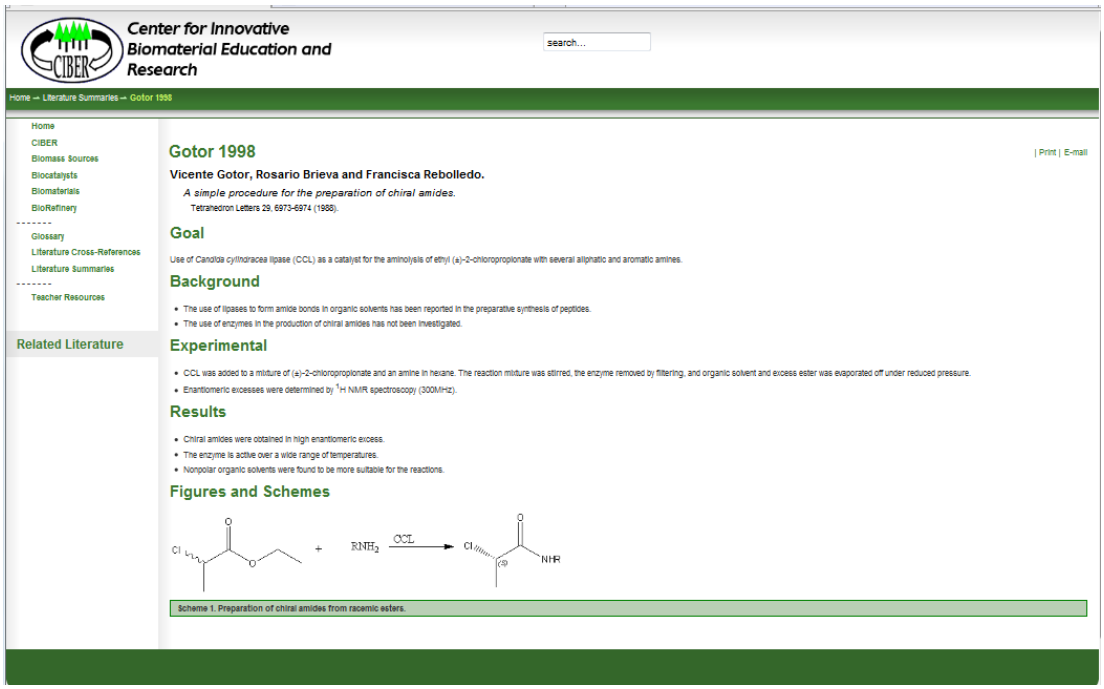

Figure 5.7. Example of literature summary found on CIBER website.[21]

A Teacher's Resource page has been added in order to provide teachers of all levels (K-12) with an easily accessible compilation of websites containing numerous activities, lesson plans, and laboratory experiments for use in teaching biomaterials and biomass sources and conversion. The websites included in this list are reputable sources of facts and information on the topics and include the U.S. Dept. of Energy and the Energy Information Administration. Linked to this page is a list of downloadable PDFs of classroom activities and laboratory experiments aimed towards high school teachers.

The CIBER website is constantly being updated and is serving as a tool to introduce the area of biomass conversion and the major problems that still remain to be solved by researchers in this area. As seen in Figure 5.6, from May 2009 to October 2009 the site was being used by an average of 243 different users each month and was generating an average of 26,865 hits per month. Navigations to the website have been referred by search engines such as Google, Yahoo and Bing.

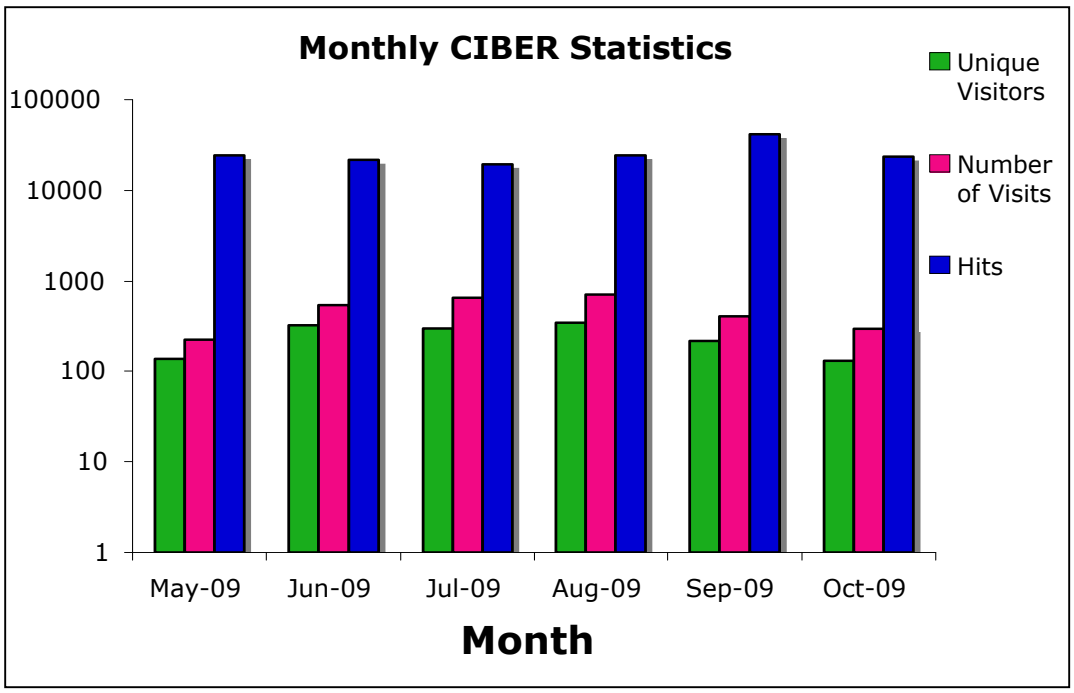

Figure 5.6. CIBER website statistics from May 2009 to October 2009.

5.4 References

1. Davis, B. G., Synthetic Methods. Part (iii) Biocatalysis and enzymes in organic synthesis. *Annu. Rep. Prog. Chem., Sect. B* **2003,** 99, 49-62.

2. Gross, R. A.; Kalra, B.; Kumar, A., Polyester and polycarbonate synthesis by *in vitro* enzyme catalysis. *Appl. Microbiol. Biotechnol.* **2001,** 55, 655-660.

3. Kato, M.; Toshima, K.; Matsumura, S., Preparation of aliphatic poly(thioester) by the lipase-catalyzed direct polycondensation of 11-mercaptoundecanoic acid. *Biomacromol.* **2005,** 6, 2275-2280.

4. Parratt, J. S.; Cripps, M. C.; Faulconbridge, S. J.; Holt, K. E.; Rippé, C. L.; Savage, S. P.; Taylor, S. J. C., Enzyme Chemistry. *Annu. Rep. Prog. Chem., Sect B, Org. Chem.* **1997,** 98, 291-307.

5. Silva, A.; Bordado, J. C., Recent delvelopments in polyurethane catalysis: Catalytic mechanisms review. *Catalysis Reviews* **2004,** 46, (1), 31-51.

6. Uppenberg, J.; Hansen, M. T.; Patkar, S.; Jones, T. A., The sequence, crystal structure determination and refinement of two crystal forms of lipase B from *Candida antartica*. *Structure* **1994,** 2, 293-308.

7. Uppenberg, J.; Öhrner, N.; Norin, M.; Hult, K.; Kleywegt, G. J.; Patkar, S.; Waagen, V.; Anthonsen, T.; Jones, T. A., Crystallographic and molecular-modeling studies of lipase B from *Candida antarctica* reveal a stereospecificity pocket for secondary alcohols. *Biochemistry* **1995,** 34, 16838-16851.

8. Cygler, M., Grochulski, Pawel; Kazlauskas, R. J.; Schrag, J. D.; Bouthillier, F.; Rubin, B.; Serreqi, A. N.; Gupta, A. K., A structural basis for the chiral preferences of lipases. *J. Am. Chem. Soc.* **1994,** 116, 3180-3186.

9. Ghanem, A. G.; Schurig, V., Lipase-catalyzed irreversible transesterification of secondary alcohols using isopropenyl acetate. *Monatsheft fur Chemie* **2003,** 134, 1151-1157.

10. Isaksson, D.; Lindmark-Henriksson, M.; Manoranjan, T.; Sjodin, K.; Hogberg, H.-E., Hemiacetals and their esters as side products in lipase-catalysed transesterifications of vinyl esters with sterically hindered alcohols. *Journal of Molecular Catalysis B: Enzymatic* **2004,** 31, 31-37.

11. Jacobsen, E. E.; Anthonsen, T., Water content influences the selectivity of CALB-catalyzed kinetic resolution of phenoxymethyl-substituted secondary alcohols. *Can. J. Chem.* **2000,** 80, 577-581.

12. Kulshrestha, A. S.; Sahoo, B.; Gao, W.; Fu, H.; Gross, R. A., Lipase catalysis: A direct route to linear aliphatic copolyesters of bis(hydroxymethyl)butyric acid with pendant carboxylic acid groups. *Macromolecules* **2005,** 38, 3205-3213.

13. Magnusson, A. O.; Rotticci-Mulder, J. C.; Santagostino, A.; Hult, K., Creating space for large secondary alcohols by rational redesign of *Candida antarctica* lipase B. *ChemBioChem* **2005,** 6, 1051-1056.

14. Parida, S.; Dordick, J. S., Tailoring lipase specificity by solvent and substrate chemistries. *Journal of Organic Chemistry* **1993,** 58, 3238-3244.

15. Raza, S.; Fransson, L.; Hult, K., Enantioselectivity in Candida antarctica lipase B: A molecular dynamics study. *Protein Sci.* **2001,** 10, 329-338.

16. Adam, W.; Lazarus, M.; Schmerder, A.; Humpf, H.-U.; Saha-Möller, C. R.; Schreier, P., Synthesis of optically active α-hydroxy acids by kinetic resolution through lipase-catalyzed enantioselective acetylation. *Eur. J. Org. Chem.* **1998**, 2013-2018.

17. Mather, B. D.; Viswanathan, K.; Miller, K. M.; Long, T. E., Michael addition reactions in macromolecular design for emerging technologies. *Prog. Polym. Sci.* **2006,** 31, 487-531.

18. Svedendahl, M.; Hult, K.; Berglund, P., Fast carbon-carbon bond formation by a promiscuous lipase. *J. Am. Chem. Soc.* **2005,** 127, 17988-17989.

19. Branneby, C.; Carlqvist, P.; Magnusson, A.; Hult, K.; Brinck, T.; Berglund, P., Carbon-carbon bonds by hydrolytic enzymes. *J. Am. Chem. Soc.* **2003,** 125, 874-875.

20. Carlqvist, P.; Svedendahl, M.; Branneby, C.; Hult, K.; Brinck, T.; Berglund, P., Exploring the active-site of a rationally redesigned lipase for catalysis of Michael-type additions. *ChemBioChem* **2005,** 6, 331-336.

21. Gotor, V.; Brieva, R.; Rebolledo, F., A simple procedure for the preparation of chiral amides. *Tet. Lett.* **1988,** 29, 6973-6974.